



UNIVERSITÀ
DEGLI STUDI
FIRENZE

PROT. N° 153319 POS III/6-21
DATA 23-10-2017

DOTTORATO DI RICERCA IN
Scienze Agrarie e Ambientali

CICLO XXX

COORDINATORE Prof. Pietramellara Giacomo

**A model library for estimating grapevine development and growth
under different pedo-climatic conditions**

Settore Scientifico Disciplinare AGR/02

Dottorando

Dott. Leolini Luisa

Tutore

Prof. Bindi Marco

Coordinatore

Prof. Pietramellara Giacomo

Anni 2014/2017

Supervisor

Prof. Marco Bindi

Department of Agri-food Production and Environmental Sciences (DISPAA)

University of Florence

Piazzale delle Cascine 18, 50144 Florence, Italy

Phone: +39 055 2755791

Email: marco.bindi@unifi.it

Co-supervisors

Dr. Simone Ugo Maria Bregaglio

Council for Agricultural Research and Economics (CREA)

Research Centre for Agriculture and Environment (AA)

Via di Corticella 133, 40128 Bologna, Italy

Phone: +39 051 6316847

Email: simoneugomaria.bregaglio@crea.gov.it

Dr. Marco Moriondo

Institute of Biometeorology of the National Research Council (CNR-IBIMET)

Via G. Caproni 8, 50145 Florence, Italy

Phone: +39 055 3288257

Email: marco.moriondo@cnr.it

To Sergi

“E non è un'invenzione
E neanche un gioco di parole
Se ci credi ti basta, perché
Poi la strada la trovi da te”
-L'isola che non c'è-

Acknowledgements

This PhD thesis is the result of three years of intense and rewarding work in which I learned a lot and shared many experiences. For this reason, it is time to acknowledge the people who helped me to reach this important goal.

I am very grateful to Prof. Marco Bindi and Prof. Marcello Donatelli for giving me this opportunity and for their professional assistance.

A special thanks goes to Dr. Marco Moriondo for his precious and irreplaceable help and for encouraging me even in the most difficult moments. He is a wonderful person and one of the more brilliant scientists who I worked with.

Many thanks also to the research team of Prof. Marco Bindi (Camilla, Roberto, Paolo, Giacomo, Lorenzo and Gloria) who always supported me. In particular, I would like to thank Dr. Lorenzo Brilli; I shared with him "philosophical" moments, funny breaks and intense but always interesting discussions that only close friends can have. A special thanks also goes to the future PhD, Gloria Padovan, a very good colleague and, above all, friend.

My sincere thanks goes to the CREA research team of Bologna who I worked with. In particular, I would like to thank Dr. Fabrizio Ginaldi and Dr. Simone Bregaglio, two excellent scientists and kind people. One of my greatest thanks goes to them for helping me in my PhD journey and for encouraging me every time. In addition, I want to thank Dr. Gianni Fila for helping me during Chapter 4 elaboration. As for Simone and Fabrizio, Gianni is a very good scientist and a fantastic person.

I would like to thank the research group of INRA in Bordeaux (France) and, especially, Dr. Zhanwu Dai who welcomed me with enthusiasm and made me feel at home. I thank my summer school's friends in Cadillac (Bordeaux), with whom I spent an unforgettable week discussing about climate, forestry, and wine. Moreover, I want to remember Junqi Zhu, Ruie Liu, Tefide Kizildeniz and Kenneth Webster for the wonderful friendship they demonstrate yesterday, today and tomorrow.

Special thanks to my family, Giovanna's lunch group, my friends and all the people who supported me. This journey was not only for me just a professional experience but rather a intense "slice" of my life. Over the unhappy moments, I want to thank all the people who helped me, more or less consciously, to carry on with my work.

Finally, very great thanks to Sergi for his sweetness, patience and love. During the saddest moments of my PhD, he stood by my side giving me the strength to carry on. For him, my gratitude and sincere love.

Table of Contents

Abstract	III
Riassunto	V
1.1. Role and importance of viticulture	9
1.2. The impact of climate change on grapevine: yield and quality	11
1.3. Grapevine and simulation models	13
1.3.1. General overview about crop simulation models	13
1.3.2. Modelling the main plant processes	14
1.3.3. Modelling the effect of abiotic stress	20
1.4. Aim and outline of the research.....	22
2. A model library to simulate grapevine growth and development: software implementation, sensitivity analysis and field level application	27
2.1. Introduction	28
2.2. Materials and Methods	30
2.2.1. Component architecture	31
2.2.2. Models description	32
2.2.3. Case study	39
2.3. Results and discussion.....	45
2.3.1. Analyzing the sensitivity of the modelling solution to weather variability and parameter changes	45
2.3.2. Field level application of the modelling solution	48
2.4. Conclusions	53
3. UNIFI.GrapeML implementation for estimating sugar content of Sangiovese grape variety	57
3.1. Introduction	58
3.2. Materials and Methods	59
3.2.1. Study area.....	59
3.2.2. Phenology and sugar content measured/observed data	61
3.2.3. Grape quality implementation	61
3.3.3. Calibration and Statistical analysis.....	63
3.3. Results	63
3.3.1. Climate analysis	63

3.3.2. Model calibration and validation.....	64
3.4. Discussion	67
3.5. Conclusions	68
4. Late spring frost impacts on future grapevine distribution in Europe	73
4.1. Introduction	75
4.2. Materials and Methods	75
4.2.1. Climate datasets.....	76
4.2.2. Phenology model.....	76
4.2.3. Grapevine varieties.....	78
4.2.4. Fruit-set Index and Frost events estimation.....	79
4.3. Results	80
4.3.1. Present period dynamics.....	81
4.3.2. Future Scenarios	84
4.4. Discussion	90
4.5. Conclusions	90
5. General Discussion.....	97
5.1. UNIFI.GrapeML implementation	97
5.2. Sensitivity analysis, calibration and validation	99
5.3. Application: the impact of mean climate change and extreme events at European scale.....	101
5.4. Future implementations	103
6. Conclusions	107
References	109
Supplementary Material	125
Supplementary Material I.....	130
Supplementary Material II.....	134
Supplementary Material III	136
List of Tables and Figures	144
Curriculum Vitae	149
Publications	150

Abstract

Grapevine (*Vitis vinifera* L.) is a valuable fruit crop characterized by a worldwide importance. In particular, Italy, France and Spain are the biggest wine-producing countries and they play a relevant role in the world wine economy. However, the specific climate conditions of the narrow geographical areas in which grapevine is currently cultivated expose the viticulture suitability to the great risk of the climate change and extreme events. In this context, the grapevine simulation models represented useful tools for investigating the main physiological plant processes under different pedo-climatic conditions. Accordingly, the objective of this thesis is to provide a new software component for estimating grapevine growth, yield and quality in different environments.

The new software component UNIFI.GrapeML is presented in Chapter 2 as an extendible model library in which the fine-granularity of the model structure allows an easier discretization and implementation of the code. In Chapter 2, UNIFI.GrapeML was tested in a specific case of study in Northeastern of Spain on a Chardonnay vineyard. A sensitivity analysis using Latin Hypercube and Sobol method was performed for evaluating the sensitivity of the model parameters on the final fruit biomass considering the environmental conditions of the study area. The results evidenced the strong impact of leaf area expansion and crop partitioning parameters on final output. The model was then calibrated on soil water content, phenology and fruit biomass data showing satisfactory results.

Afterwards, UNIFI.GrapeML was implemented with a quality approach for assessing sugar concentration during ripening period according to the berry water content. This approach was evaluated in a specific case of study in Montalcino wine-producing region (Italy) for Sangiovese variety over the period 1998-2015. In this case, the phenological phases (budbreak, flowering, veraison and maturity) of Sangiovese variety were calibrated using data from Susegana and Montalcino for determining the length of grapevine cycle. Then, the model calibration and validation on observed sugar content data was performed for Montalcino site. The results showed high correlations in both calibration and validation procedures considering the year-to-year variability of the dataset.

Finally, the impact of climate change and extreme events was evaluated on the phenological cycle of very early, early, middle and late varieties at European scale (Chapter 4). The effect of the mean climate change on phenology was assessed using a chilling-forcing model while the effect of extreme events was accounted through the frost events at budbreak and the effect of suboptimal temperatures at flowering stages (fruit-set impact implemented in UNIFI.GrapeML). The results highlighted an overall advance of budbreak and flowering phases of all varieties across a latitudinal and

longitudinal geographical gradient, especially in central/eastern Europe. In particular, the climate change showed a high impact on budbreak of late compared to very early and early varieties in western European region. Moreover, a higher decrease of frost events was evidenced in western regions compared to central/eastern Europe and a more relevant effect of these events was found on very early and early compared to late varieties. On the other hand, the estimation of the temperature stress at flowering stage evidenced a lower variability between varieties and scenarios while relevant differences were showed between European regions.

Riassunto

La vite (*Vitis vinifera* L.) è una coltura arborea caratterizzata da una diffusione ed una importanza mondiale. In particolare, Italia, Francia e Spagna sono considerati i paesi maggiori produttori di vino e giocano un ruolo chiave nell'economia viticola globale. Tuttavia, le peculiari condizioni climatiche delle principali regioni viticole rendono la viticoltura di quelle aree particolarmente esposta al forte impatto del cambiamento climatico e degli eventi estremi, mettendone a serio rischio la sostenibilità. In questo contesto, lo sviluppo di modelli che simulano la crescita della vite ha rappresentato uno strumento utile per studiare i principali processi fisiologici della pianta in varie condizioni pedo-climatiche. Pertanto, il principale obiettivo di questa tesi è fornire una nuova componente software in grado di stimare la crescita, la resa e la qualità della vite in ambienti diversi.

La soluzione di modellazione UNIFI.GrapeML è presentata nel Capitolo 2 come una libreria estendibile nella quale la fine granularità della struttura del modello permette una più semplice discretizzazione e implementazione del codice. Nel Capitolo 2, UNIFI.GrapeML è stata testata in un caso specifico nel nordest della Spagna in un vigneto di varietà Chardonnay. Un'analisi di sensitività, utilizzando gli approcci di Ipercubo Latino e Sobol, è servita per valutare i parametri più sensibili del modello che agiscono sulla resa finale considerando le condizioni ambientali dell'area di studio. I risultati hanno evidenziato il forte impatto dei parametri che riguardavano l'espansione dell'area fogliare e la ripartizione della biomassa sulla resa finale di uva. Successivamente, il modello è stato calibrato sul contenuto idrico del suolo, la fenologia e la biomassa del frutto fornendo soddisfacenti risultati.

Successivamente, UNIFI.GrapeML è stata implementata utilizzando un approccio qualitativo per valutare la concentrazione di zucchero durante il periodo di maturazione considerando il contenuto di acqua negl'acini. Questo metodo è stato testato in un caso specifico di studio nella regione viticola di Montalcino (Italia) per la varietà Sangiovese durante il periodo di studio 1998-2015. Le fasi fenologiche (germogliamento, fioritura, invaiatura e maturità) del Sangiovese sono state calibrate su dati osservati di fenologia dei siti di Susegana e Montalcino per determinare la lunghezza del ciclo fenologico della varietà. In seguito, il modello è stato calibrato e validato nel sito di Montalcino utilizzando dati osservati di grado Brix. I risultati hanno mostrato strette correlazioni per entrambe le procedure di calibrazione e validazione considerando la variabilità climatica della serie di dati.

Infine, l'impatto del cambiamento climatico e degli eventi estremi è stato valutato, a scala Europea, sul ciclo fenologico di varietà di uva molto precoci, precoci, medie e tardive (Capitolo 4). L'effetto del cambiamento climatico sulla fenologia è stato stimato utilizzando un modello basato sull'accumulo di unità di freddo e di calore mentre l'effetto degli eventi estremi è stato valutato considerando gli eventi di gelo al

germogliamento e l'effetto di temperature subottimali alla fioritura (l'impatto all'allegagione è stato implementato in UNIFI.GrapeML). I risultati hanno evidenziato un generale anticipo delle fasi di germogliamento e fioritura di tutte le varietà lungo un gradiente latitudinale e longitudinale. Il cambiamento climatico ha mostrato un forte impatto sul germogliamento nelle regioni dell'Europa centrale e, a livello varietale, un maggiore impatto è stato riscontrato sulle varietà tardive nella parte ovest dell'Europa. Inoltre, gli eventi di gelo sono fortemente diminuiti nella parte occidentale rispetto alla parte centrale e orientale dell'Europa. In questo senso, un effetto maggiormente rilevante è stato riscontrato sulle varietà molto precoci e precoci in confronto a quelle tardive. Al contrario, la stima dello stress di temperatura alla fioritura ha evidenziato una più bassa variabilità sia tra varietà che tra scenari mentre evidenti differenze sono state trovate tra regioni europee.

Chapter 1

General Background



Chapter 1 shows a general background about the importance of viticulture around the world, the impact of climate change on grapevine yield and quality and an overview of the main grapevine simulation models.

PhD candidate's contribution

Luisa Leolini wrote all sections of the chapter.

1.1. Role and importance of viticulture

Grapevine (*Vitis vinifera* L.) is a valuable crop characterized by a long history of evolution and domestication (Terral et al., 2010). The origin of grapevine cultivation was found in the area between Black Sea and Iran during Neolithic period (McGovern and Michel, 1995; Zohary, 1996). Afterwards, grapevine was spread in the near regions of Middle East and Europe where this cultivation evolved in a great range of types and forms.

Nowadays, the great economic importance of viticulture is largely recognized around the world (Fig.1.1). In 2015, the global vineyard surface area reached 7534 kha (thousands of hectares) while the global wine production rose to 274.4 mhl (millions of hectoliters; OIV, 2016). Although, the strong increase in vineyard surface area makes of China the 2nd biggest country for global area under vines and United States of America provided the second highest level of wine production with 22.1 mhl, Europe remains the first world wine producer (Bettini, 2015; OIV, 2016). The greatest amount of global wine production is provided by three European countries such as Italy, France and Spain.

In particular, Italy represents the biggest wine-producer country in 2015 (OIV, 2015) with a large number of wine-making areas distributed on the entire territory. For example, in Tuscany region the wine production covers a large part of the agriculture sector providing a wide range of high-quality wine for global and local wine economy. In this context, Sangiovese is the most important red variety and it characterizes the most famous wine brands in the region (i.e. Chianti Classico, Brunello di Montalcino, etc.).

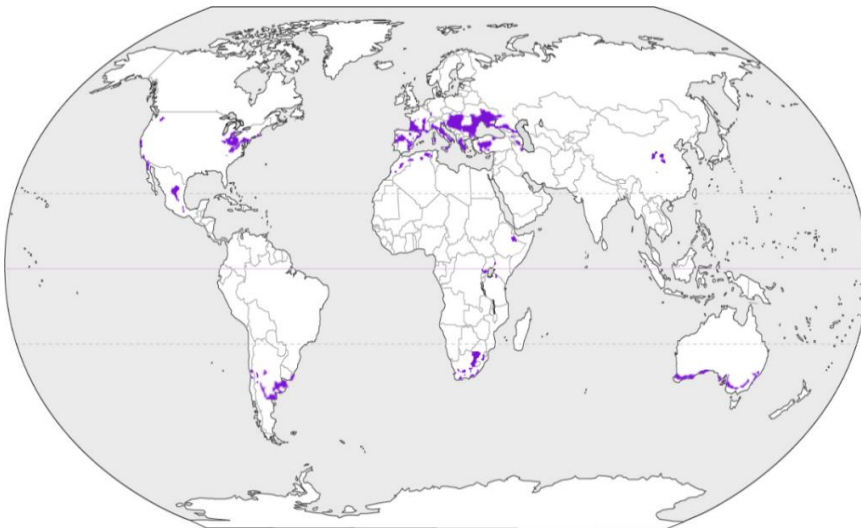


Figure 1.1. Distribution of the current suitable wine-producing regions around the world (data of current grapevine suitability extracted by Hannah et al. 2013).

These wine-producing regions are included in specific geographical areas characterized by Protected Designation of Origin (PDO) and Protected Geographical Indication (PGI) (https://ec.europa.eu/agriculture/quality_en, Last Access [14/10/2017]) which preserve the wine peculiarity. Indeed, the complex interaction of different factors (i.e. soil status, water and nitrogen dynamics), plant and human techniques are involved in the concept of *Terroir* (Seguin, 1988, 1986). The impact of different factors on *Terroir* has already been studied as the effect of singles parameters (Huglin and Schneider, 1998; Van Leeuwen and Seguin, 1994; Winkler et al., 1974) or as a complex of them on grapevine growth and production (Van Leeuwen et al., 2004).

The specific environmental conditions in which grapevine is currently cultivated have a direct impact on grapevine growth and yield and quality. According to Smart (1985), for instance, grapevine physiology may be directly altered by climate, soil and management practices and indirectly altered by variation of canopy climate. In these terms, grapevine growth, yield and quality result strongly affected by the combination of the main environmental factors which determine the taste and tipicity of the most prestigious wines (Van Leeuwen et al., 2004).

1.2. The impact of climate change on grapevine: yield and quality

The climate showed an unequivocal change around the world compared to pre-industrial times. The higher greenhouse gases (CO₂, CH₄, N₂O) concentration in the atmosphere led to a raise in the global earth's temperature. From 1880 to 2012 temperatures trend has increased of 0.85 [0.65 to 1.06] °C showing a higher frequency and magnitude of extreme events since 1950 (IPCC, 2014). Indeed, the number of cold days and nights has decreased compared to the number of warm days and nights over the period 1951-2010 (IPCC, 2014). This phenomenon is reported by several authors who investigated long series of weather data. According to Ramos et al., (2008), for example, the number of days with temperatures higher than 30°C is significantly increased over the period 1950-2006 for three locations in northeastern of Spain. Moreover, Vincent et al. (2005) showed that the percentage of cold nights in South America decreased from 1960 to 2000 especially in summer and autumn season.

The warmer temperatures conditions are associated with the increase of the variability of the precipitation that leads to a relevant discrimination between dry and wet regions. According to Zhai et al. (2005), the annual amount of precipitation and the extreme precipitation events showed a strong decrease in some regions of China over the period 1951-2000. By contrast, other Chinese regions evidenced a significant increase of extreme frequency and intensity of the precipitation. In Europe, Moberg and Jones (2005) showed that precipitation increased in terms of mean intensity and moderate extreme events especially during winter period. On the other hand, few significant results were found for changes in precipitation events over the summer period.

The impact of climate variability determine the alteration of the climate-soil-variety equilibrium with negative effects on high quality wine production (Jones et al., 2005; Jones and Davis, 2000). This phenomenon has already been found by several authors who evidenced as the changing climate conditions showed a detrimental effect on viticulture suitability. In this case, the current literature reports that the short-term climate variability and the long-term climate change negatively impact on the most famous viticulture regions (Duchêne and Schneider, 2005; Jones et al., 2005; Jones and Davis, 2000; Santos et al., 2011).

Accordingly, the threats led by the climate variability (i.e. warmer temperature, increase of frequency and magnitude of the precipitation, etc.) is expected to influence the growth cycle and the future high quality production (Fig.1.2). As mentioned before, the current wine-producing regions are located in narrow and specific climatic niches that are strongly subjected to the effect of climate change. Thus, the climate

conditions expected for future scenarios could undermine the suitability of the current viticulture regions (Hannah et al., 2013; Moriondo et al., 2013, 2011a).

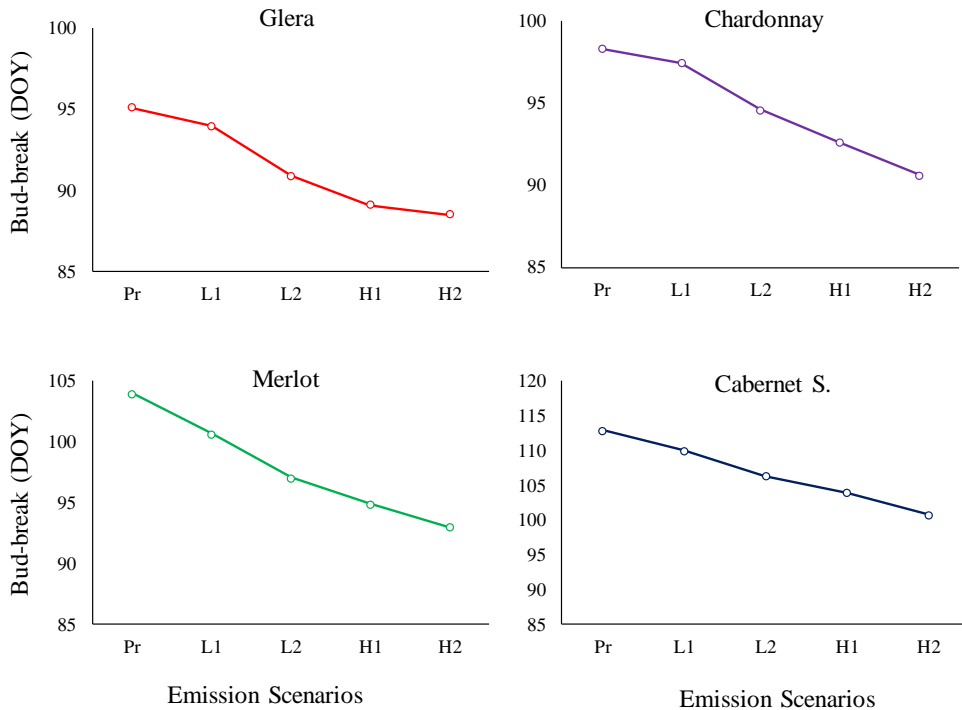


Figure 1.2. Estimation of Budbreak (Day Of Year; DOY) of four different varieties under two different climatic scenarios and two time slice in Spain (L1: RCP 4.5 2036-2065; L2: RCP 4.5 2066-2095; H1: RCP 8.5 2036-2065; H2: RCP 8.5 2066-2095).

Indeed, the influences of climate change and extreme events affect negatively crop growth, development, yield and quality. The higher temperature conditions, for example, are expected to change the occurrence of the main phenological phases leading to a shift of the grapevine growth cycle (Webb et al., 2007; Fig. 1.2). According to Dry (1988), the grapevine growing season is affected by an increase of 2°C in temperature range producing an advancement of harvest date from 12 to 30 days. The occurrence of grapevine ripening in dry and hot months leads to increase the probability of water stress conditions with consequent negative effect on grapevine yield and quality.

The relationship between yield and soil water availability in potted grapevine has already been considered in terms of reduced leaf area, photosynthesis and production (Bindi et al., 2005; Lebon et al., 2006). In drought conditions, the limited soil water

availability showed a great impact on stomatal conductance, net CO₂ assimilation and leaf transpiration as well as on grapevine yield (Medrano et al., 2003). More specifically, the water stress conditions during the flowering-veraison period is considered to have a detrimental effect on final berry weight (Becker and Zimmerman, 1984; Van Leeuwen and Seguin, 1994). By contrast, grapevine quality may be improved by moderate water stress conditions. Berries with excessive water content showed a worst quality due to an increase of berry size as well as a major dilution of the main constituents. Indeed, the relationship between vintage rating and water stress showed that moderate and severe water stress affect positively the grape quality (Van Leeuwen et al., 2009). However, the influences of severe water stress conditions and higher temperatures determine an increase of the sugar content and a decrease of total acidity compromise the sugar-acid ratio in berries (Jones et al., 2005). This aspect is considered as the main cause for the increase of wine alcohol content and the production of unbalanced wines.

1.3. Grapevine and simulation models

1.3.1. General overview about crop simulation models

Over the last years, crop simulation models have provided useful decision tools for investigating plant behavior under different environmental conditions. In most cases, the current climate change affects negatively the crop growth and farmers need to adapt their traditional agro-management practices for ensuring crop production. Accordingly, simulation models that explain the dynamics of growth, yield and quality of the most important and worldwide crops represent helpful tools especially for the next future. Indeed, the main feature of crop simulation models is related to the reproduction of the plant physiological processes using a schematic and simplified representation of the real system. By one side, the simplification provides a clear and comprehensive description of the system (i.e. few inputs for estimating the desired outputs) but, by the other side, it become the weakness point of the process. In general, the use of few inputs and parameters for estimating the final outputs allows to increase the model robustness under different climate scenarios. However, this simplified approach describes the essential processes of a complex real system with all the inherent risks (Murthy, 2004).

Based on these criteria, crop simulation models are mainly grouped in two main categories: empirical and process based models (Moriondo et al., 2015).

Empirical models usually describe linear relationships between one dependent variable (e.g. yield) and other independent variables (e.g. weather variables), but they do not consider processes such as plant growth and development or nitrogen and water dynamics. These models need of a limited amount of input data but their applications

are restricted to the environmental conditions in which relationships are defined and calibrated. According to Jones and Davis (2000), the effect of high precipitation levels on final yield is explained using empirical relationships. For example, Santos et al. (2011) found the empirical relationship between monthly mean temperature and precipitation on grapevine yield in Port wine-producing region.

On the other hand, process-based models describe the main plant processes (e.g. crop growth and development, biomass accumulation and partitioning) using mathematical relationships at different detail levels. These kind of models are generally used for describing crop yield at local scale and they include also non-climatic data such as agro-management practices or soil data. For instance, process-based models such as STICS (Brisson et al., 2009, 1998) and CropSyst (Stöckle et al., 2003) simulate crop growth cycle including specific plant and soil processes (e.g. plant gas exchange and water dynamics in the soil).

In general, both empirical and process-based models are characterized by different strength and weakness points. In empirical models, for instance, the lower use of model parameters generates a reduced uncertainty compared to process-based models. Indeed, the higher complexity of the process-based models and the large number of input data can make difficult the model running and provide a higher uncertainty in the results. However, the complex structure of the process-based models is unavoidable for describing the physiological process (i.e. phenology, biomass accumulation, etc.) at a high detail level and for understanding the dynamics of crop behavior in a context of climate change.

In the last years, grapevine simulation models have become one of the most important tools for evaluating yield and quality. The modelling of the main processes of the grapevine growth (i.e. development, growth, yield and quality) was evaluated in a context of present and future scenarios providing a useful support tools for wine-producer. According to the review of Moriondo et al. (2015), the modeling of the main grapevine physiology processes are briefly described for taking into account strength and weakness points of each model approach.

1.3.2. Modelling the main plant processes

Phenological development

The main phenological phases of grapevine (Fig.1.3) can be described using different modelling approaches (Caffarra and Eccel, 2010; Fila et al., 2014; García de Cortázar-Atauri et al., 2009a; Parker et al., 2011). The most important challenge for modelers is to improve the modelling of phenology estimation for allowing an accurate description of the plant development under changing environmental conditions. In particular, budbreak date represents the starting point for leaf unfolding

and annual vegetative growth in grapevine simulation models (e.g. Bindi et al., 1997a, 1997b; Wermelinger and Baumgartner, 1991). Accordingly, the negative effect led to higher or lower temperature on this phase may produce a shift of the entire grapevine growth cycle with a consequently detrimental effect on growth, yield and quality (Fila, 2012a; Jones et al., 2005; Jones and Davis, 2000; Molitor et al., 2014a; Webb et al., 2007). In this context, two main phenological approaches are generally used for describing grapevine behavior under present and future conditions: chilling-forcing and forcing approaches.

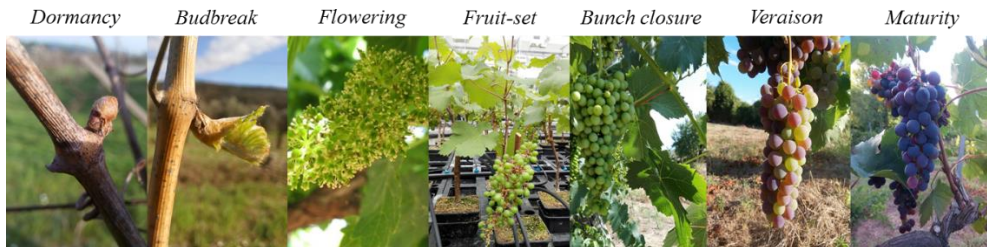


Figure 1.3. Grapevine phenological development.

In the first approach, the dormancy period is represented by endo- and eco-dormancy period (Lavee and May, 1997). During endo-dormancy, the units of chill are accumulated and the bud development is driven by endogenous factors. When the number of chills reach a specific threshold (chilling requirement), the bud development start to be influenced by esogenous factors and the forcing units are accumulated until bud-break date (Caffarra and Eccel, 2010; García de Cortázar-Atauri et al., 2009a; Hlaszny et al., 2011; Parker et al., 2011). Here, a particular approach for chilling days estimation was proposed by Fishman et al. (1987a, 1987b) that considers the dynamics sequence of cold and warm temperature as one of the fundamental aspect for determining chilling accumulation (Erez and Couvillon, 1987). On the other hand, the second approach assumes that the chilling unit requirement and the dormancy period has been already satisfied. Accordingly, the forcing units accumulation (eco-dormancy period) starts from a fixed day of the year until budbreak date is reached (Ben-Asher et al., 2006; Bindi et al., 1997a, 1997b; Cola et al., 2014).

Although the model performances of the chilling-forcing approach are not superior to the forcing approach under current climate conditions, the use of these types of models may play an important role under future scenarios (Fila et al., 2014; García de Cortázar-Atauri et al., 2009a). Indeed, the estimation of the dormancy period assumes a greater importance in a warming scenario where higher temperature

during winter may reduce the chilling accumulation determining the not fulfillment of chilling.

Despite the description of budbreak is the discriminant aspect between these two approaches, the modelling of the other phenology phases is also important. Flowering, veraison and maturity phases are generally considered in terms of thermal time accumulation and their importance on the cycle is relevant for defining the steps of the grapevine development. Flowering phase, for instance, is useful for taking into account the starting point of biomass partitioning and fruit growth while veraison phase determines the start of ripening period. Finally, maturity phase is often associated with harvest because it determines the reaching of the sugar content required for harvest. In order to describe these phenological phases, the growing degree days accumulation (GDD) or the use of sigmoid curves (UniFORC, Chuine, 2000) approaches starting from a fixed day of the year (or by the previous phenology phase) are generally used (Caffarra and Eccel, 2010; Parker et al., 2013, 2011).

Leaf area growth

The length of grapevine growing season starts with budbreak stage and finish with leaf fall. In this context, the modelling of vegetative growth is expressed in terms of the leaf area increase at different phenological stages (Bindi et al., 1997a, 1997b, Brisson et al., 2009, 1998). In Bindi et al., (1997a, 1997b), for example, the accumulation of the leaf number per shoots is based on the daily average temperature while Lebon et al., (2003) describe the increase of a simplified grapevine canopy structure using the relationship between the intercepted radiation and cumulative thermal time.

Moreover, the description of Leaf Area Index (LAI, $m^2 m^{-2}$) assumes a relevant importance because it can be directly related to grapevine production. In particular, LAI is estimated by some authors considering the plant leaf area (accounted by leaf appearance and expansion rates) and the portion of the soil occupied by the plant (Bindi et al., 1997a, 1997b). The vegetative part can be also described using the specific leaf area weight and biomass partitioned to leaves as shown by Ben-Asher et al. (2006), Nendel and Kersebaum (2004) and Wermelinger and Baumgartner (1991).

Finally, the impact of the main management practices plays a key role during leaf area growth and it is used in some grapevine simulation models as driver for canopy growth (Poni et al., 2006).

Light interception and Biomass accumulation

Biomass accumulation is estimated by the intercepted fraction of Photosynthetic Active Radiation (PAR) and Radiation Use Efficiency (RUE).

Several authors consider the intercepted radiation through the Beer-Lambert function (Vose et al., 1995) based on LAI and light extinction coefficient (Bindi et al., 1997a, 1997b, Brisson et al., 2009, 1998; Wermelinger and Baumgartner, 1991). A different case is showed by Cola et al. (2014) in which a three-dimensional canopy shape is implemented. Here, light interception is based on the approach of Oyarzun et al. (2007) considering several aspects (geographical position, aspect, slope, between and in-the-row vine spacing).

After light interception, RUE represents another important feature for describing biomass accumulation. RUE is the net dry matter production per unit of adsorbed energy (Bindi et al., 1997a, 1997b; Brisson et al., 2009; Pallas et al., 2011). In Bindi et al. (1997a, 1997b), RUE is calculated as a function of daily maximum and minimum temperatures and it is linearly correlated with the increase of CO₂ concentration in the atmosphere. Further contributions derived by Pallas et al. (2011), according to the approach proposed by Lebon et al. (2006) evidenced as RUE is affected by the Fractional Transpirable Soil Water (FTSW).

The estimation of PAR and RUE is used for accounting the daily accumulation of dry matter. However, others approaches consider biomass accumulation as derived by photosynthesis and respiration processes. According to Poni et al. (2006), the daily difference between plant photosynthesis (Charles-Edwards, 1982) and single plant organs respiration produce the total increase of biomass (after Lakso and Johnson, 1990).

Biomass partitioning

Plant biomass distribution among the single organs is called biomass partitioning (Fig. 1.4). Although, the grapevine simulation models use partitioning systems for redistributing plant biomass among single organs, this process is poorly described by literature. Hence, two main approaches have generally been used for considering the biomass partitioning dynamics: the use of fixed partitioning coefficients and the source/sink approach.

By one side, the use of fixed partitioning coefficients makes easier the modelling of plant biomass distribution considering that the plant biomass is allocated in the organs in specific development stages (Nendel and Kersebaum, 2004). By the other side, this approach makes difficult the explanation of the complex dynamics of the biomass partitioning into the plant. Accordingly, in some cases a source/sink approach is used for quantifying plant demand of assimilates for each organs considering the relationship between the available photosynthates pool and single plant organs (Pallas et al., 2011; Wermelinger and Baumgartner, 1991). This approach is based on the allocation rules that allow the distribution of dry matter among different parts of the plant.

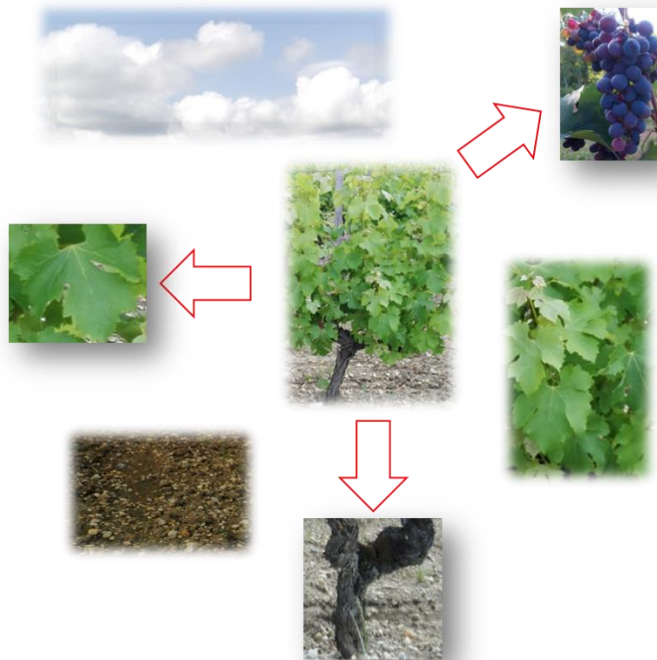


Figure 1.4. Biomass partitioning among single plant organs.

Finally, many of the previous studies are focused on the biomass partitioning between aboveground organs (Bindi et al., 1997a, 1997b; Cola et al., 2014; Poni et al., 2006). However, another important focus is related to the biomass partitioning towards root system. According to (Grechi et al., 2007), the root-shoot partitioning is mainly driven by plant carbon:nitrogen balance and this explain the effect of environmental changes on plant growth. In this way, Bota et al. (2004) showed a decrease in terms of accumulation strength of the main cluster compared to sink organs such as root and trunk in water stress conditions.

Evapotranspiration

Evapotranspiration (ET) process derives by the sum of the soil evaporation and plant transpiration process. ET is called Potential Evapotranspiration (PET) when it represents the potential amount of water removed through evaporation and transpiration processes from the environment. PET can be estimated using several approaches (Penman, Penman–Monteith, Priestley-Taylor, etc.; Allen et al., 1998) largely adopted by several simulation models. In STICS, for example, PET is estimated using the Penman–Monteith equation (Brisson et al., 2009, 1998).

On the other hand, ET is called crop evapotranspiration (ET_C) when it represents the crop evapotranspiration under standard conditions (i.e. large field and optimal agronomic and soil water status). The ET_C is derived by PET using crop coefficients (K_c) at different phenological stages or reducing specific thresholds on soil evaporation and plant transpiration (Celette et al., 2010; Lebon et al., 2003). Concerning the modelling of water loss by plant, the use of K_c that integrate the crop features and the average effect of soil evaporation has been often adopted for estimating crop evapotranspiration (FAO-56, Allen et al., 1998). The K_c varies considering the crop type and the length of the crop development stages and three different K_c are generally adopted for representing the initial (K_{ini}), middle (K_{mid}) and end (K_{end}) of the crop cycle. For grapevine, the K_{ini} , K_{mid} and K_{end} are 0.30, 0.70 and 0.45, respectively (grapevine varieties for wine; <http://www.fao.org>). Finally, K_c can be splitted in crop coefficient for crop transpiration and crop coefficient for soil evaporation. In this case, the K_{ini} , K_{mid} and K_{end} for crop transpiration in grapevine are 0.15, 0.65 and 0.40, respectively (grapevine varieties for wine; <http://www.fao.org>).

Soil evaporation is the water evaporated from an evaporating surface and it is described by several approaches (i.e. Allen et al., 1998; Campbell, 1985; Ritchie, 1972; Stöckle et al., 2003) and as shown for evapotranspiration it can be grouped in potential or actual evaporation. On the other hand, plant transpiration process is related to gas exchange by plant stomata and it can be modelled using different approaches. According to Amir and Sinclair (1991), Soltani and Sinclair (2012) and Tanner and Sinclair (1983), for example, plant transpiration is based on the daily crop dry matter production, air vapor pressure deficit and transpiration coefficient.

Grape quality

The modelling of berries sugar and acid concentration during the ripening period is one of the most important challenge for modelers due to the relevant climate change impact on grapevine quality. Although the acid concentration is currently difficult to model, the complex dynamics of sugar concentration during the grapevine growth cycle have been already shown by some authors. According to García de Cortázar-Atauri et al., (2009b), Sadras and Mccarthy (2007) and Sadras et al. (2008), the sugar concentration is negatively correlated to the berries water content over the ripening period. The behavior of the sugar content is climate, soil and variety-dependent (Matthews and Anderson, 1988) and it can be explained using the thermal time or number of days from flowering (or veraison) to harvest such as proposed by García de Cortázar-Atauri et al., (2009b). The simplified approach of García de Cortázar-Atauri et al. (2009b) can be coupled to a process-based grapevine simulation model for estimating sugar content (Brisson et al., 1998). On these basis, STICS (Brisson et al. 1998) is probably one of the few growth models able to simulate sugar concentration.

The complex dynamics of sugar concentration can be also estimated separately by the grapevine growth processes. Some types of simulation models (functional models) describe exclusively the complex dynamics of sugar concentration. Dai et al. (2009), for example, adapted the process-based functional approach of SUGAR model for estimating grape sugar concentration (SUGAR-vitis model) during the post-veraison phase.

1.3.3 Modelling the effect of abiotic stress

Extreme events impact

The low predictability and the changes in frequency and intensity level of the extreme events makes difficult to quantify their effect on plant growth, development and yield. However, the effect of extreme events and in particular of extreme temperatures showed a relevant importance on grapevine yield (Ramos et al., 2008; White et al., 2006). A clear example of extreme events that affect grapevine growth is represented by the occurrence of frost events at budbreak and heat stress at flowering. In this context, while frost events affecting buds at the first phase of development can limit leaf appearance and shoot growth (Mullins et al. 1992; Trought et al. 1999), heat stress reduces photosynthesis process and the fruit-set percentage at flowering stage (Ewart and Kliewer, 1977; Kliewer, 1977; Tukey, 1958).

Despite their relevant effect on grapevine growth, the extreme events impact is generally not account in grapevine simulation models. Only some crop models used for annual crops consider extreme events as reducing factors of the final output (Barlow et al., 2015a; Chung et al., 2014).

CO₂ concentration

The increase of CO₂ concentration is the main important driver of global warming that affect vine growth and yield. Indeed, while the excessive levels of CO₂ have a strong direct effect on the increase of plant photosynthesis, some indirect effects of CO₂ on plants are related to the increase of temperatures. For instance, a double effect on transpiration rate is expected due to the increase of CO₂ atmosphere level. By one side, transpiration is reduced by a lower stomatal conductance, by the other side the increase of vapor pressure deficit (VPD) and consequently of transpiration rate is a direct cause of global warming (Edwards et al., 2016).

Some studies have already highlighted the impact of CO₂ concentration on grapevine growth and development showing the positive effect of CO₂ on RUE and WUE at different level of CO₂ (Bindi et al., 2001a, 2001b; Flexas et al., 2013). Accordingly, some simulation models include the effect of CO₂ concentration on biomass accumulation and transpiration processes (Bindi et al., 1997a, 1997b, Brisson

et al., 2009, 1998; Cola et al., 2014; Godwin et al., 2002). For instance, Cola et al. (2014) showed the effect of the increase CO₂ from 320 to 395 ppm on the potential gross CO₂ assimilation as a factor of the photosynthesis model.

Water stress

The modelling of soil water dynamics is an important step for taking into account the impact of water stress on grapevine yield and quality (Bota et al., 2004; Dry et al., 2000a, 2000b; Santos et al., 2005).

Accordingly, simulation models coupled soil water balance models with grapevine simulation model (Brisson et al., 2009, 1998). In general, the soil water balance is defined by the difference between the water inputs (i.e. precipitation and irrigation) and water outputs (i.e. soil evaporation and plant transpiration, soil surface runoff, deep drainage) in the layers explored by roots. These soil water dynamics are estimated using different approaches (i.e. cascading approach (Ritchie, 1998) and Richard's equation (Richards, 1931) that help to determine the available soil water for plant water uptake. Thus, the aim of soil water models is to provide outputs useful for assessing the responses of the plant to unlimited or limited water conditions. For instance, the link between a soil water balance and the plant component can be useful for evaluating the variability of the Fractional Transpirable Soil Water (FTSW) and its impact on the plant (Amir and Sinclair, 1991; Soltani and Sinclair, 2012). On these basis, some experiments found that the impact of water stress can be explained through empirical relationships that consider the effect of FTSW on leaf development, photosynthesis and transpiration rate (Bindi et al., 2005; Lebon et al., 2006; Pellegrino et al., 2006).

Soil nutrients limits

The most important soil nutrient for grapevine is nitrogen. Indeed, grapevine nitrogen content plays a key role in growth, yield and quality during the entire cycle. Several authors have studied the positive correlation between vegetative plant vigor and nitrogen content (Van Leeuwen et al., 2008) as well as the effect of nitrogen supply on final grapevine yield and quality (Delgado et al., 2004; Des Gachons et al., 2005; Hilbert et al., 2003). The limited soil nitrogen content influences negatively the grapevine nitrogen dynamics showing alterations of biomass partitioning with a favorable assimilates translocation towards storage organs (Grechi et al., 2007).

In order to evaluate the effect of nitrogen stress on vegetative growth and yield, several authors coupled the nitrogen balance to their grapevine simulation models (Brisson et al., 2009; Nendel and Kersebaum, 2004; Godwin et al., 2002; Wermelinger, B. and Baumgartner, 1991). Although, some models describe soil nitrogen dynamics using a high detail level and a great number of inputs (Brisson et

al., 2009, 1998), the poor availability of the inputs data for nitrogen models lead to develop simplified approach for estimating nitrogen dynamics (Nendel and Kersebaum, 2004). The evaluation of soil nitrogen dynamics and plant nitrogen content provides a useful information for farmers during the main agro-management practices (i.e. fertilization).

Finally, sub-models able to describe the dynamics of other macro-elements (Phosphorous and Potassium) and micro-elements are not easily coupled to grapevine simulation models. Accordingly, the effect of soil nutrient limits is generally explained in terms of lacking in nitrogen concentration.

1.4. Aim and outline of the research

The aim of this research is the implementation of a new grapevine simulation model for studying vine growth and development under different pedo-climatic conditions. The original model proposed by Bindi et al. (1997a, 1997b) is implemented considering different aspects:

- I. Phenology
- II. Extreme events effect
- III. Biomass partitioning
- IV. Water Balance
- V. Quality

The objective is to improve the accuracy and the reliability of model simulation as well as to provide a helpful tool for estimating grapevine yield and quality in different pedo-climatic conditions. Moreover, the introduction of the model in the BioMA software architecture (www.biomamodelling.org) allows to obtain a fine granularity of the model structure and to allow an easier maintenance and implementation.

In this context, **Chapter 2** describes the structure of the new grapevine simulation model library (UNIFI.GrapeML) showing the model working, the architecture, the new implementations and the links with the others software components. In this Chapter, a sensitivity analysis of the model is showed for evaluating the influences of the parameters on final fruit biomass while the calibration of phenology, soil water content and grapevine yield is performed in a specific case of study in northeastern of Spain.

Chapter 3 describes the implementation of the sugar content approach as strongly related to the water supply of the berries. The introduction of a quality approach is useful for evaluating the effect of climate change on high-quality wines over the most

famous wine-producing regions. The grape sugar content is calibrated and validated in Montalcino (Siena) study area over a long-term data of observed Sangiovese sugar content.

Finally, **Chapter 4** the phenological dynamics of very early, early, middle-early and late varieties are estimated under present and future climatic scenarios at European scale level. In this study, the use of different varieties allows to consider the responses of inter-varietal variability to the effect of the mean climate change. Furthermore, the extreme events effect (i.e. frost events and suboptimal temperature during flowering) is accounted through the strong relationship with the occurrence of the phenological dates in a changing climate.

Chapter 2

A model library to simulate grapevine growth and development



Chapter 2 has been based on the study: L. Leolini, S. Bregaglio, M. Moriondo, M.C. Ramos, M. Bindi, F. Ginaldi. A model library to simulate grapevine growth and development: software implementation, sensitivity analysis and field level application. (*submitted*). *European Journal of Agronomy*.

PhD candidate's contribution

Luisa Leolini, Fabrizio Ginaldi and Simone Bregaglio are the developers of the model library presented in this chapter. The authors jointly implemented, developed, explored the behaviour, and tested the component as stand-alone and in a modelling solution.

2. A model library to simulate grapevine growth and development: software implementation, sensitivity analysis and field level application

L. Leolini¹, S. Bregaglio², M. Moriondo³, M.C. Ramos⁴, M. Bindi¹, F. Ginaldi²

¹ DiSPAA, University of Florence, Piazzale delle Cascine 18, 50144 Florence, Italy.

² CREA - Council for Agricultural Research and Economics, Research Centre for Agriculture and Environment, via di Corticella 133, I-40128 Bologna, Italy

³ CNR-IBIMET, Via G. Caproni 8, 50145, Florence, Italy

⁴ Department of Environment and Soil Science, University of Lleida, Alcalde Rovira Roure, 191, E-25198, Lleida, Spain

Abstract

Simulation modelling applied to grapevine is a promising tool to unravel the tight interactions between agricultural management and pedo-climatic conditions, and their impact on yield variability. This is an urgent need in current conditions, and in light of climate change, which is expected to deeply affect the performances of vine cropping systems. Here we present a BioMA software component (UNIFI.GrapeML), which is a model library of grapevine physiological processes. We developed a new grapevine model considering the impact of soil water availability on yield, selecting a Spanish vineyard as a case study (Chardonnay variety). We inspected its behavior with sensitivity analysis techniques, to select the most relevant parameters to be calibrated to match reference data. The accuracy in reproducing phenology ($\bar{R}=0.58$), soil water content ($\bar{R}=0.70$) and yield ($R=0.59$) proved its capability to respond to weather variability, and the efficiency of BioMA software architecture in developing agricultural models.

Keywords

BioMA platform, Chardonnay, Latin Hypercube Sampling, simplex optimization, Sobol' total order, Vineyard.

Highlights

We present a new software library with models of grapevine physiological processes.

The adoption of BioMA platform facilitated the composition of a new grape model.

The library was coupled with sensitivity analysis and automatic optimization tools.

The comparison of simulated and reference field data led to a good model accuracy.

2.1. Introduction

Grapevine (*Vitis vinifera* L.) is the top cash crop worldwide (Williams and Ayars, 2005), being cultivated on 7.5 million hectares in 2015 (OIV, 2017) with a total production of nearly 75 Mt (FAOSTAT, 2016). The resulting global wine production remained quite stable under the 21st century, ranging between 257 Mhl in 2002 to 276 Mhl in 2015 (OIV, 2017), with the European Mediterranean region contributing to a quarter of total wine production, followed by South America (27.6 Mhl), United States (22.1 Mhl), Australia (12.0 Mhl), and China (11.2 Mhl).

The qualitative and quantitative performances of grapevine production systems are known to be largely affected by the complex interactions between environmental drivers (Seguin, 1988; Jones et al., 2005; Ramos et al., 2008), grapevine varieties (Lavee and May, 1997; Huglin and Schneider, 1998) and soil conditions (Seguin, 1986; Van Leeuwen and Seguin, 1994), including water and nutrients dynamics (Costantini and Bucelli, 2014). The evidence of global warming is thus posing a concrete threat to the economy of the three top producing countries - Italy, France and Spain – as their uppermost wine regions are placed in very sensitive areas to climate change (Gao and Giorgi, 2008), whose impacts are expected to vary even at low spatial resolution (Gao et al., 2006).

Available studies indeed evidenced the impacts of climate change on vine development, yield and quality (Jones and Davis, 2000; Jones et al., 2005; Hannah et al., 2013; Moriondo et al., 2013). The beneficial effects on photosynthesis due to the increase of CO₂ concentration (Bindi et al., 2001b; Moutinho-Pereira et al., 2006; Salazar-Parra et al., 2012a, 2012b) are expected to be counterbalanced by the negative impacts of rising temperatures and perturbed precipitation patterns, even in the short-term future. The length of grapevine cycle is expected to be further shortened in Australia (Webb et al., 2007), whereas an advancement of vine harvest date has been already recorded in Mediterranean wine regions in the last 30-50 years (Jones and Davis, 2000). The combination of a shorter cycle with the occurrence of heat stress during and after fruit-set phase has been associated with a decrease of berries growth, leading to the end of sugar accumulation (Greer and Weston, 2010), up to their abscission (Kliewer, 1977).

The associated impacts on wine quality in Australian viticulture were quantified by Webb et al. (2008) in the range -7% ÷ -39% and to -9% ÷ -76% in the short- (2030) and medium- (2070) term, respectively. The advancement of budbreak date could also increase the risk of frost events in early spring (Mullins et al., 1992; Narciso et al., 1992), leading to shoot damages and yield losses. This phenomenon has been already documented in outstanding wine regions as the French Champagne (Brun and Cellier, 1992) and the Luxembourgish (Molitor et al., 2014). The changing pattern of rainfall

distribution during the vine cycle is also expected to contribute increasing the year-to-year yield variability. Prolonged water stress reduces stomatal conductance, net CO₂ assimilation and leaf transpiration (Medrano et al., 2003), whereas moderate stressful conditions during berry ripening may have beneficial effects on grape yield and quality (Ojeda et al., 2002; Chaves et al., 2007, 2010; Van Leeuwen et al., 2009).

Despite the recognized limitations of current process-based crop models (Rötter et al., 2011; Asseng et al., 2013), they are considered as the only viable mean to obtain reliable projections of crop yield in response to climate variability (Bannayan and Crout, 1999), as they can deal with the non-linear interactions between environmental drivers and plant physiology, also considering the impacts of management practices (Donatelli et al., 2006; Therond et al., 2011). Their adoption in viticulture was recently reviewed by Moriondo et al. (2015), who highlighted that available models (e.g., Wermelinger and Baumgartner, 1991; Bindi et al., 1997a, b; Godwin et al., 2002; Nendel and Kersebaum, 2004; Pallas et al., 2011; Cola et al., 2014) share a limited set of modelling approaches for the simulation of the main vine physiological processes, i.e., development, biomass accumulation, biomass partitioning, gas exchange, and fruit quality. Differently from field crop simulators, which are increasingly used in model ensembles to evaluate their accuracy and to identify areas of improvement (e.g. maize, Bassu et al., 2014; rice, Li et al., 2015; wheat, Martre et al., 2015), no model comparison studies were performed on grapevine, thus limiting our understanding of models' limits and performances.

Here we present a software library, UNIFI.GrapeML, implementing a set of modelling approaches for the simulation of the main physiological processes related to grapevine growth and development. We used the BioMA software architecture (www.biomamodelling.org), which adopts the component-oriented programming to develop software units which can be shared among the modellers community and extensible with new/alternate approaches (e.g., Cappelli et al., 2014; Stella et al., 2014; Donatelli et al., 2014; Bregaglio and Donatelli, 2015). We then developed a new grapevine simulator using UNIFI.GrapeML, and we coupled it with a soil water model to release a modelling solution reproducing vine growth and development as affected by water stress. We finally demonstrated the capability of this BioMA modelling solution to be interfaced with platform specific sensitivity analysis and automatic optimization tools, using an experimental dataset collected on a Spanish grapevine orchard (1998-2012, Chardonnay variety) as a case study.

2.2. Materials and Methods

	Activity	Objective	BioMA tools
Step A	Development of the UNIFI.GrapeML software component	Release of a software library with models for vine development and growth	Domain Class Coder (DCC) API Class Coder (ACC) Strategy Class Coder (SCC)
Step B	Coupling UNIFI.GrapeML with models for soil water uptake and redistribution	Release of a new grapevine model to reproduce the impact of soil water availability on vine growth and yield	Composition Layer Interactive Coder (CLIC)
Step C	Calibration of the phenological development using field observations (multi-start simplex method)	Adjustment of the simulation of the main phenological stages before running the sensitivity analysis	Optimizer, automatic calibration tool
Step D	Sensitivity analysis with the Latin Hypercube Sampling method	Screening of the most relevant parameters in influencing simulated fruit biomass variability	Library User Interface for Sensitivity Analysis (LUISA)
Step E	Sensitivity analysis with the Sobol' Total Variance method	Identification of the subset of parameters to be automatically calibrated	Library User Interface for Sensitivity Analysis (LUISA)
Step F	Calibration of the fruit biomass accumulation using field observations (multi-start simplex method)	Demonstrate the capability of the modelling solution to simulate the year-to-year yield variability	Optimizer, automatic calibration tool

Figure 2.1. Workflow of the activities presented in this study, with relevant objectives and BioMA tools, downloadable at www.biomamodelling.org.

Fig. 2.1 presents the activities performed in this study, with a reference to the BioMA tools used for code generation and model analysis. After the development of the UNIFI.GrapeML software library (Step A, section 2.2.1 and 2.2.2), we developed a new model using available approaches for the reproduction of grapevine morpho-physiological processes. We then coupled it with a set of models to simulate crop water uptake and soil water redistribution in the soil profile (Step B, section 2.2.3, Modelling solution).

The parameters of this modelling solution were calibrated to reproduce observed phenological development in an experimental vine orchard in 1998-2012 (Step C, section 2.2.3, Experimental reference dataset). This activity laid the basis for a two-step global sensitivity analysis: at first, a screening method (i.e., Latin Hypercube Sampling) was applied on all the parameters of the modelling solution (Step D, section 2.2.3, Sensitivity analysis experiment); then the sub-set of the most important parameters was further inspected using a variance based method (Sobol' Total Variance, Step E, section 2.2.3, Sensitivity analysis experiment). Using the information coming from the sensitivity analysis, an automatic calibration allowed to increase the accuracy of the modelling solution in reproducing the reference soil water content and yield data (Step F, section 2.2.3, Calibration and evaluation of the modelling solution).

2.2.1. Component architecture

UNIFI.GrapeML is a BioMA component collecting models of the main physiological processes of grapevine. The definition of the input/output (I/O) data structures (UNIFI.GrapeML.Interfaces) is separated from the modelling approaches which use them (UNIFI.GrapeML.Strategies), according to an implementation of the Bridge pattern (Fig. 2.2, Del Furia et al., 1995), in order to let third parties to extend and re-use the modelling domain in custom applications.

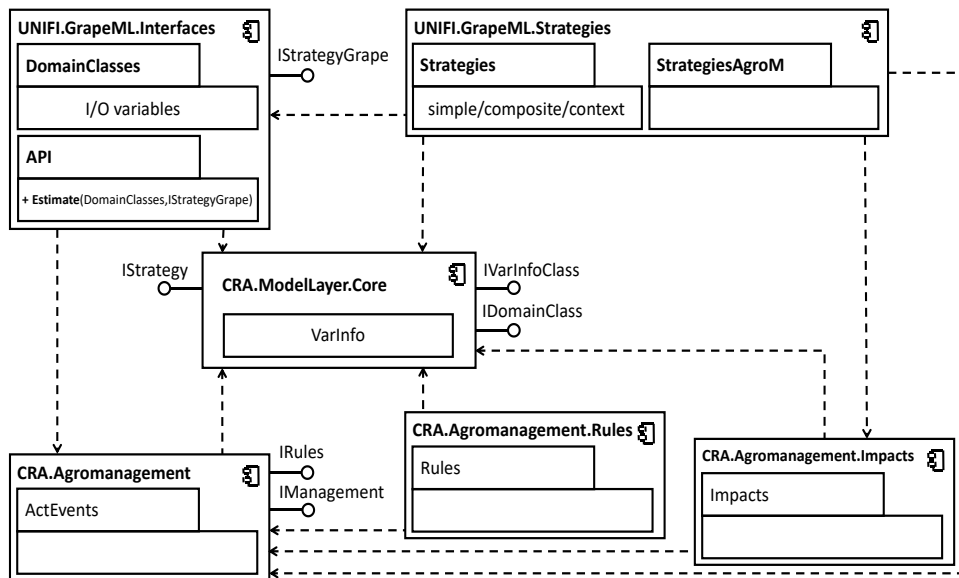


Figure 2.2. Unified Modelling Language (UML) component diagram of the UNIFI.GrapeML component. Software units (*UNIFI.GrapeML.Interfaces* and *UNIFI.GrapeML.Strategies*) have a dependency (arrow dotted line) to *CRA.Core.ModelLayer* and *CRA.AgroManagement* component, belonging to the core of the BioMA framework.

I/O variables are collected in domain classes, according to the ontology proposed by Forrester (1961) for system dynamics. The domain classes of UNIFI.GrapeML are States (states variables, e.g., leaf area index, grape aboveground biomass), Rates (rates variables, e.g., rate of change of leaf area index), Auxiliary (intermediate derived variables, e.g., bud-break date), Exogenous (driving variables, e.g., air maximum and minimum temperature) and ExternalStates (external state variables, e.g., soil water and nitrogen content). The *CRA.ModelLayer.Core* component, from which UNIFI.GrapeML depends, provides methods to perform quality check of input (preconditions) and output (post-conditions) variables and model parameters,

according to their ontology (minimum, maximum and default value, unit, type, and description).

Models are implemented in UNIFI.GrapeML.Strategies as *simple strategies* (e.g. ShootLeafNumber and LeafAreaGrowth, Fig. 2.3), which are units of code (C# classes) isolating an algorithm for a specific morpho-physiological process of grapevine. *Composite strategies* (e.g., LeafAreaIndex, Fig. 2.3) allow to compose simple strategies into higher-level models to represent part-whole hierarchies, while keeping the same programming interface. Available *composite strategies* refer to plant macro-processes as phenological development, evapotranspiration, leaf growth and biomass accumulation, biomass partitioning, extreme events affecting fruit biomass. *Context strategies* (Strategy design pattern, e.g., Phenology, Fig. 2.3) are used to switch between *simple* or *composite strategies* presenting alternative modelling approaches for the same process (e.g., chilling-forcing (CF) unit or growing degree days (GDD) to simulate vine development) or to user choices (e.g., activation of extreme events in limiting fruit set).

2.2.2. Models description

The workflow of the *strategies* currently implemented in UNIFI.GrapeML is showed in Fig. 2.3. Phenological development starts with the accumulation of chilling units from a user-defined day of the year and continues until the end of the endodormancy period. Afterwards, forcing units are accumulated until bud-break (**Phenological development Section**). Then, leaf appearance and expansion on shoots are simulated to derive the total plant leaf area and the leaf area index (**Leaf Area Growth Section**). The emission of leaf area index triggers the light interception, which is converted into biomass, using a radiation use efficiency (RUE) approach. The daily value of RUE is modulated according to CO₂ concentrations and as a function of air temperature (Ritchie and Otter, 1984; Van Keulen and Seligman, 1987; **Light interception and biomass accumulation Section**). The daily growth rate of aboveground biomass is entirely allocated into vegetative organs from bud-break to flowering, whereas it is partitioned to fruits during flowering-harvest period according to user-defined coefficients. The fruit biomass is thus reduced according to the fruit-set index based on the effect of high or low temperatures around flowering (**Extreme event impact and Biomass partitioning Section**).

A water stress index (Fractional Transpirable Soil Water, FTSW, 0-1), computed as the ratio between the Available Transpirable Soil Water in the rooted zone (ATSW) and the Total Transpirable Soil Water (TTSW) acts reducing the leaf development and transpiration (Bindi et al., 2005; **Evapotranspiration Section**) and stimulating root elongation (Bota et al., 2004; Dry et al., 2000b).

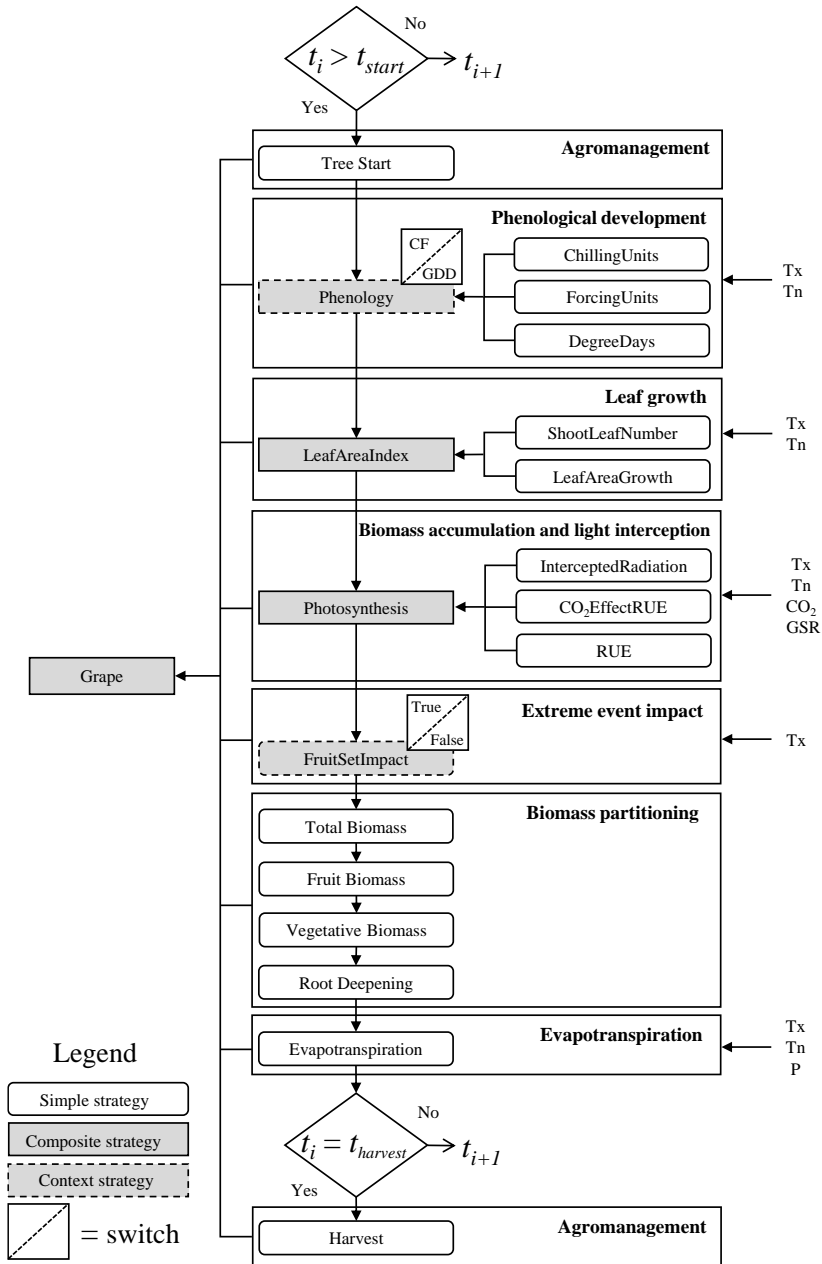


Figure 2.3. Workflow of the strategies currently implemented in UNIFI.GrapeML. The scheme presents the logical order in which models are called during a daily time step. T_x = daily maximum air temperature ($^{\circ}\text{C}$), T_n = daily minimum air temperature ($^{\circ}\text{C}$), P = precipitation (mm), GSR = global solar radiation (MJ m^{-2}), CF = Chilling-Forcing, GDD = Growing Degree Days.

Phenological development

Chilling-forcing method

A parallel CF approach (Caffarra and Eccel, 2010) is available in UNIFI.GrapeML. The dormancy period until bud-break date is simulated considering the accumulation of chilling and forcing units. The chilling units accumulation starts at the end of the previous growing season and ends when a chilling requirement threshold is reached, then the accumulation of thermal units (forcing units) begins. The effect of chilling accumulation on forcing units decreases from the first day of chilling accumulation up to the day when the effect of chilling temperature on forcing units ends (Table 2.1, Eq. 2.1, 2.2, 2.3). Bud-break is reached when both chilling and forcing requirements are satisfied. The subsequent estimation of flowering, veraison, and maturity dates is performed using three sigmoidal curve of forcing accumulation and defined by three thresholds of forcing requirement (Table 2.1, Eq. 2.4, 2.5, 2.6).

Table 2.1. Equations of the CF method to simulate phenological development in the four main phenological stages of grapevine (Caffarra and Eccel, 2010).

Phenological phases	Equations	
Budbreak	$ChillingUnit = \sum \frac{2}{1 + e^{aParam(T_{avg} - cParam)^2}}$	Eq. 2.1
	$ForcingBudbreak = \sum \frac{1}{1 + e^{-db(T_{avg} - eb)}}$	Eq. 2.2
	$ForcingCritic = Col \cdot e^{co2 \cdot ChillingUnitState}$	Eq. 2.3
Flowering	$ForcingFlowering = \sum \frac{1}{1 + e^{-df(T_{avg} - ef)}}$	Eq. 2.4
Veraison	$ForcingVeraison = \sum \frac{1}{1 + e^{-dv(T_{avg} - ev)}}$	Eq. 2.5
Maturity	$ForcingMaturity = \sum \frac{1}{1 + e^{-dm(T_{avg} - em)}}$	Eq. 2.6

$aParam, Col, co2$ =curve shape parameters; $cParam$ = optimum chilling temperature; T_{avg} = daily average temperature; db, df, dv, dm = forcing units rates and eb, ef, ev, em = optimum forcing temperatures.

Growing degree days approach

UNIFI.GrapeML provides an alternative model for phenological development, based on the accumulation of growing degree days (GDD, °C d⁻¹, Bindi et al., 1997a).

GDD are accumulated starting from a user-defined day of the year until the fulfillment of the thermal requirement for budbreak (Eq. 2.7).

$$GDD = \sum_{t_0}^{t_1} T_{avg} - BaseTemperature \quad \text{Eq. 2.7}$$

where T_{avg} is the daily average temperature (°C), t_0 is the starting point for GDD accumulation, t_1 is the phenological phase (bud-break, flowering, veraison, and maturity) and $BaseTemperature$ (°C) is the minimum temperature for GDD accumulation. Then, GDD are computed until flowering, when a minimum number of leaves (model parameter) is used to trigger flowering stage. GDD accumulation is also computed for the lag phase when berry weight does not increase; then, the veraison stage is triggered and GDD are accumulated until the maturity stage.

Leaf growth

Leaf area growth is simulated as a function of leaf appearance and expansion on the actively growing shoots (Bindi et al., 1997; Eq. 2.8, 2.9, 2.10).

$$LeafNumberRate = (SLNI + LAR1 \cdot T_{avg}) \cdot (1 + LAR2 \cdot ShootLeafNumber) \quad \text{Eq. 2.8}$$

$$LeafNumberRate = LeafNumberRate * (1 / (1 + SLN1 \cdot e^{(-SLN2 \cdot FTSW)})) \quad \text{Eq. 2.9}$$

$$ShootLeafNumberStress = ShootLeafNumberStress + LeafNumberRate \quad \text{Eq. 2.10}$$

where $LeafNumberRate$ is the daily rate of leaf appearance (number leaves d⁻¹), $SLNI$ ($ShootLeafNumberIntercept$, unitless, default value -0.28), $LAR1$ ($LeafAppearanceRate1$, unitless, default 0.04) and $LAR2$ ($LeafAppearanceRate2$, unitless, default 0.015) are curve shape parameters, $SLN1$ (unitless, default, 25.9) and $SLN2$ (unitless, default, 17.3) are the parameters of water stress impact on $LeafNumberRate$, and $ShootLeafNumberStress$ is the number of leaves appeared on the shoot considering the water stress effect on leaf development (unitless; Bindi et al., 2005). The total leaf area per shoot ($ShootLeafArea$, cm²; Eq. 2.11) and plant leaf area ($PlantLeafArea$, cm²; Eq. 2.12) are finally computed during season progress considering the number of shoot per plant.

$$ShootLeafArea = SLAS \cdot (ShootLeafNumberStress)^{SLAE} \quad \text{Eq. 2.11}$$

$$PlantLeafArea = ShootLeafArea \cdot ShootNumber \quad \text{Eq. 2.12}$$

where $SLAS$ ($ShootLeafAreaSlope$, unitless, default value 5.39) and $SLAE$ ($ShootLeafAreaExponential$, unitless, default value 2.13) are curve shape parameters and $ShootNumber$ is the number of shoots per plant. Finally, $LeafAreaIndex$ (m² m⁻²;

Eq. 2.13) is computed considering the soil occupied by the plant (*PlantArea*, m²) and the proportion of the area shaded by plant (*ProportionShadedArea*, unitless).

$$LeafAreaIndex = (PlantLeafArea/10000)/(ProportionShadedArea \cdot PlantArea) \text{ Eq. 2.13}$$

2.13

Light interception and biomass accumulation

Biomass accumulation is simulated considering the radiation intercepted by the canopy and the radiation use efficiency (RUE, g MJ⁻¹) affected by air temperature and CO₂ concentration. The fraction of radiation intercepted (*RadIntercepted*, 0-1, unitless, Eq. 2.14) is calculated using the Beer-Lambert law (Vose et al., 1995), considering the *LeafAreaIndex* (m² m⁻²) and the crop extinction coefficient (*CropCoeff*, unitless).

$$RadIntercepted = 1 - e^{(-CropCoeff \cdot LeafAreaIndex)} \text{ Eq. 2.14}$$

RUE (g MJ⁻¹, Eq. 2.15) represents the effective biomass accumulated per unit of global solar radiation, modulated by the effect of temperature. It is calculated according to an initial value dependent by CO₂ concentration in the atmosphere and a temperature based function.

$$RUE = RUE_{max} \cdot (1 - (0.0025 \cdot ((0.25 \cdot T_n + 0.75 \cdot T_x - 25)^2))) \text{ Eq. 2.15}$$

Where *RUEmax* is the initial RUE that assumes different values depending on CO₂ concentration thresholds of 350, 550 and 700 ppm (Eq. 2.16, 2.17, 2.18), *T_x* is the daily maximum temperature and *T_n* is the daily minimum temperature. Accordingly,

If CO₂ is equal to 350 ppm:

$$RUE_{max} = InitialRUE \text{ Eq. 2.16}$$

Where *InitialRUE* is equal to 1.001 g MJ⁻¹.

If CO₂ >350 ppm and CO₂ ≤ 550 ppm:

$$RUE_{max} = mRUE550 \cdot CO_2 + qRUE550 \text{ Eq. 2.17}$$

While if CO₂ >550 ppm and CO₂ ≤ 700 ppm:

$$RUE_{max} = mRUE700 \cdot CO_2 + qRUE700 \text{ Eq. 2.18}$$

where CO₂ is the atmosphere CO₂ concentration (ppm), *mRUE550* (0.00105 g MJ⁻¹ ppm⁻¹), *qRUE550* (0.633 g MJ⁻¹ ppm⁻¹), *mRUE700* (0.000468 g MJ⁻¹ ppm⁻¹), and *qRUE700* (0.954 g MJ⁻¹ ppm⁻¹) are empirical parameters for the linear increase of

RUE_{max} (g MJ⁻¹) according to different CO₂ concentration thresholds. Finally, the daily photosynthesis rate of the plant (g m⁻² day⁻¹; Eq. 2.19) is calculated taking into account the effect of GSR (MJ m⁻²), $RadIntercepted$, $ProportionShadedArea$, and the water stress effect (unitless) on the daily photosynthesis rate ($PhotoRate$, g m⁻² day⁻¹).

$$PhotoRate = Radiation \cdot RadIntercepted \cdot ProportionShadedArea \cdot RUE_{max} \cdot (1 / (1 + PHO1 \cdot e^{(-PHO2 \cdot FT_{SW})})) \quad \text{Eq. 2.19}$$

Extreme event impact

The impact of extreme events on fruit set is simulated according to a fruit-set index ($FruitSetIndex$, unitless, Eq. 2.19), considering the impact of the 7-days average maximum temperatures around flowering stage.

$FruitSetIndex$ (0, minimum, to 1, maximum) is modulated as the temperature factor function such as described after Farquhar and Caemmerer (1982) for photosynthesis (Eq. 2.20):

$$FruitSetIndex = \left(\frac{T - T_{min}}{T_{opt} - T_{min}} \right)^q \cdot \left(\frac{T_{max} - T}{T_{max} - T_{opt}} \right) \quad \text{Eq. 2.20}$$

where T is the daily average maximum air temperature (°C), T_{max} , T_{opt} and T_{min} (°C) are the maximum, optimum and minimum temperature for optimal fruit-set and q (unitless) is a curve shape parameter.

Biomass partitioning

The $TotalBiomass$ ($TotBio$, g m⁻², Eq. 2.21) represents the total aboveground biomass at day⁻¹, computed as the daily accumulation of photosynthesis rate (Eq. 2.19).

$$TotBio = TotBio + PhotoRate \quad \text{Eq. 2.21}$$

The partitioning of total biomass among vegetative and fruit biomass is driven by phenological phases. Before flowering ($TriggerBudbreak = 1$ and $TriggerFlowering = 0$), the daily rate of aboveground biomass is partitioned to the vegetative pool ($VegetativeBiomass$, $VegBio$, g m⁻² day⁻¹, Eq. 2.22, 2.24) whereas $FruitBiomass$ ($FruBio$, g m⁻² day⁻¹, Eq. 2.23) is computed using a linear relationship between total biomass and a daily increase of harvest index. The $FruBio$ is affected by the value of $FruitSetIndex$ estimated after flowering.

If $TriggerBudbreak > 0$ and $TriggerFlowering < 1$:

$$VegBio = TotBio \quad \text{Eq. 2.22}$$

If $TriggerFlowering > 0$:

$$FruBio = TotBio \cdot HarvestIndex \cdot FruitSetIndex \quad \text{Eq. 2.23}$$

$$VegBio = TotBio - FruBio \quad \text{Eq. 2.24}$$

Finally, the biomass partitioned to the root system is computed in terms of root deepening into the soil. According to Nendel and Kersebaum (2004), a vineyard when reaches maturity stage showed a very low root growth rate. However, Dry et al. (2000b) demonstrated that low water availability stimulates root growth increase. In UNIFI.GrapeML, the root elongation ($RootDepthRate$, cm day⁻¹, Eq. 2.25, 2.26) in wet conditions is driven by $RootGrowthBasic$ (0.001, cm day⁻¹), while in water stress conditions ($FTSWLimitRoot=0.5$ and $DayForStress=2$) the increased root growth rate is computed as $RootGrowthStress$ (0.05, cm day⁻¹).

If $FTSW > FTSWLimitRoot$:

$$RootDepthRate = RootGrowthBasic \quad \text{Eq. 2.25}$$

If $FTSW < FTSWLimitRoot$ and $DayCountStress > DayForStress$:

$$RootDepthRate = RootGrowthStress \cdot (1 - FTSW)$$

Eq. 2.26

Evapotranspiration

Crop transpiration is estimated considering the $PhotoRate$ (g m⁻² day⁻¹), the air vapor pressure deficit (VPD , kPa) and the water use efficiency (WUE , Pa), that represents the biomass accumulated per gram of water transpired by the plant (Eq. 2.27).

$$TranspirationRate = (PhotoRate \cdot VPD) / (WUE) \quad \text{Eq. 2.27}$$

The $TranspirationRate$ of the previous equation is expressed in mm day⁻¹ then it is converted in cm day⁻¹.

Moreover, the evaporation rate is calculated considering the intercepted radiation by the plant, the air and the slope of the saturated curve versus temperature as shown in (Amir and Sinclair, 1991; Soltani and Sinclair, 2012; Eq. 2.28 and 2.29).

$$Delta = e \left(\left(21.255 - \frac{5304}{(273 + T_{avg})} \right) - \frac{5304}{(273 + T_{avg})^2} \right) \quad \text{Eq. 2.28}$$

$$EvaporationRate = (GSR \cdot 0.25 + GSR \cdot 0.75 \cdot RadIntercepted \cdot Delta + 0.68 \cdot 0.4 \cdot VPD) / (Delta + 0.68) \quad \text{Eq. 2.29}$$

where T_{avg} is the daily average temperature, GSR is the global solar radiation, $RadIntercepted$ the intercepted radiation and $Delta$ ($mbar \text{ } ^\circ K^{-1}$) is the slope of the saturated vapor pressure deficit curve.

Then, potential evaporation is, in turn, converted in actual evaporation decreasing its value as a function of the elapsed days ($LastDayRain$) since last rainfall event (Amir and Sinclair, 1991 and Soltani and Sinclair, 2012; Eq. 2.30):

$$EvaporationRate = EvaporationRate \cdot (\sqrt{LastDayRain + 1} - \sqrt{LastDayRain}) \quad \text{Eq. 2.30}$$

The $EvaporationRate$ of the previous equation is expressed in $mm \text{ day}^{-1}$ using the same approach of Amir and Sinclair (1991) and Soltani and Sinclair (2012).

2.2.3 Case study

Modelling solution development

The *strategies* implemented in UNIFI.GrapeML were composed to give a new grapevine model simulating the whole processes connected to growth and development, represented by the *composite strategy* Grape in Fig. 2.3. The model was then coupled with the two components: UNIMI.SoilW (Donatelli et al., 2014), collecting models to simulate crop water uptake and redistribution in the soil profile, and CRA.AgroManagement (Donatelli et al., 2006), which handles the implementation of agricultural management events. The resulting modelling solution (MS, Fig. S.2.1) was developed with the software CLIC (Composition Layer Interactive Coder, www.biomamodelling.org) and interfaced with a generic weather and soil data provider. The MS can be re-used both as stand-alone unit and in BioMA-type applications (i.e., BioMA-Site, BioMA-Spatial, www.biomamodelling.org).

The soil profile was split into ten layers (1st layer = 0.03 m, 2nd layer = 0.07 m, 3rd-10th layer = 0.1 m) and soil water redistribution was simulated with a tipping-bucket approach (Ritchie, 1998), assuming that water can move to the (i+1)-th layer when field capacity of the i-th layer is exceeded. The root depth simulated by UNIFI.GrapeML is used as input to compute crop water uptake, which considers crop potential transpiration as the plant demand, according to the EPIC model (Williams et al., 1989).

Soil evaporation was derived by daily evapotranspiration considering the fraction of light intercepted by the canopy (Ritchie, 1974), setting an evaporation layer of 0.1 m. The minimum and maximum soil water content in each layer were set to wilting point and field capacity, respectively, both derived by pedo-transfer functions from soil texture. The interception of precipitation by the canopy was computed according to Von Hoyningen-Huene (1981), with the remaining quote infiltrating into the soil.

CRA.AgroManagement is a software component to simulate the timing and the effects of management events in an agricultural simulation model (Donatelli et al., 2006). It formalizes the decision making process via the rule-impact approach: a management action requires that a set of conditions based on the state of the system (a "rule") is met to be applied. When it happens, a management action is triggered. This approach allows de-coupling the agro-management operations from biophysical models. In this study, we used it to set the starting the day of year (244) for chilling units accumulation and the end of the grape growing season (305), respectively.

Experimental reference dataset

We selected a vineyard located about 40 km Northwest (NW) of Barcelona in the Catalan Prelitoral Depression (lat. 41.531 N, long. 1.769 E, 340 m. a.s.l., Penedès Depression) as the location of our case study. This area has a long tradition of vine cultivation within the Designation of Origen Penedès, with vines representing about 80% of the cultivated land (IDESCAT, 2013). The climate is Mediterranean, with average maximum (T_x) and minimum (T_n) air temperature in 1998-2012 during budbreak-flowering equal to 19.7 °C (SD = 1.3 °C) and 8.9 °C (SD = 0.8 °C), respectively, whereas during veraison-harvest period equal to 30.3 (T_x , SD = 1.7°C) and 18.7 (T_n , SD = 1.7°C). Precipitation are mainly concentrated in spring and autumn, with average cumulated values of 118.8±71.2 mm, and then decrease during veraison-harvest phase (cumulated values = 39.9±17.7, Table 2.2). The soil of the experimental vineyard is Typic Xerorthents and Fluventic Haploxerepts (Soil map of the Penedès, DAR, 2008), with soil depth ranging from 0.8 to 1.5 m. Soil particle distribution (Gee and Bauder, 1986) and organic matter content (Allison, 1965) were evaluated in samples collected at three locations (up, mid and down slope). The soil texture is loam, with bulk density equal to 1.5 g cm⁻³, and organic matter = 1.3 % (Ramos and Martínez-Casasnovas, 2014).

Trained vines of Chardonnay variety (3.1 m × 1.3 m, 16 nodes per vine) were planted after land levelling in 1989. The vineyard is orientated NNE-WSW, with 7% average slope. Phenological observations in 1998-2012 were available at budbreak (BBCH code 5), flowering (BBCH code 57), veraison (BBCH code 81) and harvest. Grapevine fresh yield (t ha⁻¹) in 1998-2010 was provided by the farmer, whereas in 2011-2012 the yield of 15 plants was sampled (Ramos and Martínez-Casasnovas, 2014). Dry fruit biomass was derived as the 23% of total berry fresh weight (García de Cortázar-Atauri et al., 2009b; Girona et al., 2009). Soil water content was measured in two cropping seasons (2011-2012) at four soil depths (0.3 m; 0.5 m; 0.7 m; 1 m), using soil moisture probes (Time Domain Reflectometry, TDR). Daily meteorological data as input for the models were obtained from a weather station placed in close proximity to the orchard. (Els Hostalest de Pierola, 41.531 N; 1.808 E; 316 m a.s.l.). Available variables were maximum and minimum temperature, precipitation and

wind speed in the period 1997-2012 (Table 2.2 and Table S.2.1). Global solar radiation was estimated using the Hargreaves method (Hargreaves and Samani, 1982), reference evapotranspiration via Penman-Monteith equation (Monteith, 1965).

Table 2.2. Average and standard deviations of maximum (T_x) and minimum (T_n) air temperatures, cumulated precipitation ($Prec$) and evapotranspiration (ET_0) in the grapevine growing seasons (1998-2012) in the study area.

Meteorological variables	Unit	Budbreak-Flowering	Flowering-Veraison	Veraison-Maturity
T_x	°C	19.7±1.3	27.6±1.4	30.3±1.7
T_n	°C	8.9±0.8	15.8±0.9	18.7±1.03
$Prec$	mm	118.8±71.2	65.8±51.1	39.9±17.7
ET_0	mm	296.5±47.4	413.6±76.3	241.9±56.7

Sensitivity analysis experiment

The modelling solution presented in **Modelling solution development Section** was interfaced with a library of methods for model sensitivity analysis, LUISA (Library User Interface for Sensitivity Analysis, Donatelli et al., 2009, available at www.biomamodelling.org), to evaluate the contribution of model parameters and of their interaction on the variability of simulated grapevine yield at harvest.

A two-step global sensitivity analysis was performed (Saltelli et al., 1995, 1999; Confalonieri et al., 2010). A screening regression method (Latin Hypercube Sampling, LHS, McKay et al., 1979) was used to select the most relevant parameters of the modelling solution at a low computational cost (Table 2.3). In the second step, the subset of parameters explaining most output variability was evaluated with the Sobol' variance-based method, to decompose it into fractions to be attributed to each parameter or sets of parameters.

The LHS regression method independently and randomly sample each parameter without replacement, to give a matrix of X rows (number of simulations) and n columns (number of varied parameters). The modelling solution was iteratively run using each combination of parameter values, and grapevine yield was recorded after each simulation. The non-parametric Spearman correlation between each parameter under evaluation and model output was then computed, as suggested for biophysical models by Zacharias et al. (1996) and Bellocchi et al. (2010). This screening method was applied for each cropping season in the period 1998-2012, in order to quantify the variation of model sensitivity to parameters change under varying weather conditions. The model parameters related to phenological development were excluded from the sensitivity analysis, as they were calibrated to match reference data (see

Calibration and evaluation of the modelling solution Section). Model parameters were sampled from a uniform distribution ranging from -15% to +15% of default values (Table 2.3). The LHS method was run with a shuffle seed of 1234567, by setting the convergence to 0.025 (i.e., the maximum average difference of Spearman correlations between model parameters and grapevine yield in consecutive evaluations). The convergence was firstly evaluated after 6000 runs, and then every 1000 runs.

The parameters with average Spearman's correlation higher than 0.1 ± 0.025 in the 15 years were then investigated with the Sobol' method. This method, recognized as a standard in global sensitivity analysis applied to biophysical simulation models (Varella et al., 2010; Stella et al., 2014), highlights the portion of the total variance explained by the contribution of the single parameters, or even including parameters interactions (Tang et al., 2007). This second step of sensitivity analysis was performed with the same settings for model parameters values and for input weather data used by the LHS method. Convergence was expressed as the maximum difference of Sobol' Total Order index in two consecutive runs and set to 0.01, with a first check after 85000 runs, and then testing it every 17000 runs.

Table 2.3. Acronyms, description, default value and unit of the model parameters evaluated via sensitivity analysis, with relevant source of information. CU =Chilling Units, FU=Forcing Units, SLN= Shoot Leaf Number, SLA= Shoot Leaf Area, WS= Water Stress.

Parameter	Description	Min	Max	Default	Unit
Phenological development					
aParam	Curve shape parameter	0.002	0.008	0.005 ^a	unitless
cParam	Optimal chilling temperature	1.12	4.48	2.8 ^{a,b,c,d,e}	°C
ChillingReq	Chilling requirement	31.48	125.91	78.692 ^a	CU
db	Slope of forcing unit eq. (budbreak)	-0.42	-0.11	-0.26 ^a	unitless
df	Slope of forcing unit eq. (flowering)	-0.42	-0.11	-0.26 ^a	unitless
dv	Slope of forcing unit eq. (veraison)	-0.42	-0.11	-0.26 ^a	unitless
dm	Slope of forcing unit eq. (maturity)	-0.42	-0.11	-0.26 ^a	unitless
eb	Base forcing temperature (budbreak)	6.41	25.70	16.06 ^a	°C
ef	Base forcing temperature (flowering)	6.41	25.70	16.06 ^a	°C
ev	Base forcing temperature (veraison)	6.41	25.70	16.06 ^a	°C
em	Base forcing temperature (maturity)	6.41	25.70	16.06 ^a	°C
Col	Curve shape parameter	70.50	282.02	176.26 ^a	unitless
co2	Curve shape parameter	-0.024	-0.006	-0.015 ^a	unitless
LimitForcingReq	Last day of CU effect on forcing req.	94	374	234 ^a	day
FloweringReq	Forcing requirement for flowering	9.88	39.54	24.71 ^{a,b,d,e}	FU
VeraisonReq	Forcing requirement for veraison	20.46	81.82	51.146 ^{a,b,d,e}	FU
MaturityReq	Forcing requirement for maturity	-	-	-	FU
Leaf growth					
ShootNumber	Number of shoots per plant	13.6	18.4	16 ⁱ	Number
ShootLeafNumberIntercept	Curve shape param. of SLN eq.	-0.32	-0.24	-0.28 ^f	unitless
LeafAppearanceRate1	Curve shape param. of SLN eq.	0.03	0.05	0.04 ^f	unitless
LeafAppearanceRate2	Curve shape param. of SLN eq.	-0.017	-0.013	-0.015 ^f	unitless
ShootLeafAreaSlope	Curve shape param. of SLA eq.	4.58	6.2	5.39 ^h	unitless
ShootLeafAreaExp	Curve shape param. of SLA eq.	1.81	2.45	2.13 ^f	unitless
ProportionShadedArea	Proportion of the area shaded by plant	0.64	0.86	0.75 ^f	unitless
PlantingDensity	Squared meters of soil per plant	3.4	4.6	4 ⁱ	m ² plant ⁻¹
SLN1	Coeff. of WS eq. on leaf develop.	22.09	29.80	25.9 ^{j,k}	unitless
SLN2	Coeff. of WS eq. on leaf develop.	14.71	19.90	17.3 ^{j,k}	unitless
Light interception and biomass accumulation					
CropCoeff	Extinction coefficient for RadIntercept	0.51	0.69	0.6 ⁱ	unitless
InitialRUE	Initial RUE at 350 ppm of CO ₂	0.85	1.15	1.001 ^f	g MJ ⁻¹
qRUE550	Intercept of the CO ₂ 550 ppm eq.	0.54	0.73	0.633 ^m	g MJ ⁻¹
mRUE550	Coeff. of the CO ₂ 550 ppm eq.	0.00089	0.0012	0.00105 ^m	g MJ ⁻¹ ppm ⁻¹
PHO1	Coeff. for WS effect on photosyn.	10.97	14.84	12.9 ^{j,k}	unitless
PHO2	Coeff. for WS effect on photosyn.	11.99	16.22	14.1 ^{j,k}	unitless
qRUE700	Intercept of the CO ₂ 700 ppm eq.	0.81	1.09	0.954 ^m	g MJ ⁻¹
mRUE700	Coeff. of the CO ₂ 700 ppm eq.	0.0004	0.00053	0.000468 ^m	g MJ ⁻¹ ppm ⁻¹
Biomass partitioning					
FTSWLimitRoot	FTSW Limit for Root Growth	0.42	0.58	0.5	unitless
DayForStress	N° Days for water stress on root	1.7	2.3	2	day
HarvestIndex	Slope of Fruit Biomass Index eq.	0.0038	0.0051	0.00443 ^h	d ⁻¹
HarvestIndexCutOff	Harvest Index cut off	0.43	0.58	0.5	d ⁻¹
InitialRootLength	Initial value of root depth	85	115	100 ^{n,i}	cm
RootGrowthBasic	Root growth rate for not limit water	0.0009	0.0012	0.001	cm day ⁻¹
RootGrowthStress	Root growth rate for limiting water	0.043	0.058	0.05	cm day ⁻¹
Evapotranspiration					
WUE	Water use efficiency	3.05	9.15	6.1 ^{l,i}	Pa
Extreme events impact					
Tmax	Max temp. for fruit-set at flowering	35	47	41 ^{o,p,q,r}	°C
Tmin	Min temp. for fruit-set at flowering	0.9	1.2	1 ^{o,p,q,r}	°C
Topt	Optimum temp. for fruit-set at flower.	21	28	25 ^{o,p,q,r}	°C
q	Curve shape param.	1.62	2.19	1.9 ^{o,p,q,r}	unitless

References: ^aCaffarra and Eccel (2010);^bPouget, (1963);^cPouget, (1968);^dDokoozlian, (1999);^eBotelho et al. (2007);^fBindi et al. (1997a);^gDos Santos et al. (2003);^hBindi et al. (1997b); ⁱRamos and Martinez-Casasnovas (2014);^jBindi et al. (2005);^kLebon et al. (2006);^lPoni et al. (2006);^m(Bindi et al., 2001a, 2001b);ⁿ derived by Nendel

and Kersebaum (2004) considering a vineyard from 3 to 18 years; °derived by: Kliewer (1977);^eEwart and Kliewer (1977);^gTukey (1958);^f Haeseler and Fleming (1967).

Calibration and evaluation of the modelling solution

The modelling solution was coupled with the software application Optimizer (available at www.biomamodelling.org), to perform automatic calibration of parameter values in order to increase the accuracy in reproducing reference data. The parameters sets related to phenological development were calibrated prior to sensitivity analysis by minimizing the root mean square error between simulated and reference data, considering 60% of variation from default values (Caffarra and Eccel, 2010, Table 2.3). Dates of budbreak, flowering and veraison were recorded as field observations, whereas we assumed the day in which physiological maturity was simulated as harvest date.

The most relevant parameters from sensitivity analysis were subjected to automatic calibration using the multi-start downhill simplex algorithm (Nelder and Mead, 1965) as modified by Acutis and Confalonieri (2006). This algorithm explores the N-dimensional parameters space, with N as the number of the parameters under evaluation, following the gradient of the objective function, which in our case was Root Mean Square Error (RMSE). A geometrical figure with N+1 vertexes (i.e., the simplex) is created when the optimization starts, with N as the number of parameters under evaluation. After each simulation run, the objective function is evaluated at each vertex of the simplex, which moves via reflection, contraction, or expansion towards the minimization of RMSE between reference and simulated data. The optimization ends when the difference of RMSE value in the simplex vertexes is below a tolerance range (i.e., 0.001). We launched five simplexes at each optimization run, with the same domain of model parameters used for the sensitivity analysis assessment.

The evaluation of model performance in reproducing phenology, soil water content and fruit dry biomass was based on the following statistical metrics (Green and Stephenson, 1986; James and Burges, 1982; Loague and Green, 1991, Eq. 2.31 - 2.35):

Root Mean Square Error (RMSE, Equation 2.31):

$$RMSE = \left[\sum_{i=1}^n \frac{(P_i - O_i)^2}{n} \right]^{0.5} \quad \text{Eq. 2.31}$$

and the normalized form (RRMSE, Equation 2.32):

$$RRMSE = RMSE \cdot \frac{100}{O} \quad \text{Eq. 2.32}$$

Modelling Efficiency (EF, Equation 2.33):

$$EF = \frac{\left(\sum_{i=1}^n (O_i - \bar{O})^2 - \sum_{i=1}^n (P_i - O_i)^2 \right)}{\sum_{i=1}^n (O_i - \bar{O})^2} \quad \text{Eq. 2.33}$$

Pearson's Coefficient (r , Equation 2.34):

$$r = \frac{\sum_{i=1}^n (O_i - \bar{O}_i) \cdot (P_i - \bar{P}_i)}{\sqrt{\sum_{i=1}^n (O_i - \bar{O}_i)^2 \cdot \sum_{i=1}^n (P_i - \bar{P}_i)^2}} \quad \text{Eq. 2.34}$$

Coefficient of Residual Mass (CRM, Equation 2.35):

$$CRM = \frac{\left(\sum_{i=1}^n O_i - \sum_{i=1}^n P_i \right)}{\sum_{i=1}^n O_i} \quad \text{Eq. 2.35}$$

where P_i are the predicted values, O_i are the observed values; n is the number of samples; and \bar{O} is the mean of the observed data.

2.3. Results and Discussion

2.3.1. Analyzing the sensitivity of the modelling solution to weather variability and parameter changes

The results of the sensitivity analysis are presented in Fig. 2.4, showing the Spearman's correlation coefficient (SC) (Fig. 2.4a) among model parameters and fruit biomass variability and Sobol' Total Orders (STL) (Fig. 2.4b) for each parameter of the modelling solution.

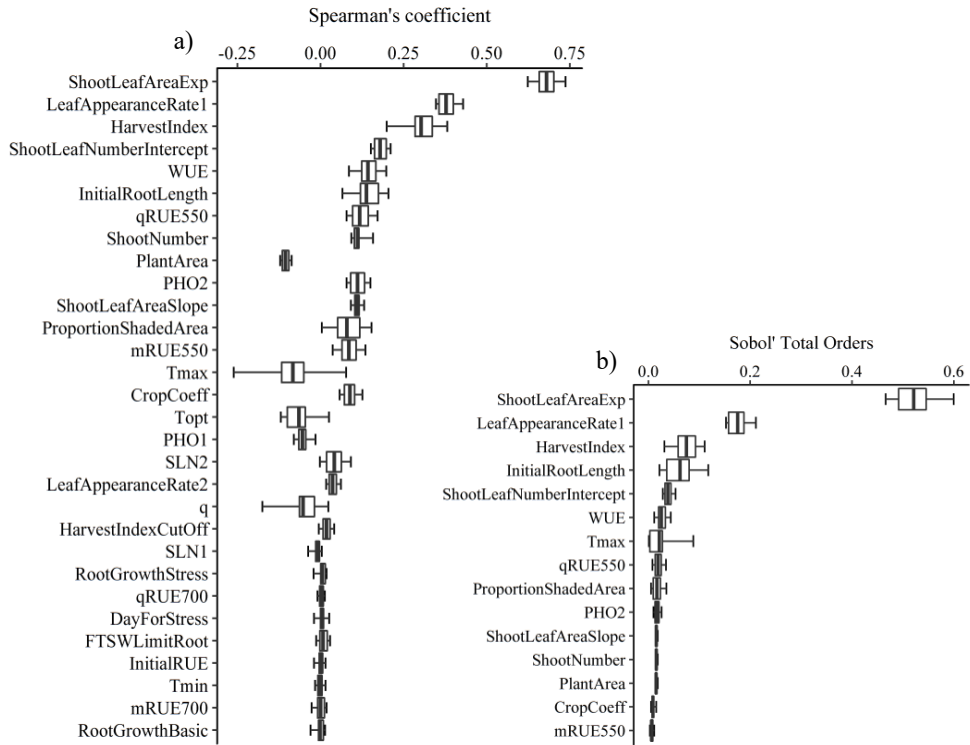


Figure 2.4. Sensitivity Analysis (SA) using LHS and Sobol' methods. The Spearman's correlation coefficient (Fig. 2.4a) and Sobol' Total Order (Fig. 2.4b) were used as metrics to determine which parameters of the modelling solution is more sensitive.

According to LHS results, the two top ranked parameters in explaining the variability of fruit biomass were related to shoot leaf area growth, i.e., the exponential coefficient driving the shoot leaf area expansion (*SLAE*, Eq. 2.11), and the slope of the temperature-dependent linear function related to the daily rate of leaf appearance (*LARI*, Eq. 2.8). The parameter *SLAE* showed a higher average Spearman's correlation ($\overline{SC}_{SLAE} = 0.680$, cv 20%) than *LARI* ($\overline{SC}_{LARI} = 0.378$, cv 13%), suggesting that shoot leaf area expansion has a prominent influence on the simulated leaf area, which in turn resulted as the most relevant process in influencing fruit biomass. The key role of leaf area expansion is further proved by the high relevance of other connected empirical parameters, i.e., the intercept of the temperature-dependent linear function estimating shoot leaf number (*SLNI*, 4th ranked) and the slope of the shoot leaf area function (*SLAS*, 11th ranked). The third most important parameter in explaining fruit biomass variability was the harvest index (*HI*), which showed a high positive correlation with the model output ($\overline{SC}_{HI} = 0.3$), with a large variability between years (cv. 17%): the higher the yield, the stronger the parameter correlation. Our results agree with Wang et al. (2013), who identified the parameters related to the

leaf area expansion as the most prominent in affecting simulated corn yield variability in the WOFOST model, and with Ruget et al. (2002) and Dzotsi et al. (2013), who evidenced via sensitivity analysis that wheat, maize, peanut and cotton yields were mainly affected by leaf development and crop partitioning parameters. Another study by Wang et al. (2005) confirm that *HI* is one of the most sensitive parameters in crop models when yield is the target simulated variable, using FAST sensitivity analysis on EPIC crop growth model.

The MS showed a high sensitivity to the parameters linked to the water use (water use efficiency, *WUE*, 5th ranked, and *InitialRootLength*, *Root_{ini}*, 6th ranked) rather than to the ones modulating the radiation use efficiency (*mRUE550* and *qRUE550*, 7th ranked and 13th ranked, respectively). *Root_{ini}* determines the depth of the root zone, therefore it substantially impacted on the potential plant water reserve, while *WUE* represents the capability of the plant to convert the available water in aboveground biomass. According to Spearman analysis, these two parameters were positively correlated to simulated fruit biomass ($\overline{SC}_{WUE} = 0.143, \overline{SC}_{Rootini} = 0.139$), with similar strength. The variability in the correlations of these parameters with fruit biomass (cv. *WUE* = 4%, cv. *Root_{ini}* = 3%) in the period of interest reflected the high year-to-year fluctuations of thermal conditions and cumulated precipitation in the study area (Table 2.2). Our results are in agreement with findings by Vanuytrecht et al. (2014), who demonstrated using the EFAST sensitivity analysis method that variations in the parameters related to root growth deeply affect maize yield in the AquaCrop model.

The MS resulted more responsive to the variation of the intercept value (*qRUE550*) rather than the slope (*mRUE550*, 13th ranked) of radiation use efficiency function, probably due to the ranges of values selected in this study. The *ShootNumber*, *PlantArea*, and *ProportionShadedArea* (8th, 9th, and 12th ranked, respectively), related to the representation of canopy characteristics and vine training systems, showed less importance in explaining fruit yield variability via their impact on the intercepted radiation rate. The *PlantArea* was the only parameter showing a negative correlation with fruit biomass, as it represents the inverse of planting density.

The *Tmax*, *Topt* parameters were determinant in influencing fruit biomass variability, despite their low average correlation with this variable, modulating the impact of air temperatures (from budbreak to flowering) on the fruit set process (data not shown).

Fifteen parameters were included in the second step of the sensitivity analysis assessment (Sobol' Total Order, Fig. 2.4b). The ranking of the parameters most influencing fruit biomass variability after Sobol' sensitivity analysis reflected LHS results. The main difference between the two rankings was the parameter *Root_{ini}*, which gained relevance after Sobol' (4th ranked, $\overline{STL}_{Rootini} = 0.06$), highlighting the large influence of root water uptake on fruit biomass, with a deep year-to-year

variability (cv. 47%). The parameter *SLAE* ($\overline{STL}_{SLAE} = 0.521$, cv. 8 %) consistently resulted as the most relevant, and even increased its relative importance with respect to *LARI* ($\overline{STL}_{LARI} = 0.176$, cv. 12%) and *HI* ($\overline{STL}_{HI} = 0.075$, cv. 31%), the latter confirming the high importance of partitioning rules on simulated output. The *Tmax* parameter (7th ranked, $\overline{STL}_{Tmax} = 0.02$, cv. 134%) presented the highest year-to-year variability in Sobol' Total Order index.

2.3.2. Field level application of the modelling solution

Phenological development

The comparison of observed and simulated days of the year corresponding to the main phenological phases (budbreak, flowering, veraison and maturity) of the Chardonnay variety are showed in Fig. 2.5 and the list of the calibrated parameter values is reported in the supplementary material, Table S.2.2. The modelling solution was more accurate in reproducing flowering ($r=0.64$; $RMSE=4.39$; $EF=0.41$) and maturity ($r=0.69$; $RMSE=4.45$; $EF=0.56$) stages, compared to budbreak ($r=0.52$; $RMSE=5.05$; $EF=0.26$) and veraison ($r=0.44$; $RMSE=4.88$; $EF=0.09$). Results were in line with Parker et al. (2011), who tested four phenological models (Spring Warming, Spring Warming from 1st of January, UniFORC, UniCHILL) on several grape varieties on a large dataset. Parker et al. (2011) evidenced similar ranges (from 5.4 to 6.1 and from 8.0 to 10.2) of RMSE values for flowering and veraison stages, respectively, even with better r . Caffarra and Eccel (2010) obtained similar r (0.53-0.81) and RMSE (5.6-6.9) on budbreak phase of Chardonnay variety (data extracted from charts), using the same chilling-forcing model adopted here. Finally, higher performance for estimating harvest date was showed by Fraga et al. (2015) (r : 0.69 vs 0.83) for Aragonez, Touriga-Franca and Touriga-Nacional varieties.

Although some authors (Parker et al., 2011; Fila et al., 2014) claimed that CF models did not lead to higher accuracy than pure forcing models in current climate, the adoption of a CF approach to simulate phenological development is considered adequate especially in warmer climate conditions (García de Cortázar-Atauri et al., 2009a). Indeed, high temperatures influence the release of the dormancy phase altering chilling-forcing requirements and producing an erratic estimation of budbreak in simple forcing models. The worse performances in reproducing budbreak could be partially explained by the uncertainty of its detection in the field, as the duration of the 'greentip' (C for Baggioolini; 4 for Eichorn-Lorenz modified, 07 for extended BBCH-scales) period can be very short (Lavee and May, 1997). Also the occurrence of the veraison stage is subjected to high large year-to-year variability, and presents spatial patterns within a vineyard and, more particularly, even between berries within each cluster (Coombe, 1992). Hence, the exact timing of colour change, especially in white varieties, is difficult to identify.

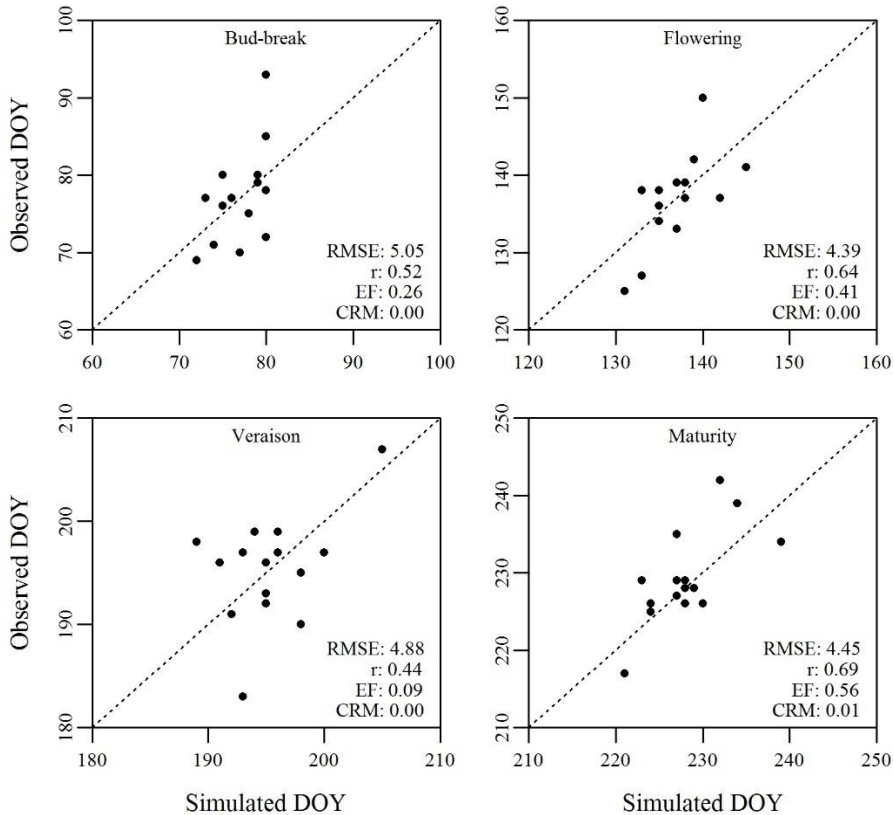


Figure 2.5. Scatterplots presenting the comparison of simulated (X-axis) and observed (Y-axis) day of the year (DOY) referred to the main phenological phases of the Chardonnay variety (budbreak, flowering, veraison and maturity). Within each plot, the values of root mean square error (RMSE), Pearson's coefficient (r), the modelling efficiency (EF), and the coefficient of residual mass (CRM) are reported.

The calibrated optimal temperature for chilling accumulation was set to 1.8 °C, leading to the accomplishment of chilling requirements around the end of December (endo-dormancy). This agrees with experimental studies in which optimal chilling requirement ranged from 0 to 10°C (Pouget, 1963, Pouget, 1968; Dokoozlian, 1999; Botelho et al., 2007; Caffarra and Eccel, 2010). After endo-dormancy period, the accumulation of forcing units until budbreak proceeded at a forcing rate of 0.23, with 15°C as optimal temperature. This is in agreement with Chuine (2000), where the best temperature conditions for forcing units accumulation ranged from 10°C to 25°C in several arboreal trees. The calibrated optimal temperatures for vine development increased from flowering to maturity, ($T_{opt}Flowering= 9.43$ °C; $T_{opt}Veraison= 10.93$ °C; $T_{opt}Maturity= 17.24$ °C), as reported in Zapata et al. (2015) and Oliveira (1998), as well as the forcing unit accumulation rate ($FloweringRate= 0.13$; $VeraisonRate=$

0.40; *MaturityRate*= 0.40). The calibrated threshold to reach veraison phase (57.31 FU) was higher than the flowering phase (38.47 FU), as in Caffarra and Eccel (2010). A lower thermal requirement was determined for maturity phase (30.73 FU), due to the higher forcing accumulation rate and the shorter length of the veraison-maturity period.

Soil water content

The comparison of simulated (lines) and measured (points) soil water content (SWC, mm mm^{-1}) at different depths in the experimental field is presented in Figure 2.6, considering the data availability limited to November 2010-September 2012 (Ramos and Martínez-Casasnovas, 2014).

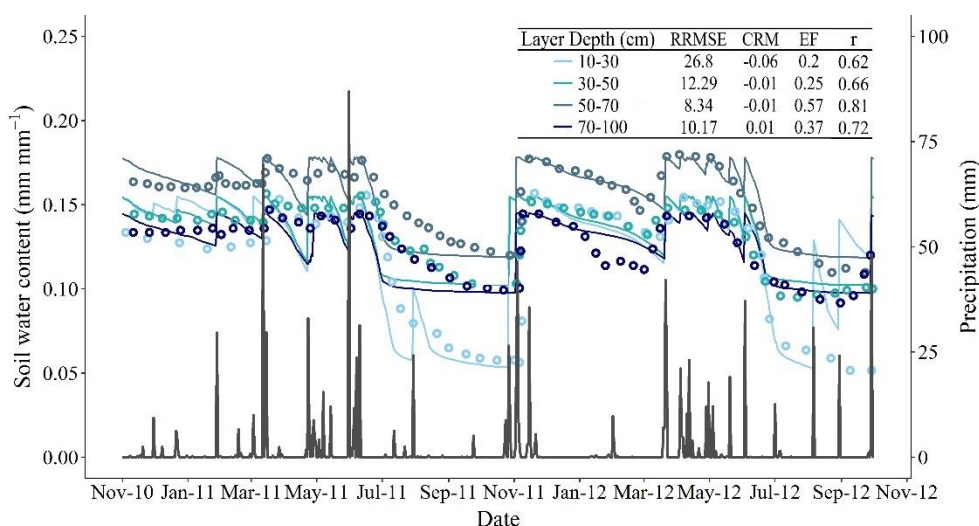


Figure 2.6. Simulated (continuous lines) and observed (empty points) soil water content at different depths in two cropping seasons (2010-2012) in the experimental vineyard. Precipitation is reported on the secondary y-axis as grey line. The table at the top right of the figure resumes the performances of the modelling solution in the different layers, considering the relative root mean square error (RRMSE), the coefficient of residual mass (CRM), the modelling efficiency (EF), and the Pearson's coefficient (r).

The 2011 cropping season was characterized by 86.3 mm of cumulated precipitation during budbreak-flowering period, 184.6 mm in flowering-veraison - concentrated in few high intensity events - and 17.67 mm in the last part of the vine cycle. This determined a steep SWC decline in the whole profile in early June, with no recharge until the end of the cropping season. In 2012, larger precipitation events (217.8 mm) occurred during budbreak-flowering period. The corresponding measured

and simulated SWC was higher, with field capacity in the whole profile kept until the beginning of July. Later in the season, very small precipitation events were recorded, thus determining a low SWC until harvest date.

The first soil layer (10-30 cm), affected by soil evaporation, presented a larger water holding capacity (field capacity = 0.16 mm mm^{-1} wilting point = 0.05 mm mm^{-1}) than deeper layers. The modelling solution correctly reproduced SWC measurements, with RRMSE values ranging from acceptable (1st layer, 26.8%) to excellent performances ($< 10\%$) in the whole soil profile (Jamieson et al., 1991). RRMSE values in the four soil layers are consistent with published simulation studies where SWC was simulated (Markewitz et al., 2010; Constantin et al., 2015; Bregaglio et al., 2016). The lower accuracy obtained in the surface soil layer is due to its sudden refill up to field capacity as a consequence of small precipitation events during simulation. Indeed, this layer was characterized by a systematic overestimation of SWC (CRM = -0.06), whereas no bias emerged in the deeper layers ($-0.01 \leq \text{CRM} \leq 0.01$). Our results agree with Molina-Herrera et al. (2016), where the Pearson's coefficient between observed and simulated SWC at 10 cm depth ranged from 0.28 to 0.79 in several agricultural sites. The modelling efficiency (EF) was positive throughout the soil profile, proving the accuracy of the modelling solution in reproducing SWC, which decreased as a consequence of root water uptake during vegetative seasons. The r and EF are consistent with the results reported by Toumi et al. (2016) (r : 0.71-0.82; EF: -2.62-0.55) in which the soil water content (0-55 cm) is simulated considering the inputs of rainfall and irrigation under limited water conditions. The increase of SWC in our case study is solely determined by precipitation, as no irrigation was applied in the two cropping seasons.

Fruit biomass

The comparison of measured and simulated fruit dry biomass (kg ha^{-1}) in the period 1998-2012 is shown in Fig. 2.7. The overall correlation was significant ($r = 0.59$, $p < 0.05$), and proved the capability of the modelling solution in reproducing the large year-to-year variability characterizing reference yield data.

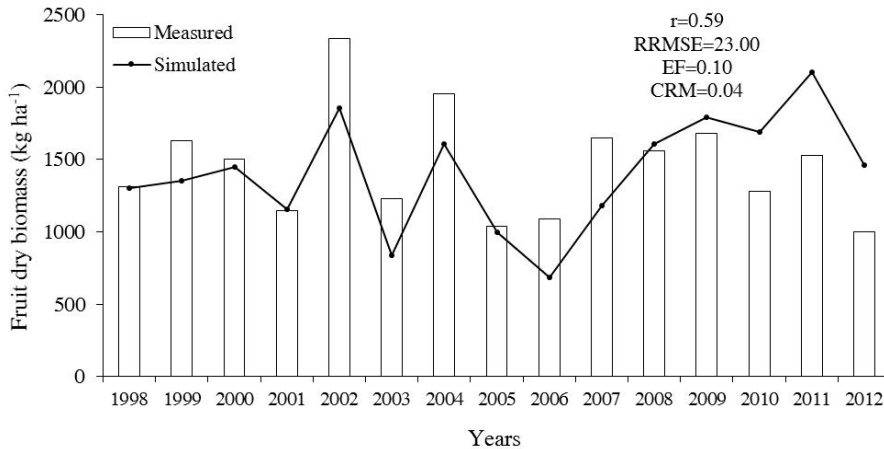


Figure 2.7. Comparison of simulated (lines) and measured (histogram) fruit dry biomass (kg ha^{-1}) over the period 1998-2012. In the top right of the figure, the values of Pearson's coefficient (r), relative root mean square error (RRMSE), the modelling efficiency (EF) and the coefficient of residual mass (CRM) are reported.

The values of RRMSE (23%) and EF (0.1) supported the ability of the modelling solution in reproducing measured yields. There were not leaf area index (LAI) measurements in the reference dataset to further test the performances of our modelling solution. Indeed, simulated LAI in 1998-2012 (data not shown) ranged from 0.76 to 1.19 $\text{m}^2 \text{m}^{-2}$, which agrees with results by Pérez et al. (2013) and Chacón et al. (2009), who measured it in rainfed Spanish vines trained with a similar number of buds ha^{-1} .

The modelling solution correctly simulated low yields in 2001, 2003, 2005, and 2006, which were characterized by high water deficit during the flowering-veraison period (Ramos and Martínez-Casasnovas, 2014). Conversely, high yields were simulated in the years 2000, 2004 and 2011, according to field measurements. The modelling solution tended to overestimate reference yield data in the period 2007-2012. A possible reason is the adoption of a fixed coefficient to convert fresh to dry fruit biomass. The alternation of wet-dry conditions could indeed have determined a variable berry water concentration, with the years 2011 and 2012 being characterized by higher water deficit before harvest time. A specific case was represented by the year 2002, in which the rainfall recorded immediately before harvest may have affected the wet-dry ratio of annual grapevine production. As a consequence, the percentage of dry weight at harvest can vary according to soil water availability (Girona et al., 2009), with the high water stress around harvest reducing both dry matter production (Reynolds et al., 2007) and berry water content (García de Cortázar-Atauri et al., 2009b; Petrie et al., 2000).

2.4. Conclusions

The availability of grapevine simulators to be used as in-season supporting tools or in mediumlong term forecasting activities is recognized as a priority by the community, given the paramount importance of this key cash crop worldwide. The research products which are presented and released with this paper are meant to contribute to this aim, providing a starting point to further extend their implementation and use. The fine granularity adopted in model development allows third parties to independently extend the UNIFI.GrapeML software library, and the availability of BioMA tools for code generation and model analysis facilitates the fulfillment of these objectives.

The new modelling solution proved to be adequate in reproducing a reference field dataset containing phenological, soil water content and yield data, although its operational application for climate change assessments must be limited to the explored variety and study area. Further, new models need to be implemented to capture the effect of extreme events on phenological development and on the qualitative aspects of grape yield, to give a comprehensive model representation of this complex cropping system.

Chapter 3

Grape quality implementation



Chapter 3 has been based on the study: L. Leolini, L. Brilli, M. Moriondo, G. Buscioni, M. Gardiman, S. Costafreda-Aumedes, M. Bindi. UNIFI.GrapeML implementation for estimating sugar content of Sangiovese variety (*forthcoming paper*).

PhD candidate's contribution

Luisa Leolini implements the grape quality approach in the model library. She produced the results and she and the others co-authors wrote the sections of the chapter.

3. UNIFI.GrapeML implementation for estimating sugar content of Sangiovese variety

L. Leolini¹, L. Brilli², M. Moriondo², G. Buscioni³, M. Gardiman⁴, S. Costafreda-Aumedes¹, M. Bindi¹

¹ DiSPAA, University of Florence, Piazzale delle Cascine 18, 50144 Florence, Italy.

² CNR-IBIMET, Via G. Caproni 8, 50145, Florence, Italy

³ FoodMicroTeam s.r.l, Via Santo Spirito 14, 50125, Florence, Italy

⁴ CREA - Council for Agricultural Research and Economics, Research Centre for Viticulture and Enology viale XXVIII Aprile 26, 31015, Susegana, Treviso, Italy

Abstract

The grape sugar content is one of the most important factors for determining the quality of the future wines. However, the most famous wine-producing regions (i.e. Montalcino, Tuscany) characterized by valuable grapevine varieties (Sangiovese) and specific *Terroir* are currently influenced by the increase of temperature with detrimental consequences on grape quality. In order to cope the impact of climate change and to maintain the high quality production of these areas, grapevine simulation models represent a promising tool for investigating the accumulation of berries sugar content under different environmental conditions. Accordingly, the aim of this study is the implementation of a grape quality approach in UNIFI.GrapeML for estimating Brix degree during the grapevine ripening period. In this context, the phenological development of the Sangiovese variety was calibrated on the observed phenological data from Susegana (Treviso, Italy) and Montalcino (Siena, Italy) study areas. The estimation of the main phenological phases was useful for determining the Brix degree in Montalcino area over the period 1998-2015. The results showed satisfactory performances for phenological calibration and high correlation between of observed and simulated Brix degree in Montalcino area highlighting the reliability of the model to estimate the sugar content considering the intra and inter-annual climate variability. On these basis, our study represents the first step towards the estimation of Brix degree and further works are need for investigating the sugar content dynamics in the most famous wine-producing regions under changing environmental conditions.

Keywords

Grape quality, Sangiovese, sugar content, Montalcino

3.1. Introduction

The importance of grape quality plays a key role on the future wine influencing the consumer decision-making process (Corduas et al., 2013; Sáenz-Navajas et al., 2014, 2013). In this perspective, the understanding of which factors affect grape quality may be fundamental to cope in advance with winemaking issues (Yuyuen et al., 2015). Despite sugar content represents one of the most important factors for grape quality (Boulton et al., 1996), grape aroma compound and titratable acidity play a key role in future wine production (De la Hera-Orts et al., 2005; Oberholster et al., 2010; Somers and Verette, 1988). The physiological pattern of berry ripening moves from flowering to harvest and consists of three stages: a) rapidly cell multiplication and enlargement; b) slow growth (lag phase); c) cell enlargement only. The last stage is highly important since concerns the increase of sugar concentration (Swanson and El-Shishiny, 1958) which, after the fermentation process, determines the final alcohol content in the wine. Accordingly, grapes in which the sugar sweetness at harvest is balanced by a satisfactory level of titratable acidity show positive traits for future wine production and conservation.

The reaching of a specific level of sugar content at harvest mainly depend on the climate conditions affecting the grapes (Bock et al., 2013; Teslic et al., 2016). For instance, Duchêne and Schneider (2005) found the higher sugar content in cv Riesling at harvest in correspondence of the warmer temperature recorded during the period 1972-2004. Jones and Davis (2000) and Jones et al. (2005) observed as the impact of warmer temperature influenced the behavior of acid and sugar content and, consequently, the vintage ratings. According to the current widespread literature, changes in mean climate conditions and extremes are expected to be more frequent in the next decades (Fraga et al., 2016; Hannah et al., 2013; Moriondo et al., 2013). This may carry out significant negative impacts on grape quality, especially at harvest time, where an overly increase in berry sugar content may lead to unbalanced wines. In order to overcome this risk, the most appropriate harvest is established in advance, thus re-organizing the winemakers scheduling of field operations (Webb et al., 2011).

Accordingly, the changes in vineyard macro and microclimate as well the adoption of specific agro-management practices and the use of specific varieties play a key role on grape and wine quality (Brilli et al., 2014; Smart et al., 1990). In Tuscany, for example, where the variety Sangiovese is widely spread, the sugar content required for high-quality performance classes is generally higher than 22°Brix while values lower than 20°Brix are considered not sufficient for optimum wine quality (Bucelli et al., 2010).

In this context, the use of simulation models for predicting berries sugar content at harvest date may be useful. Currently, two distinct type of approach have been used for assessing grape quality: empirical and process-based. The empirical approaches

are based on weather variables, which are considered the only driver for estimating grape quality. For instance, Jones et al. (2005) and Moriondo et al. (2011) account the vintage quality positively related to average temperature during the grapevine growing season, whilst the occurrence of rainfall over the ripening phase leads to dilution effect of berry juice with consequent negative impact on sugar accumulation. By contrast, process-based approaches describe the main plant processes (i.e. plant growth, development, fruit growth and yield) which affect the grape quality. For instance the process-based model STICS (Brisson et al., 1998) can estimate the sugar content at harvest date considering the number of days or the thermal time above 10°C and crop temperature from flowering to harvest period. Also Genard et al. (2003) for peach and Dai et al. (2009) developed process-based model for grapevine able to simulate fruit growth and sugar accumulation metabolism in relation to water supply. Despite the ability of these models at reproducing specific processes, they were not still dynamically introduced into crop simulation models (Moriondo et al., 2015).

Building on these premises, the aim of this study is the implementation of the UNIFI.GrapeML (Chapter 2) with the approach proposed by García de Cortázar-Atauri et al. (2009b) for estimating berries sugar content. After phenological calibration, an 18 years-long dataset of berries sugar content for the most representative and economics relevant variety in the Montalcino area (cv. Sangiovese), will be used for assessing model calibration and validation performance.

3.2. Materials and Methods

3.2.1. Study area

Data from two different Italian sites have been considered for model calibration (Fig. 3.1). Phenological data have been primarily collected at the grapevine germplasm repository of CREA Research Centre for Viticulture and Enology Susegana (CREA-VE, Treviso, 45°51'00"N, 12°15'31"E, 83 m a.s.l., Fig. 3.1a) and at Montalcino (Siena, 43°03'33"N; 11°29'26"E; 326 m a.s.l., Fig. 3.1b), whilst quality data have been obtained only from Montalcino site.

Susegana: The climate conditions of the area is humid mesothermal (Thornthwaite, 1948), characterized by hot summers and mild winters. The mean annual air temperature was 13°C, over the period 1975-2012. Along this period, the average maximum air temperature was found in July (28.7 °C) while the average minimum air temperature was found in January (-0.83°C). The mean annual precipitation was 1077 mm over the period 1975-2012 with the most of rainfall concentrated in spring and autumn (<http://agri4cast.jrc.ec.europa.eu/>). According to World Reference Base (WRB) soil classification, the soil is Haplic Cambisols (Hypereutric, Orthosiltic) with high level of water saturation, few calcareous content

and a good drainage (IUSS Working Group, 2014; <http://ows.provinciatreviso.it/suoli/map.phtml>). The vineyard is characterized by a Sylvoz training system with row spacing of 3x1.5m and an interrow permanently grass covered.

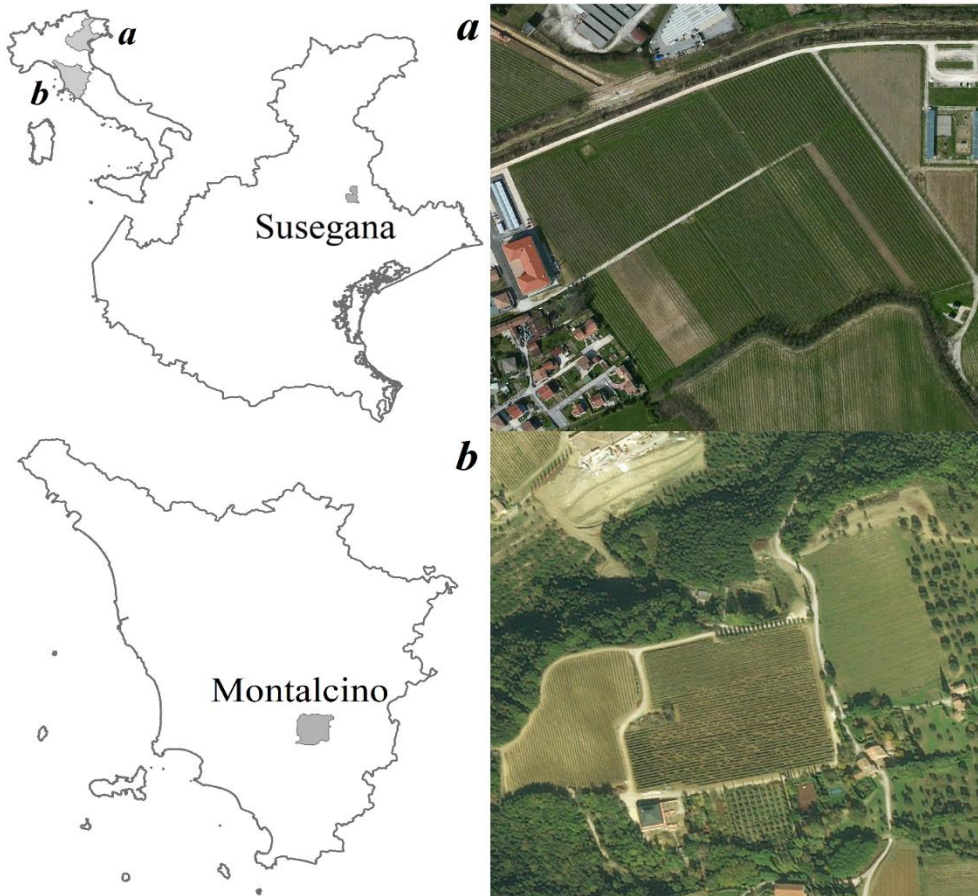


Figure 3.1. Study Area: (A) Susegana (Treviso, $45^{\circ}51'00''N$, $12^{\circ}15'31''E$) and (B) Montalcino (Siena, $43^{\circ}03'33''N$; $11^{\circ}29'26''E$).

Montalcino: The climate is Mediterranean characterized by hot-dry summers and mild winters with rainfall mainly concentrated in autumn and spring (Köppen classification, after Köppen, 1936). The mean annual air temperature is around $14^{\circ}C$ over the period 1975-2012. Along this period, the average maximum air temperature was found in July ($30.5^{\circ}C$) while the average minimum air temperature was found in January ($-1.3^{\circ}C$). The mean annual precipitation was 807 mm over the period 1975-2012 with the most of rainfall concentrated in spring and autumn

(<http://agri4cast.jrc.ec.europa.eu/>). According to the international soil classification system (IUSS Working Group, 2014), the soil is Haplic Calcisols characterized by a silty-loam texture. The vineyard is characterized by a double cordon training system with row spacing of 1x3 m and an interrow grass covered (*Cyndon dactylon*, *Equisetum arvense*, *P. officinalis*, *Aegopodium podagraria*). The agro-management practices are the most commonly adopted in the area (i.e. weeding, topping, green pruning, fruit thinning, etc.).

3.2.2. Phenology and sugar content measured/observed data

Data related to budbreak, flowering, veraison and harvest were collected at Susegana site during 38 years from 1964 to 2005 (excluding 1982, 1983, 1984, 2003 for missing data). Two years (2015-2016) of budbreak, flowering and veraison phenological data was collected for Montalcino site and the harvest date from 1998 to 2015 of Montalcino site was used for phenology calibration. In our study, we assume that the maturity date (phenological stage) coincides with harvest event (data from phenological dataset).

Several grape sugar content data per year were provided for Montalcino site over the period 1998-2015. After harvest, *Vitis vinifera* cv. L. Sangiovese clusters were pressed and placed in stainless-steel tank. The must samples were extracted after pumping over the grape dregs before the addition of sulfur dioxide. Then, the samples were conserved at 4°C in a sterilized plastic bag before of chemical analysis. The sugar content on the must sampling was analyzed using refractometry technique according to the method OIV-MA-AS2-02 Type I (<http://www.oiv.int/>) and expressed as g/l of sugar content. The sugar data were then converted in Brix value considering the specific gravity of the must (<http://www.musther.net/vinocalc>).

3.2.3. Grape quality implementation

The structure of the UNIFI.GrapeML (see Chapter 2) consists of several plant strategies reproducing phenological development, leaf growth, biomass accumulation and light interception, extreme event impact, biomass partitioning and evapotranspiration. The model, previously calibrated in northeastern of Spain (Chapter 2), has been now improved through the implementation of grape quality strategy (Fig. 3.2).

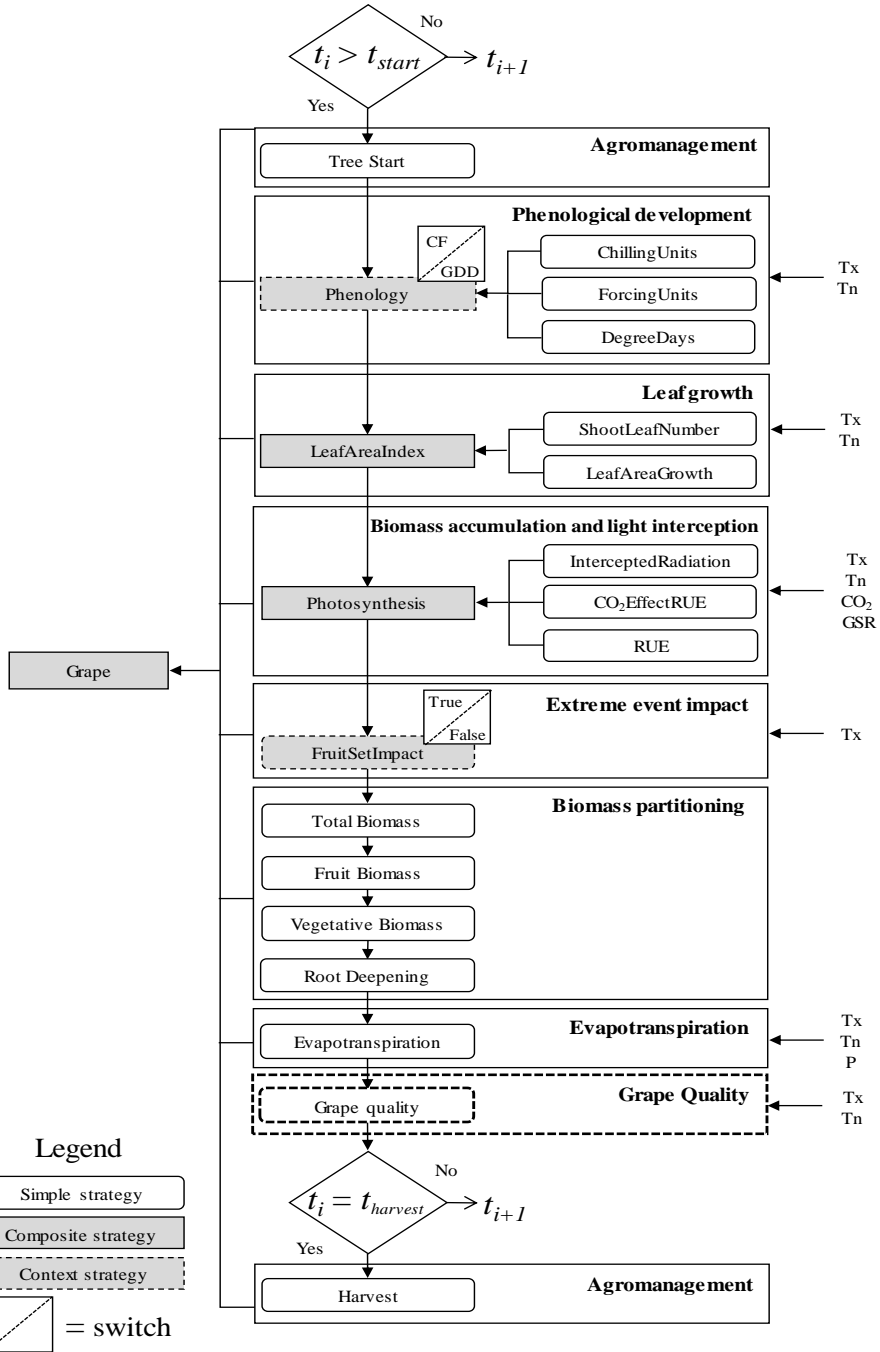


Figure 3.2. UNIFI.GrapeML workflow modified with the implementation of grape quality strategy.

In this strategy, grape sugar content is estimated following the approach proposed by García de Cortázar-Atauri et al. (2009b) in which the sugar concentration (Brix degree) is a function of the berry water content decrease during the berry ripening period. The Brix degree is calculated considering the growing degree days (base temperature= 10°C) accumulated from veraison to harvest (Eq. 3.1):

$$BrixValue = - \frac{((aBrix \cdot \sum_{\text{veraison}}^{\text{harvest}} GDD^2) + (bBrix \cdot \sum_{\text{veraison}}^{\text{harvest}} GDD) + cBrix - (dBrix \cdot (CanopyTemp - T_{avg}) - 94.40))}{0.82} \quad \text{Eq. 3.1}$$

where $aBrix$, $bBrix$, $cBrix$ and $dBrix$ are the parameters of the curve shape; GDD are the growing degree days considering a base temperature of 10°C; T_{avg} is the daily average air temperature and $CanopyTemp$ is the average crop canopy temperature.

The canopy temperature was based on a daily energy balance depending on solar radiation, leaf area index, soil evaporation and plant transpiration (Jamieson et al., 1998; Lawless et al., 2005; Soltani and Sinclair, 2012).

3.2.4. Calibration and Statistical analysis

The calibration of phenology and quality was performed using the Self-Organising Migrating Algorithm of the package *soma* (Clayden, 2014) in R software environment (R Core Team, 2015, version 3.4.0). The phenology and quality parameters were calibrated considering a uniform distribution with a 30% of variation from the default value of Caffarra and Eccel (2010) and (García de Cortázar-Atauri et al., 2009a), respectively. Phenology and quality parameters calibration was based on the minimization of RMSE function.

Finally, the Root Mean Squared Error (RMSE), the modelling efficiency (EF) and the Pearson's coefficient (r) have been used for statistical analysis (Green and Stephenson, 1986; James and Burges, 1982; Loague and Green, 1991).

3.3. Results

3.3.1. Climate analysis

A climatic analysis over the period 1998-2015 was performed for evaluating the trend of the main weather variables in Montalcino study area (Fig. S.3.1 and S.3.2). In Fig. S.3.1, the Brix dynamics of the observed data are compared to the average air temperature, precipitation and thermal excursion. The figure evidences as the trend of the observed Brix data was correlated to the average air temperature ($r=0.41$) and especially average minimum air temperature ($r=0.62$) while negative correlation was found considering the observed Brix data and precipitation ($r=0.35$).

In Fig. S.3.2, a Long-Term Average (LTA) analysis during the ripening period (August-September) for all simulation years (1998-2015) was presented in order to classify the different years according to the main weather variables. Fig. S.3.2 showed the LTA analysis for the main weather variables considering the percentage of variation around the average value. The LTA analysis of the maximum air temperature (T_{\max}) showed an average maximum temperature and a standard deviation of $27 \pm 2.11^\circ\text{C}$. On these basis, the years with T_{\max} higher (2011, 2012 and 2013) and lower (2002) the range of standard deviation represent years with extreme maximum temperatures. The LTA analysis of the minimum air temperature (T_{\min}), instead, evidenced an average minimum temperature and a standard deviation of $15.97^\circ\text{C} \pm 0.87$. Accordingly, the years with T_{\min} higher (2009 and 2003) and lower (2014, 2005, 2007 and 2002) the range of standard deviation are classified as years with extreme minimum temperatures. Moreover, the LTA analysis of the average air temperature (T_{avg}) showed an average temperature and a standard deviation of $21.49^\circ\text{C} \pm 1.37$. The years with T_{avg} higher (2011 and 2012) and lower (2005, 2007 and 2002) the range of standard deviation are considered years with extreme average temperatures. Finally, the LTA analysis on precipitation (Prec) showed an average precipitation and a standard deviation of 108.55 ± 65.04 mm. In this context, the years with Prec higher (2006) and lower (2011) the range of standard deviation are considered the wetter and driest years.

3.3.2. Model calibration and validation

Model calibration has been performed for four different phenological phases (budbreak, flowering, veraison and maturity; Table 3.1). For the budbreak date, the chilling requirement was reached at the end of December with 89 chilling units accumulated at the optimal temperature of 3.5°C (endo-dormancy). Then, the optimal temperature for accounting forcing units (amount of heat units) during the eco-dormancy period was 19.7°C . For flowering phase, the optimal temperature for accounting forcing units was 17.8°C . The forcing requirement (i.e. maximum threshold for reaching flowering) was reached using 23 forcing units. For veraison and maturity phases, the optimal temperatures were 11.8°C and 11.1°C , while forcing requirement were reached at 60 and 41 forcing units, respectively.

The correlation between observed and simulated data of the main phenological phases analyzed showed the ability of the model to reproduce the main trend (Fig. 3.3). Statistical analysis confirmed the good performances for flowering (RMSE: 4.54; r: 0.78, EF: 0.61) and whilst lower performances were found for budbreak (RMSE: 5.96; r: 0.63, EF: 0.39), veraison (RMSE: 6.85; r: 0.57, EF: 0.25) and maturity (RMSE: 10.84; r: 0.39, EF: 0.05).

Table 3.1. Calibration of the UNIFI.GrapeML parameters for assessing grapevine phenology and sugar content in Sangiovese.

<i>Type of process</i>	<i>Phenological phase</i>	<i>Model parameter</i>	<i>Parameter value</i>
Phenology	Budbreak	Col	145.679
		co2	-0.014
		aParam	0.004
		cParam	3.477
		ChillingReq	89.438
		db	-0.207
	Flowering	eb	19.662
		LimitForcingReq	278.45
		df	-0.228
		ef	17.793
		FloweringReq	23.013
	Veraison	dv	-0.269
		ev	11.782
		VeraisonReq	60.269
	Maturity	dm	-0.336
em		11.058	
MaturityReq		44.19	
Quality	aBrix	-3.67E-06	
	bBrix	-0.0023	
	cBrix	82.21	
	dBrix	0.0358	

The UNIFI.GrapeML was also calibrated and then validated for assessing sugar content over a long-term data (1998-2015). The correlations between observed and simulated sugar content were reported in Fig. 3.4. Statistical analysis indicated that model calibration (1998-2008; RMSE: 1.00; r: 0.82; EF: 0.71) and validation (2009-2015; RMSE: 1.91; r: 0.63; EF: 0.33) highly performed.

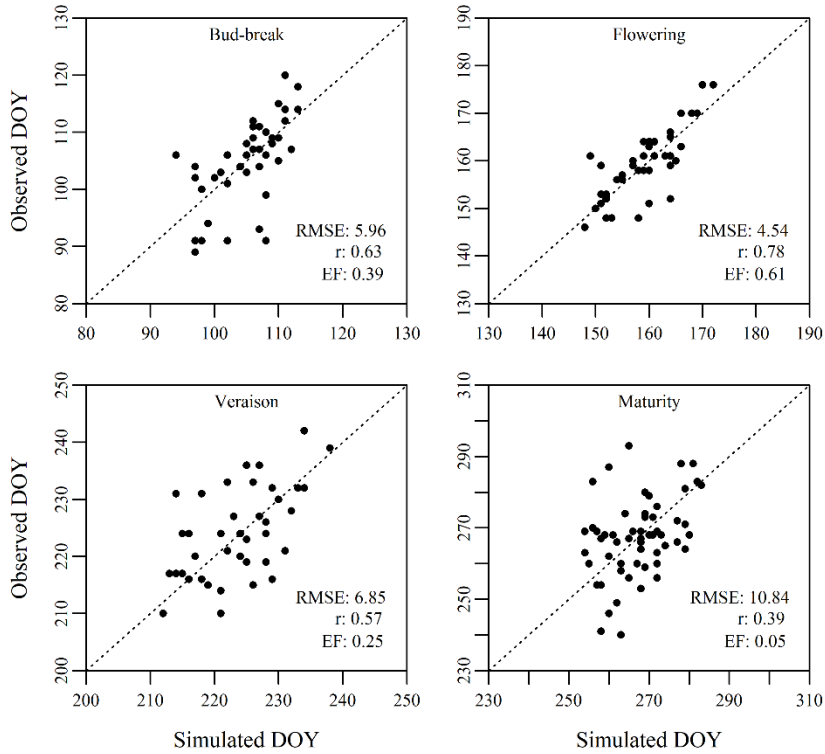


Figure 3.3. Model calibration of the four phenological phases (i.e. budbreak, flowering, veraison and maturity) at Susegana (TV) and Montalcino (SI).

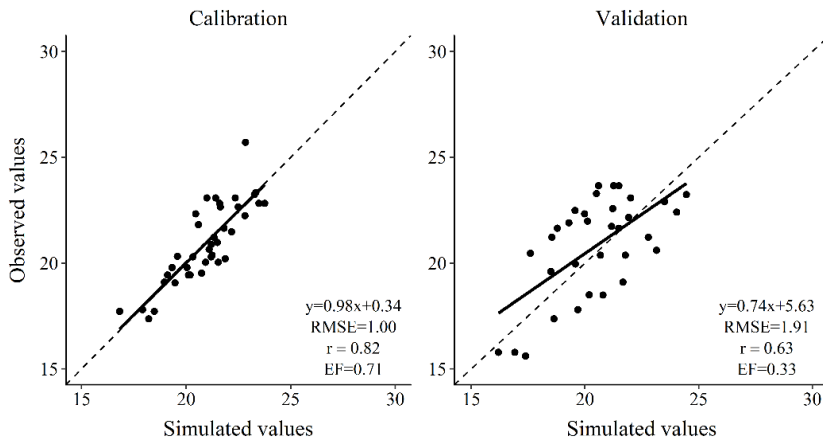


Figure 3.4. Correlations between observed and simulated Brix data in Montalcino area: model calibration and validation.

3.4. Discussion

The high quality wine production is strongly affected by climate change that modify the characteristic *Terroir* of the most famous wine-making regions (Fraga et al., 2016; Hannah et al., 2013; Moriondo et al., 2013).

In our study, the berries sugar content was, indeed, correlated to the temperature conditions of the study area (Fig. S.3.1) In particular, the years characterized by warmer temperature conditions evidenced an increase of sugar concentration compared to wet years. Over the entire period (1998-2015), the years characterized by warmer average temperatures generally showed the high values of Brix degree (e.g. 2003, 2011 and 2012; Fig. S.3.1 and S.3.2). A particular case is represented by the year 1999, in which despite average temperatures are not especially high, the minimum temperature plays a key role on Brix degree increase. The years characterized by lower temperature conditions, instead, (e.g. 2002 and 2014) evidenced lower sugar content. Finally, negative correlation was showed comparing Brix degree and precipitation that evidenced a decrease trend over the last period.

Based on these premises, the UNIFI.GrapeML was considered a good predictive tool for estimating the sugar concentration in grapes.

Firstly, phenology was calibrated for determining the main development stages of grapevine cycle. The overall set of parameters used in the model for all phenological phases (Table 3.1) is consistent with the calibration results derived by Caffarra and Eccel (2010). For budbreak phase, the chilling requirement was satisfied at the end of December as found by Fila et al. (2012) for cv. Sangiovese. The threshold for chilling requirement, ranging from 5 to 100 chilling units, reflects the findings of several grapevine experiments (Bernstein, 1984; Botelho et al., 2007; Dokoozlian, 1999; Pouget, 1968, 1963 and 1972). The optimal chilling temperature was found at 3.4°C, which are in agreement with the range found by several literatures (i.e. from 1 to 10°C, Bernstein, 1984; Botelho et al., 2007; Dokoozlian, 1999; Pouget, 1968, 1963 and 1972). Moreover, the range of forcing units accumulation rate and the optimal temperatures are still in agreement with several studies (Caffarra and Eccel, 2010; Chuine, 2000; Fila, 2012).

Concerning grape quality analysis, the estimation of grape sugar concentration is performed through the approach proposed by García de Cortázar-Atauri et al. (2009b) in which the increase of sugar content is determined by a decrease of berry water content over the flowering-harvest period. Additionally, the relationship between the berry water content and sugar concentration was also found by others authors (Sadras et al. 2008). Despite the approach proposed by García de Cortázar-Atauri et al. (2009b), Brix degree estimation was concentrated during the ripening period

(veraison-harvest) since the sugar content accumulation is mainly concentrated after veraison (Coombe, 1992).

On these basis, we estimated the sugar content (°Brix) evidencing high performances. More specifically, the parameter calibration and the correlation results (RMSE, r) were in agreement with the study of García de Cortázar-Atauri et al., (2009b) on Grenache N, Pinot Noir, Chardonnay and Syrah. Moreover, the evaluation of Brix degree in our study evidenced higher performance compared to the potential alcohol level (linearly correlated to Brix degree) estimated by Fraga et al. (2015) for Aragonese, Touriga-Franca and Touriga-Nacional varieties.

Over the entire simulation period (1998-2015), the UNIFI.GrapeML showed high performances in reproducing the trend of grape sugar content in Montalcino site. However, some differences were found, compared to the observed data trend, when the extreme years were simulated (e.g. 2003, 1999, 2009 and 2015). Based on these premises, Petrie and Sadras (2008) highlighted that the advancement of maturity date caused by warmer temperature over the period 1993-2006 in Australia determined the increase of sugar concentration for Cabernet S. and Shiraz. In some years (2003; 2011-2015), the increase of temperature and thermal excursion linked to lower precipitation (Fig. S.1 and S.2) determined an increase in °Brix degree estimation. This pattern was in agreement with the findings of several studies which suggest as highest temperature in conjunction with lower precipitation can affect grape quality through an increase of sugar content (Duchêne and Schneider, 2005; Jones et al., 2005; Jones and Davis, 2000). By contrast, during the years 2002, 2004 and 2010 characterized by lower temperatures and higher precipitation amount the Brix content was lower and the model tends to a slight underestimation. According to Coombe (1989), the increase of sugar concentration is mainly determined by the inhibition of shoot growth which move the carbohydrates to fruits. However, this increase reaches a maximum over specific temperature extremes. For instance, Kliewer (1977) evidenced as the rate of sugar accumulation did not increase when day and night temperatures were higher than 37 and 32°C, respectively. This is likely due to the inhibition of enzyme systems.

3.5. Conclusions

The climate change influences the viticulture suitability of the most traditional wine-producing regions producing detrimental effects on grapevine development and quality. In particular, the main phenological phases and sugar content accumulation result strongly affected by the impact of warmer temperatures with relevant consequences on the growth cycle and quality features of the future wine (i.e. potential alcohol).

Accordingly, process-based models can represent a useful tool for describing grape growth cycle and estimating grape quality under changing environmental

conditions. In our study, the UNIFI.GrapeML was used for describing the sugar content dynamics of Sangiovese in Montalcino area. After a preliminary satisfactory calibration of the phenological phases (budbreak, flowering, veraison and maturity), the ripening period (veraison-harvest) was selected as the most important stage for sugar increase and the starting point for sugar content estimation. On these basis, the results of Brix degree correlations showed the reliability of the model to capture both the long term average trend that the inter-annual dynamics of sugar content.

This study represents a first step for describing the behavior of berries sugar content under climate conditions. Further studies should be focused on the evaluation of the berry quality dynamics (i.e. sugar and acidity) considering the changing climate on the most famous wine-producing regions.

Chapter 4

Climate change and extreme events affect grapevine varieties



Chapter 4 has been based on the study: L. Leolini, M. Moriondo, G. Fila, S. Costafreda-Aumedes, R. Ferrise, M. Bindi. Late spring frost impacts on future grapevine distribution in Europe. (*in press*). *Field Crops Research*.
<https://doi.org/10.1016/j.fcr.2017.11.018>

PhD candidate's contribution

Luisa Leolini produced the results of the phenological model used for further elaborations and she and the others co-authors wrote the sections of the chapter.

4. Late spring frost impacts on future grapevine distribution in Europe

L. Leolini^{1*}, M. Moriondo², G. Fila³, S. Costafreda-Aumedes,¹ R. Ferrise¹, M. Bindi¹

¹ DiSPAA, University of Florence, Piazzale delle Cascine 18, 50144, Florence, Italy

² CNR-IBIMET, Via G. Caproni 8, 50145, Florence, Italy

³ Council for Agricultural Research and Economics, Center for Agriculture and Environment (CREA – AA), Via di Corticella 133, 40128, Bologna, Italy

Abstract

Viticulture is a worldwide agricultural sector with a relevant economic importance, especially in regions where the climate and environmental conditions meet requirements for the production of high quality wines. The impact of climate change combined with the increased frequency of extreme events predicted for the next future has already shown its potential detrimental effects on viticulture suitability, but few studies currently explored the effect of long-term climate change and extreme events by considering the inter-varietal variability of grapevine. In this study, the combined effect of mean climate change and extreme events (frost events at budbreak and suboptimal temperatures for fruit-set) under future scenarios (RCP 4.5 and 8.5 for two time slices 2036–2065 and 2066–2095, respectively) was evaluated considering four grapevine varieties with very early, early, middle-early and late phenological cycles. The UniChill model calibrated for these varieties was applied in Europe to assess phenological dynamics (budbreak and flowering) using the outputs of a statistical downscaling procedure. Frost impact around budbreak stage as well as the impact of suboptimal temperature around flowering was estimated under present and future scenarios. The results showed a general earlier occurrence of budbreak and flowering stages with a particular relevance on northeastern Europe. The effect of warmer temperatures had a greater effect on late compared to very early and early varieties in western regions. The frequency of frost events at budbreak ($T_{\min} < 0\text{ }^{\circ}\text{C}$) showed wide variability across Europe, with a strong decrease in western regions (e.g. Spain and UK) and an increase in central Europe (e.g. Germany) for future scenarios. The decrease in the frequency of frost events was especially evident for very early and early varieties. The impact of suboptimal temperatures at flowering evidenced a significant variability across a latitudinal gradient while this effect did not show significant results when comparing cultivars and scenarios. The results of these studies highlighted that in a warmer climate frost events rather than stress at flowering will reshape the distribution of grapevine varieties in Europe.

Keywords

Extreme events, climate change, viticulture, grapevine phenology, statistical downscaling

Highlights

Budbreak and flowering are expected to occur earlier under future scenarios.

Frost impacts around budbreak will decrease in western Europe.

The variability of fruit-set will be related to the earlier flowering.

Frost impacts variability is higher on very early and early varieties.

4.1. Introduction

Viticulture is a worldwide agricultural sector with a relevant economic importance and a long history of development and evolution (Johnson, 1985; Terral et al., 2010). The most famous wine-producing regions are located in narrow geographical areas with optimal combinations of environmental and human factors, which are described by the *Terroir* concept (Seguin, 1988; Seguin, 1986; Van Leeuwen et al., 2004). The long history of viticulture adaptation that identifies a specific *Terroir* contributes to characterizing the profile and features of its high-quality wines. However, the high specificity of these climatic niches exposes grapevine growth to the effects of climate change.

More specifically, mean seasonal climate change, inter-annual variability and the increase in frequency and magnitude of extreme weather is expected to strongly affect viticulture in the main wine-producing regions. The impact of mean climate change on the current viticultural regions has already been shown by several authors (Duchêne and Schneider, 2005; Jones et al., 2005; Santos et al., 2012; Santos et al., 2011). Some authors highlighted that warmer temperatures will determine an earlier occurrence of grapevine phenology with a consequent negative impact on grape yield and quality (Fraga et al., 2016; Hannah et al., 2013; Jones et al., 2005; Moriondo et al., 2013; White et al., 2006). These changes will therefore also have detrimental effects on the suitability of the most famous wine-producing regions, determining a shift from current suitable areas towards new ones in the future (Hannah et al., 2013; Moriondo et al., 2013). According to Fraga et al. (2016), viticulture is predicted to reach 55°N by 2070 with a consequent potential increase of wine-producing areas. Although the combined effect of mean climate and variability has long been indicated as detrimental for grape yield and quality (White et al., 2006), climate change impact assessments performed so far on grapevine according to different approaches did not consider these possible impacts (Ferrise et al., 2016; Fraga et al., 2016; Hannah et al., 2013; Moriondo et al., 2013).

Moreover, the combined effect of mean climate change and extreme events (i.e. days with $T_{\max} > 30\text{--}35\text{ }^{\circ}\text{C}$, or days with $T_{\min} < 0\text{ }^{\circ}\text{C}$) have a greater impact compared to just the long-term climate change (Ramos et al., 2008; White et al., 2006). In this case, the reduction of suitable areas for high-quality wine production is expected to exceed 50% (White et al., 2006). In particular, the frequency of frost impacts has increased over the last years in different regions (i.e. France, Brun and Cellier, 1992; Canada, Quamme et al., 2010; England, Mosedale et al., 2015; Romania, Bucur and Babes, 2015). However, future warmer temperatures are expected to move in advance late frost events more than budbreak, leading to a reduction of frost damage in some wine-producing areas (Molitor et al., 2014; White et al., 2006).

On these bases, studies are currently investigating the detrimental effects (i.e. high crop yield variability, decrease in suitable crop areas, etc.) of changing climate conditions on the most valuable crops such as wheat or grapevine (Giannakopoulos et al., 2009; Moriondo et al., 2010; Olesen and Bindi, 2002; Tomasi et al., 2011). A frequently adopted approach is to apply macro-scale analysis for a spatially-explicit assessment of changes affecting grapevine growing suitability at regional, national or continental level (Hannah et al., 2013 ; Moriondo et al., 2013). Area suitability for growing grapevines is generally evaluated with climatic indices based on a limited number of variables, e.g. heat accumulation and day length during the growing season (Huglin, 1978; Winkler et al., 1974; Zapata et al., 2017). In this context, Jones et al. (2010) showed a spatial analysis on climate variability across wine-producing regions in NW United States using four climatic indices (Huglin Index, Winkler Index, biologically effective degree-day index and average growing season temperatures), which are combined for improving the description of climate and suitability of the regions. Tonietto and Carbonneau (2004) used three complementary indices (Huglin Index, Dryness Index and the Cool Night Index) for a multicriteria climate classification of the most important wine-producing regions. Other studies, such as White et al. (2006), suggest that the use of these indices should be combined with others able to capture the extreme events effect. In this context, the study of Gabaldón-Leal et al. (2017) showed the impact of mean climate change and extreme events around olive tree flowering.

Building on these premises, the aim of this study is to estimate the dynamics of budbreak and flowering of varieties characterized by very early (VE), early (E), middle-early (ME) and late (L) phenological cycles (Fila, 2012) according to the mean variability of the climate and the unpredictable and severe effect of extreme events. The study includes: (i) the use of a chilling-forcing model for evaluating the impact of climate change on grapevine phenology at European scale; (ii) the assessment of extreme events effect through the estimation of phenological stages (budbreak and flowering).

4.2. Materials and Methods

4.2.1. Climate datasets

The impact of climate change and future climate variability was evaluated considering Representative Concentration Pathways (RCP; 4.5 and 8.5) proposed by the fifth Assessment Report of the Intergovernmental Panel on Climate Change (AR5, IPCC) (IPCC, 2014). The daily outputs of the Aire Limitée Adaptation dynamique Développement InterNational (ALADIN) Regional Climate Model (RCM) (<https://www.medcordex.eu/>; Ruti et al., 2016) spaced 44×44 km, were statistically applied over an observed gridded weather (OBS) dataset covering Europe (MARS

project; <http://mars.jrc.ec.europa.eu>) using Long Ashton Research Station-Weather Generator LARSWG; Semenov and Barrow, 1997) at a spatial resolution of 50×50 km.

According to the proposed procedure, OBS observed daily weather data such as minimum and maximum temperature and rainfall (T_{\min} , T_{\max} and R) for the period 1980–2010 were firstly used to calibrate LARS-WG.

After calibration, 300 years of synthetic daily weather were generated for each grid point at a spatial resolution of 50 km (n° grids = 1732) in Europe to represent the baseline (Present period; Pr). The daily outputs of ALADIN RCM were used to derive climatic factors to perturb the present baseline. These were expressed as monthly average differences of T_{\max} and T_{\min} and relative change in rainfall between the relevant RCM baseline (1980–2010) and two different time slices for RCP 4.5 and RCP 8.5, namely: RCP 4.5 2036–2065 (Low CO₂ emission scenario 2036–2065; L1), RCP 4.5 2066–2095 (Low CO₂ emission scenario 2066–2095; L2), RCP 8.5 2036–2065 (High CO₂ emission scenario 2036–2065; H1) and RCP 8.5 2066–2095 (High CO₂ emission scenario 2066–2095; H2). These differences were computed for each RCM grid point covering the European domain.

The relative change in standard deviation of T_{\max} and T_{\min} and duration of wet and dry spells of R were also calculated. These gridded delta changes were applied over the relevant grids of OBS dataset to perturb the climatology of the baseline. Given the mismatch between the spatial resolution of OBS and RCM, a nearest neighbor approach was used to overlap the different grids finally generating stochastically 300 years of daily data for each 50×50 km grid point. The weather variables obtained for present and future climatic conditions were then used as input of the phenological model for evaluating the responses of changing climate at European NUTS2 region scale (<http://ec.europa.eu/eurostat/web/nuts/overview>).

4.2.2. Phenology model

'UniChill' is a Chilling-Forcing (CF) model proposed by Chuine (2000) used for evaluating the grapevine response to different climate change conditions. In relation to the traditional forcing models, which accumulate heat units starting from a fixed date under the assumption that chilling requirement has already been met, (Chuine et al., 1999; Hunter and Lechowicz, 1992), CF model estimates the endo-dormancy duration (the period in which budbreak is inhibited by endogenous factors). Using this kind of model appears more appropriate for future scenario analysis, as winters are predicted to become milder and shorter (Schultz, 2000; Tate, 2001), with a very likely influence on dormancy (García de Cortázar-Atauri et al., 2009).

The length of the endo-dormancy period is calculated by accumulating chilling units from the 1st of September until a critical sum (Crit) is reached, which quantifies

the specific chilling requirement of the genotype. Starting from this moment, forcing units are accumulated until the specific forcing requirement is met, which initiates budbreak (eco-dormancy refers to the period during which dormancy of the buds is caused by environmental conditions). Flowering date is calculated in a similar manner: starting from the previous stage the forcing units are accumulated until another critical sum is reached. In this context, the simulation is considered failed if flowering is not reached before the 31st of December of the year following the beginning of chilling accumulation.

Table 1 shows the equations to calculate chilling (Eq. (1)) and forcing units (Eq. (2)). Budbreak stage is described by both equations while flowering stage is described only by Eq. (2).

Table 4.1. Equations of UniChill model for chilling and forcing accumulation (Chuine, 2000).

UniChill model	
$ChillingUnit = \sum \frac{1}{1 + e^{a_c \cdot (T_{avg} - c_c)^2 + b_c \cdot (T_{avg} - c_c)}}$	Eq. 4.1
$ForcingUnit = \sum \frac{1}{1 + e^{b_f \cdot (T_{avg} - c_f)}}$	Eq. 4.2
<p>a_c, b_c, c_c, b_f, c_f parameters for the curve shape; T_{avg} is the daily average temperature (°C); <i>ChillingUnit</i> represents chilling units accumulated (CU) while <i>ForcingUnit</i> the forcing units accumulated (FU).</p>	

4.2.3. Grapevine varieties

The phenological traits of four grapevine varieties (*Vitis vinifera* L.) were considered for evaluating the effect of mean climate change and extreme events, by means of the UniChill model.

The budbreak and flowering parameters proposed by Fila (2012) for a VE (Glera), E (Chardonnay), ME (Merlot) and L variety (Cabernet Sauvignon) were applied on all grid points in Europe. The varieties were calibrated against an observational dataset made up of field and experimental data, the latter obtained using grapevine cuttings exposed to a wide range of chilling durations to mimic the effect of short winters. The model calibrated on such a dataset should therefore be able to capture the variability expected in the future. The calibration parameters used for simulating grapevine phenology are given in Table 2.

Table 4.2. UniChill model calibration for different varieties. Source: Fila (2012).

Varieties	a_c	b_c	c_c	b_f	c_f	C_{crit}	F_g	F_f
Glera	1.441	-14.719	-2.369	-0.191	18.216	20.776	12.122	33.209
Chardonnay	1.525	-5.317	3.531	-0.200	16.090	13.752	16.603	39.261
Merlot	0.927	7.400	7.464	-0.189	19.155	12.224	12.853	30.605
Cabernet S.	6.790	17.241	6.962	-0.194	17.187	6.853	19.734	40.341

a_c, b_c, c_c, b_f, c_f parameters for the curve shape; C_{crit} is the chilling requirement threshold (CU); F_g is the forcing requirement threshold for budbreak stage (FU) while F_f is the forcing requirement threshold for flowering stage (FU).

4.2.4. Fruit-set Index (FSI) and Frost events estimation

The impact of frost was quantified by calculating the number of years with at least one day with minimum temperature lower than 0 °C ($T_{min} < 0$ °C) during the seven days interval around budbreak (frost events), and expressed as percentage over the 300 years of simulation. The frost events are associated to extreme weather for their severe and unexpected occurrence at a specific phenological stage (budbreak) that leads to considerable bud injuries. FSI estimates fruit-set as a function of air temperature during flowering. This index was obtained from greenhouse experiments described in the literature in which several grapevine varieties with different phenological cycles were exposed to varying diurnal temperatures around flowering time to evaluate their effect on fruit-set (Ewart and Kliewer, 1977; Haeseler and Fleming, 1967; Tukey, 1958; Table 3).

Table 4.3. Control temperature experiments used for describing the fruit-set index curve.

Varieties	Diurnal temperature treatment	Outputs	References
Cabernet S.	25/32.5/35/37.5/40°C	Number of berries per cluster	Kliewer (1977)
Tokay	25/32.5/35/37.5/40°C	Number of berries per cluster	Kliewer (1977)
Pinot noir	25/35/40°C	% of fruit-set	Kliewer (1977)
Carignane	25/35/40°C	% of fruit-set	Kliewer (1977)
Sylvaner	^a 25/15°C	% of fruit-set	Ewart and Kliewer (1977)

Table 4.3. Control temperature experiments used for describing the fruit-set index curve (continue).

Varieties	Diurnal temperature treatment	Outputs	References
Cabernet S.	^a 25/15°C	% of fruit-set	Ewart and Kliewer (1977)
Zinfalden	^a 25/15°C	% of fruit-set	Ewart and Kliewer (1977)
Concord (<i>Vitis labrusca</i>)	^b 65°F/69°F/79°F/89°F	Number of berries per cluster	Tukey (1958)
Concord (<i>Vitis labrusca</i>)	^c 60-65°F/75-80°F/90-95°F	% of fruit-set	Haeseler and Fleming (1967)

^a Only the grapevine that receive no nitrogen treatment was considered; ^b the experiment of 1956 was considered; ^c the average of the interval of temperature treatment was considered.

The outputs of the previous experiments (number of berries per cluster or fruit-set percentage) were used for describing the FSI curve (Table 3). In this context, the temperature of 25 °C was considered as optimum value for fruit-set and berry growth (Hale and Buttrose, 1974; Kozma, 2003; May, 2004; Vasconcelos et al., 2009; Winkler et al., 1974). Accordingly, the results obtained at different temperature treatments were standardized in relation to this optimal condition (T = 25 °C).

Based on this criterion, the equation of the temperature factor as shown in the photosynthesis scheme after Farquhar and von Caemmerer, 1982 was adopted for describing FSI (Eq. (3)):

$$FSI = \left(\frac{T - T_0}{T_{opt} - T_0} \right)^q \cdot \left(\frac{T_0' - T}{T_0' - T_{opt}} \right) \quad \text{Eq. 4.3}$$

where T is the average maximum temperature of seven days around flowering, and T_0' , T_{opt} and T_0 are the maximum, optimum and minimum temperature for growth, respectively, whilst q is a curve shape parameter. After calibration, the T_0' , T_{opt} , T_0 and q were 41 °C, 25 °C, 1 °C and 1.9, respectively. These parameters refer to the maximum, optimum and minimum threshold of daily average maximum temperature in seven days around flowering. The FSI ranges from 0 to 1, where 1 corresponds to the fruit-set obtained at the optimal temperature of 25 °C while values lower than 1 show a decrease of FSI for higher and lower temperature conditions.

4.3. Results

4.3.1. Present period dynamics

The earliest occurrences of budbreak and flowering stages are in south-western Europe (Fig. 1, Fig. 2, Fig. 3; Fig. 4 and Supplementary Material Fig. A.1, A.2, A.3 and A.4). In general, budbreak is expected to occur after the 1st of March (Day Of Year, DOY 60), flowering after the 15th of May (DOY 135).

In Spain, for example, the budbreak date for all varieties ranges on average from DOY 95–113 and from DOY 109–124 in Italy, whilst budbreak is predicted later in northern regions, e.g. around DOY 125–142 in Germany. There is also a west-east oriented variation, i.e. from the Atlantic coast to the continental interior. In the United Kingdom, for instance, budbreak date ranges on average from DOY 109 and 133 considering all varieties (minimum values for Glera and maximum for Cabernet Sauvignon), which is much earlier than in Poland (DOY 136–151). A similar response was shown by flowering, which tends to occur earlier in Mediterranean regions (i.e. DOY 157–163 on average in Spain; DOY 160–166 on average in Italy) than central and northern regions (i.e. DOY 181–190 on average in Germany). More specifically, the four varieties showed differences in phenology dynamics between VE, E, ME and L phenological cycles. For budbreak, Glera showed the earliest occurrence in Europe (DOY 87–150) and Cabernet Sauvignon the latest (DOY 100–165). Instead, lower differences were found for flowering stage between early and late varieties (Glera: DOY 144–208; Cabernet Sauvignon: DOY 146–212).

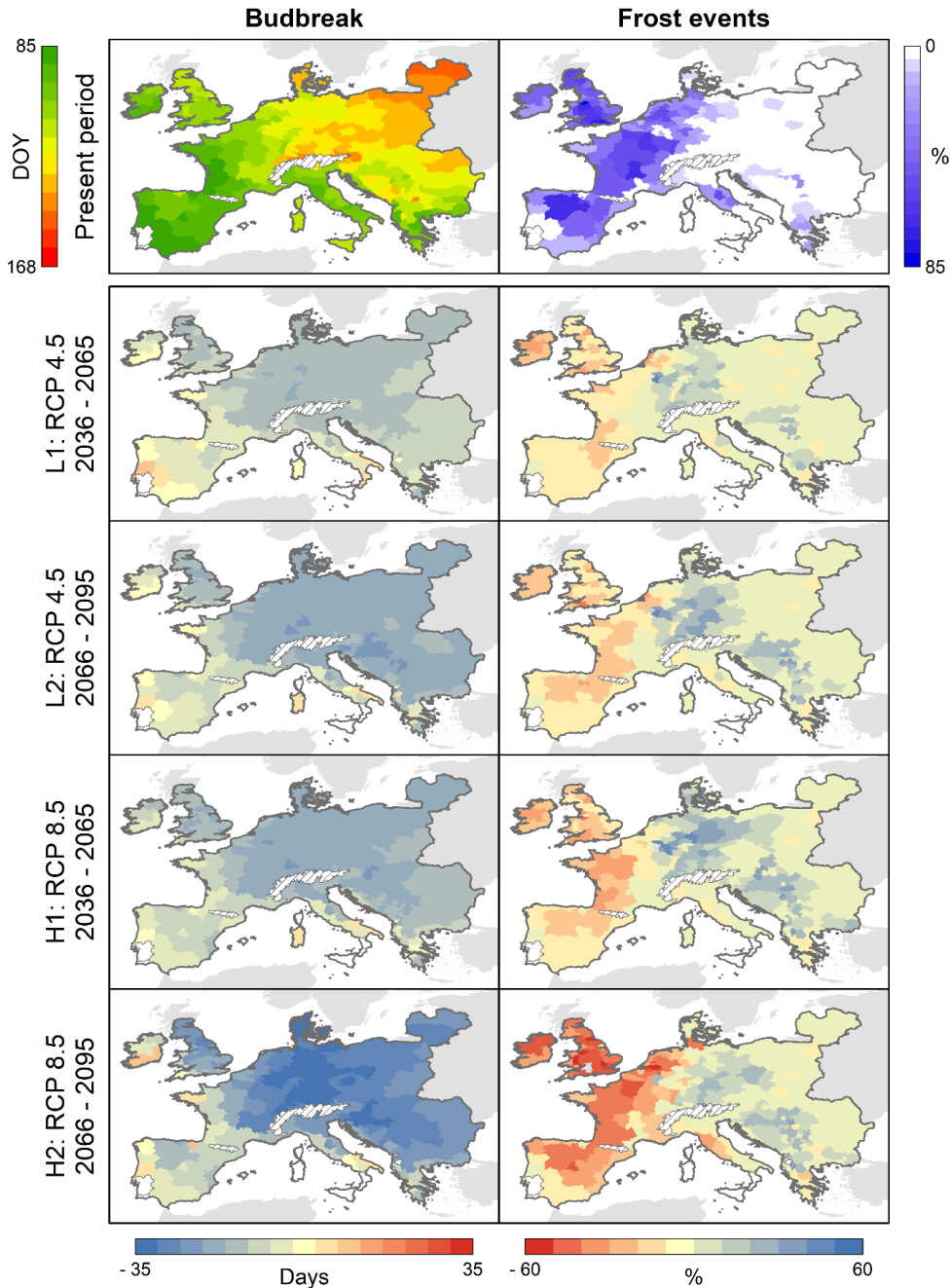


Figure 4.1. Budbreak stage and frost events for Glera variety at European NUTS2 regional scale. The maps of future emission scenarios (L1, L2, H1, H2) are obtained comparing present with future data (Days = number of days in advance or delay compared to the present period). The white areas on the map correspond to the NUTS2 zones in which budbreak is not reached while the stippled areas refer to the grid points excluded by the simulation.

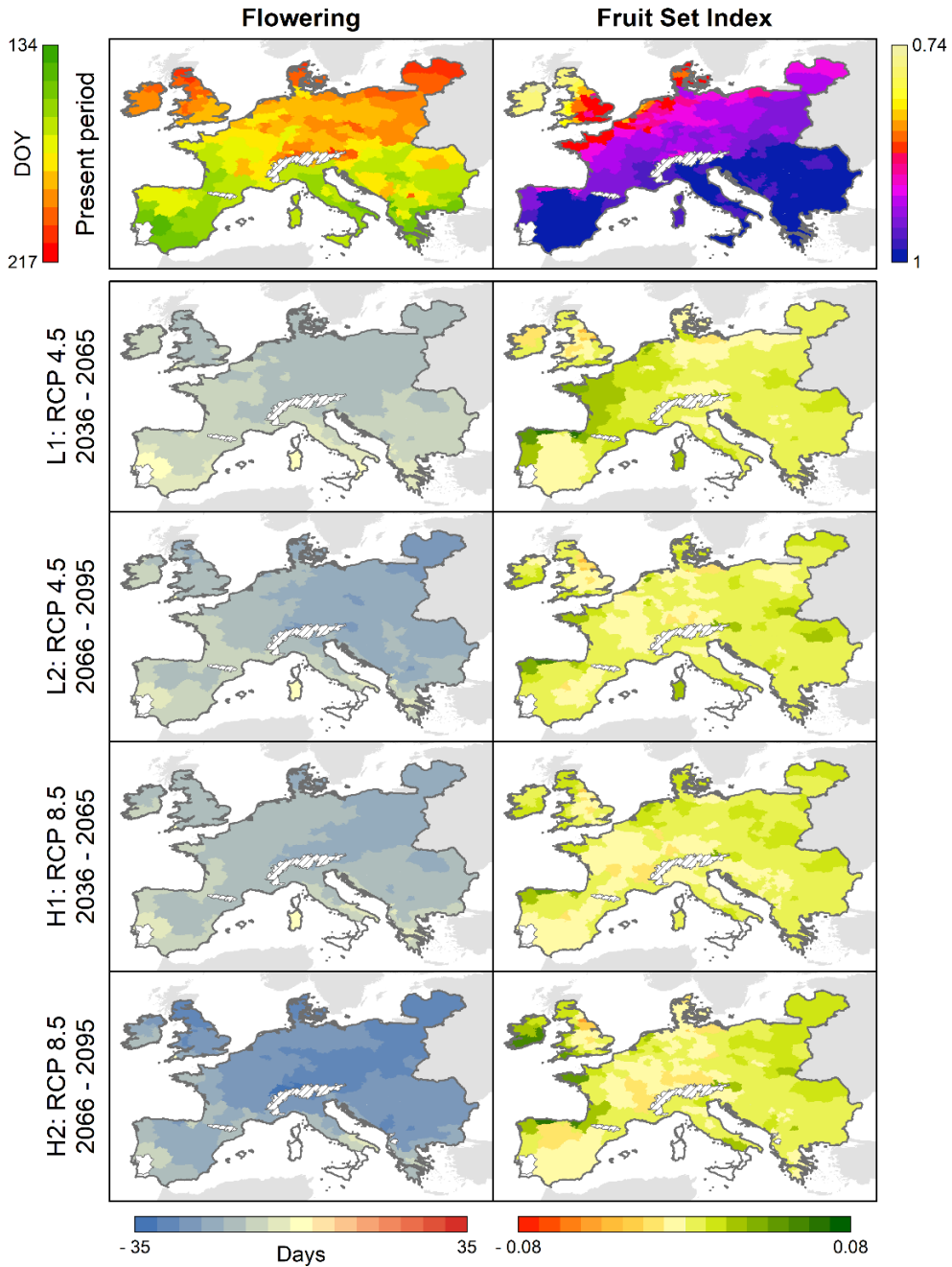


Figure 4.2. Flowering stage and fruit-set index for Glera variety at European NUTS2 regional scale. The maps of future emission scenarios (L1, L2, H1, H2) are obtained comparing present with future data (Days = number of days in advance or delay compared to the present period). The white areas on the map correspond to the NUTS2 zones in which budbreak is not reached while the stippled areas refer to the grid points excluded by the simulation.

The geographical phenology variability is associated to a corresponding impact of extreme events. A higher frequency of frost events during budbreak was estimated for western Europe where budbreak occurs earlier, most notably in Spain, France and the UK (i.e. in Spain: from 9 to 30%; France: from 3 to 41%; UK: from 3 to 50%). Conversely, Germany and Italy showed fewer frost events, which varied from 0% to 16% and from 1% to 11%, respectively (Fig. 5 ; Fig. 6). On the other hand, FSI showed a geographical variability that ranges, on average, from 0.74 to 1 for all varieties with greater differences from northern to southern Europe (Fig. 7). Earlier flowering affected FSI results (Supplementary Material Fig. A.5, A.6, A.7 and A.8). Lower FSI values were obtained in northern than in southern regions. Spain, for instance, showed higher FSI than the UK (0.97 vs 0.81). The variability in phenological cycles of the four varieties showed higher risk of frost events for VE compared to L varieties. For instance, the earlier budbreak of Glera led to a higher frequency of frost events in France (42% on average) compared to Cabernet Sauvignon (3% on average). The VE and E varieties showed the highest frequency of frost events in western Europe, L was the least affected while ME was intermediate (Fig. 1; Fig. 3 and Supplementary Material Fig. A.1 and A.3). Finally, the effect of extreme temperatures on FSI (e.g. higher and lower than the optimal range for flowering) was the same for all varieties (Fig. 2; Fig. 4 and Supplementary Material Fig. A.2 and A.4).

4.3.2. Future Scenarios

All varieties showed earlier budbreak and flowering, which was more pronounced in central and eastern regions. In H2 estimates for Germany, budbreak shifts on average from a minimum of 28 to a maximum of 31 days earlier than the present period considering all varieties, whilst in Spain budbreak shifts by 7–11 days. Budbreak is earlier in all emission scenarios with H2 changing the most. In France, for example, the variation of budbreak time is on average from 8 to 11 days in L1 and from 16 to 22 days in H2 for all varieties.

Earlier flowering was also predicted across Europe (Fig. 2; Fig. 4 and Supplementary Material A.2 and A.4). In France, the flowering stage advanced on average by 18–21 days for all varieties in the scenario with the highest variability (H2), while a slightly lower variation was predicted for Italy (on average from 16 to 18 days). Moreover, a higher variation of flowering stage is expected in Spain moving from L1 (from 2 to 5 days on average) to H2 (from 15 to 16 days on average) considering all varieties.

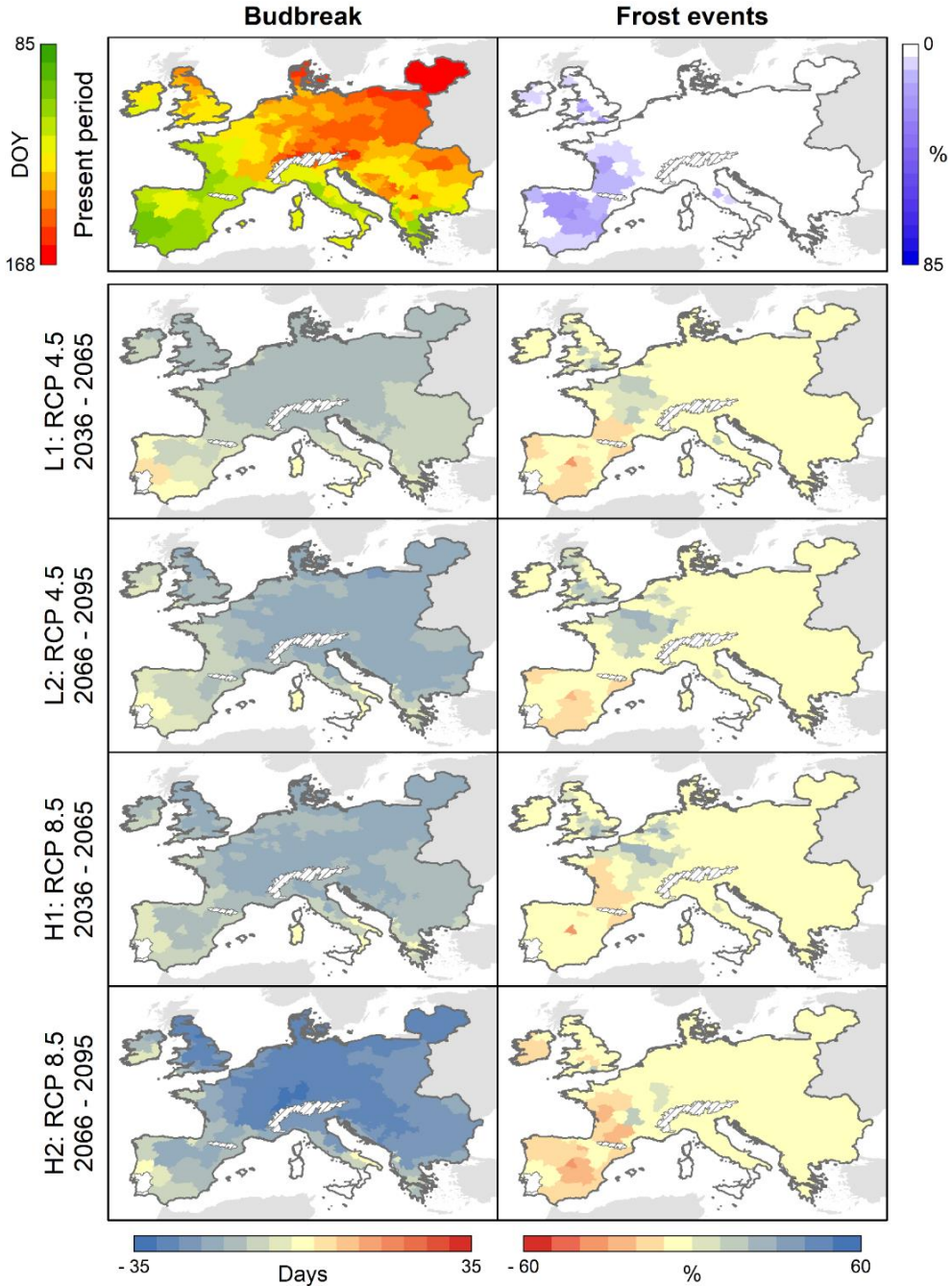


Figure 4.3. Budbreak stage and frost events for Cabernet Sauvignon variety at European NUTS2 regional scale. The maps of future emission scenarios (L1, L2, H1, H2) are obtained comparing present with future data (Days = number of days in advance or delay compared to the present period). The white areas on the map correspond to the NUTS2 zones in which budbreak is not reached while the stippled areas refer to the grid points excluded by the simulation.

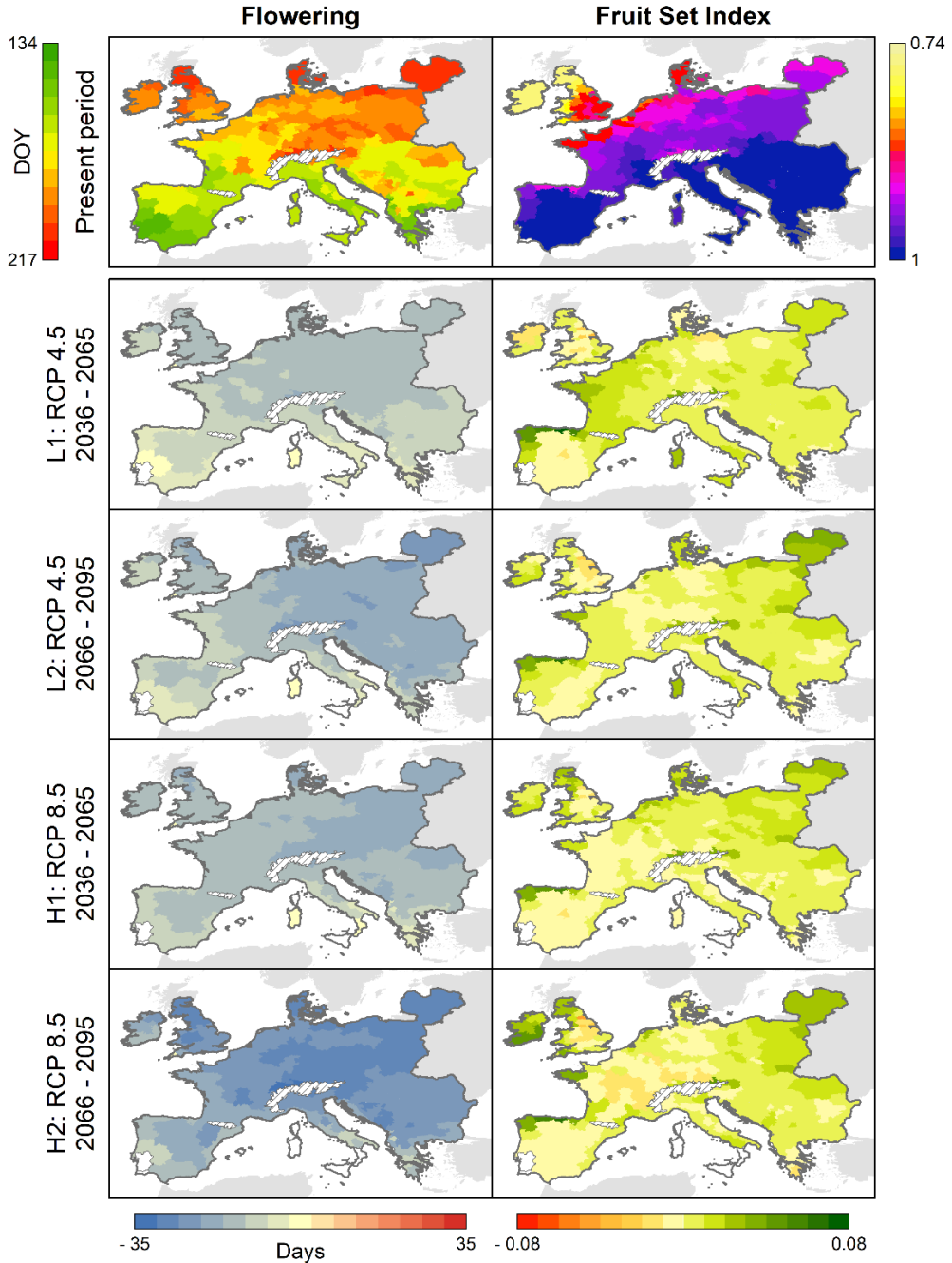


Figure 4.4. Flowering stage and fruit-set index for Cabernet Sauvignon variety at European NUTS2 regional scale. The maps of future emission scenarios (L1, L2, H1, H2) are obtained comparing present with future data (Days = number of days in advance or delay compared to the present period). The white areas on the map correspond to the NUTS2 zones in which budbreak is not reached while the stippled areas refer to the grid points excluded by the simulation.

On this basis, a higher impact of climate change is estimated on budbreak for ME and L compared to VE and E varieties in western Europe. In France, for instance, Glera and Chardonnay showed the lowest variability between the present period and H2 (on average 16 days) while Merlot and Cabernet Sauvignon resulted as more affected by climate change (on average 21–22 days). Moreover, less difference in flowering time is expected between Chardonnay and Glera (on average 18–19 days) compared to Merlot and Cabernet Sauvignon (on average 21 days). In some regions such as Sardinia and Sicily, the model failed at calculating budbreak and flowering in H2 (e.g. stages not reached) because these stages were not completed within the time window allowed (white areas on the maps).

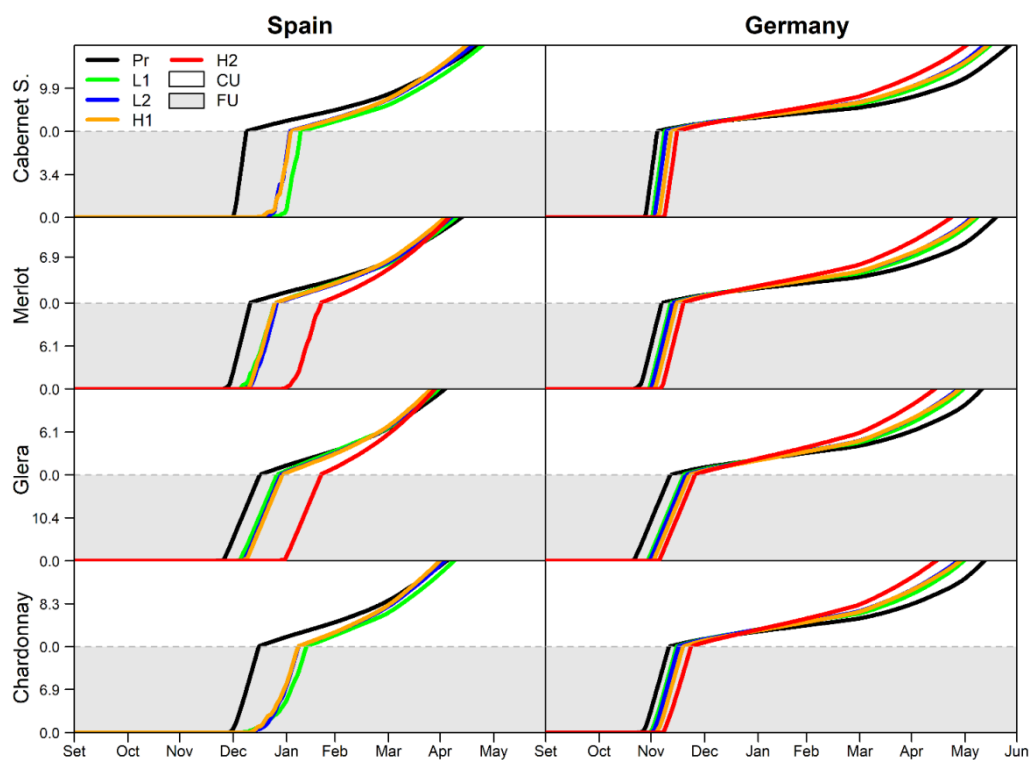


Figure 4.5. Trend of endo-dormancy and eco-dormancy period under different climatic scenarios considering an average year calculated using the mean of each day of 300 years of simulation on two representative grid points of Spain and Germany (Pr=Present; L1=Low emission Scenario RCP 4.5 2036-2065; L2=Low emission Scenario RCP 4.5 2066-2095; H1=High emission Scenario RCP 8.5 2036-2065; H2=High emission Scenario RCP 8.5 2066-2095; CU =Chilling Units; FU = Forcing Units).

Depending on the predicted earlier budbreak, frost events were estimated to increase in central Europe. In Germany, frost events increase from L1 (0.3-28%) to H1 (4–39%), whilst they decrease for H2 (0.4–21%), considering Cabernet Sauvignon as the minimum value and Glera as the maximum (Fig. 6). By contrast, a marked reduction of frost risk is predicted for the Atlantic regions, notably France, Spain and the UK. In Spain for instance, frost events decrease for Glera from L1 (25%) to H2 (11%), respectively, whilst in the UK where frost events will range on average from 40% for L1 to 7% for H2 compared to the present period considering all varieties. In this context, the increasing temperature under the future scenarios determines a decrease in frost events percentage for Glera (i.e. from 42% in the present period to 18% for H2 on average) while a slight increase is expected for Cabernet Sauvignon in France (i.e. from 3% in the present period to 5% for H2 on average). However, the frequency of frost events remains higher for Glera compared to Cabernet Sauvignon across Europe.

Although the spatial variability of FSI followed a latitudinal and longitudinal gradient with different results between countries (e.g. UK vs Italy, Fig. 2; Fig. 4), the use of varieties with different phenological cycles and different emission scenarios did not produce a strong variability on FSI (Fig. 2; Fig. 4 and Supplementary Material Fig. A.2 and A.4). According to the lesser shift of flowering stage, the greater improvement of FSI was expected for northern Europe (e.g. UK) while a decrease of FSI was particularly evident in southern Europe (e.g. south of Italy).

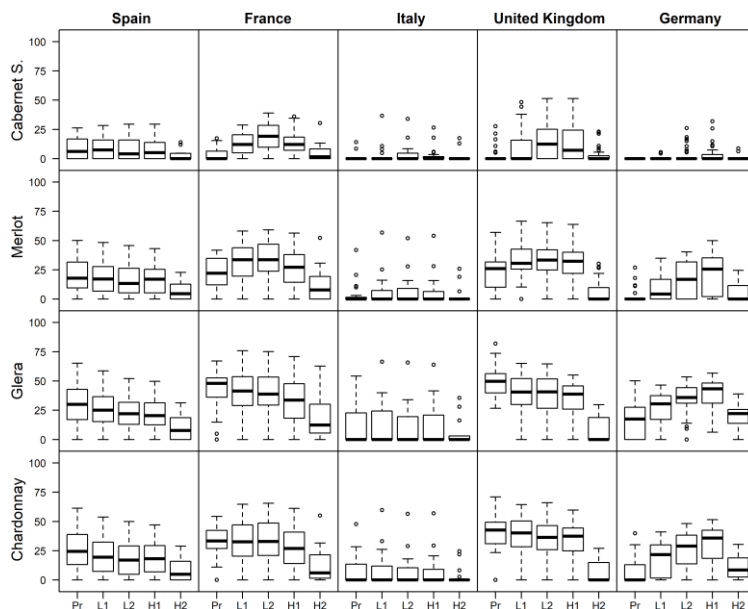


Figure 4.6. Distribution of frost events for present and future scenarios for each variety and country (Pr=Present; L1=Low emission Scenario RCP 4.5 2036-2065; L2=Low emission Scenario RCP 4.5 2066-2095; H1=High emission Scenario RCP 8.5 2036-2065; H2=High emission Scenario RCP 8.5 2066-2095).

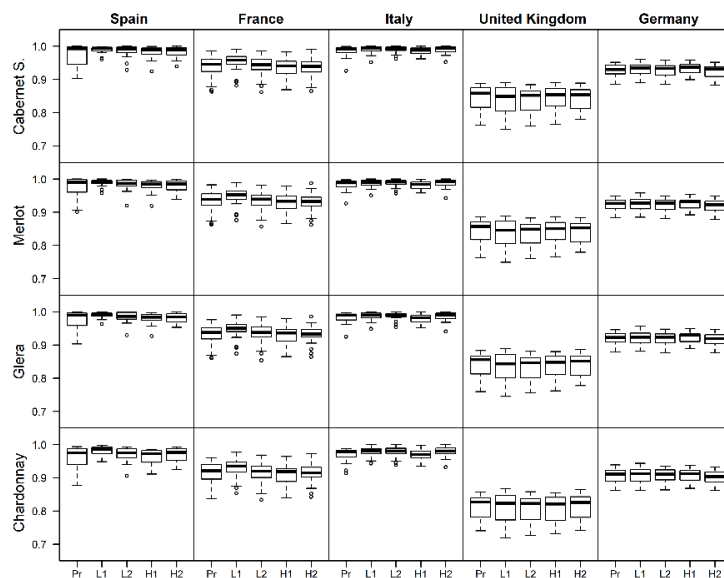


Figure 4.7. Distribution of the fruit-set index for present and future scenarios for each variety and country (Pr=Present; L1=Low emission Scenario RCP 4.5 2036-2065; L2=Low emission Scenario RCP 4.5 2066-2095; H1=High emission Scenario RCP 8.5 2036-2065; H2=High emission Scenario RCP 8.5 2066-2095).

4.4. Discussion

Over the last decades, the relationships between mean climate change and phenological timing have already been investigated using long-term datasets of several varieties (Tomasi et al., 2011). In this context, the combined effect of mean climate change and extremes is expected to become a fundamental crop yield-determining factor under future scenarios (Challinor et al., 2014; Yang et al., 2017), so an impact assessment must be performed considering both these issues (Moriondo and Bindi, 2007; Moriondo and Bindi, 2006).

Accordingly, in this work we applied a statistical downscaling that, while removing the biases in RCM outputs, allowed for the reproduction of changes in climate variability as outlined by RCM simulations (Moriondo et al., 2010; Semenov and Stratonovitch, 2010).

The simulation results showed that in future scenarios budbreak and flowering advanced and this trend was more evident in the northeastern than southwestern regions of Europe. Similar results were obtained by Fraga et al. (2016), who evidenced an earlier occurrence for southern/western Spain as compared to northern/eastern European regions considering a standard variety suitable for several wine-producing regions. By contrast, the evaluation of the performance of varieties with different development timing (VE, ME, E, and L) in this paper emphasized that the effect of climate change and extreme events differs depending on the length of phenological cycles.

This study evidenced, especially for western Europe, that L grapevine varieties were earlier than VE and E while ME was intermediate. These results are in accordance with the simulations of Webb et al. (2007), which highlighted that warmer climate conditions had greater influence on the budbreak stage of L compared to E in five out of six locations investigated in Australia.

The warmer climate showed a relevant impact on phenology stages, especially on budbreak estimation. Unlike previous studies in which the prediction of budbreak date is exclusively based on thermal time models (e.g. Zapata et al., 2017), this study highlights that the effect of chilling temperatures during dormancy period affects the budbreak simulation. These results are supported by a stable calibration in which field and grapevine cuttings data were used to calibrate and validate the phenology model. By contrast, the use of only field phenology data such as shown in Webb et al. (2007) may not allow to capture a wider range of variability (i.e. cold and mild winter) that affects dormancy period to be explored. Indeed, as the endo-dormancy period depends on a narrow temperature interval according to the adopted model, it is possible that in some environments high winter temperatures do not completely meet chilling requirements (Nendel, 2010), leading to slow dormancy exit (i.e. Spain). This

study showed that in the near future, some Mediterranean regions (i.e. Sardinia and Sicily in H2), may suffer from excessive temperatures that result in a lack of chilling units accumulation and finally in a missed budbreak. This was predicted for other species like olive trees (Gabaldón-Leal et al., 2017) in which the lack of chilling units in southern Andalusia (Spain) suggests as these areas will be less suitable for olive growth in the near future. These results are supported by this study in which the increased temperatures in southern regions (i.e. Spain) are expected to lead to a strong delay of chilling accumulation during the first part of the dormancy period in future scenarios (Fig. 5). On the other hand, the higher temperatures in late winter influence the eco-dormancy period by reducing the forcing accumulation time. As an example (Fig. 5), the chilling requirement in Germany is expected to be already satisfied in early winter while a longer eco-dormancy period is shown until budbreak date. In this case, the impact of increasing temperatures is greater for the European regions characterized by a longer dormancy cycle.

The effect of increased temperature on budbreak is not the only issue that influences grapevine phenology. In general, an earlier budbreak results in an earlier following stage (flowering) even if with generally less pronounced effects, as also observed by Fraga et al. (2016). This is especially due to the shift of budbreak that projects the following stage into a relatively cooler climate window that slows the thermal unit accumulation finally leading to a less evident advancement of flowering stage (Sadras and Moran, 2013). The shift of budbreak and flowering also determines an earlier physiological maturity in hotter and drier months (Dry, 1988).

Importantly, the results obtained in this study highlighted that for grapevine, as for other species like maize, wheat and olive tree (Barlow et al., 2015b; Chung et al., 2014; Gabaldón-Leal et al., 2017), changes in the occurrence of phenology stages may expose grapevine to a higher frequency of extreme events and this effect is strictly dependent on the varietal phenological cycle.

In particular, we focused on budbreak and flowering stages variability that is known to have detrimental effects on final grape yield and quality (i.e. yield reduction: Molitor et al., 2014; Trought et al., 1999; production of unbalanced wine: Jones et al., 2005). The sensitivity of grapevine tissues to frost events and the consequent bud injury has a strong impact on grape growth and yield. According to Mullins et al. (1992) and Trought et al. (1999), the occurrence of early frost events determines the depletion of reserves needed for shoot growth, leading to a decrease in shoot development and lower fruit yield with several economic repercussions. This study evidenced that a warmer climate resulted in a general decrease of frost events frequency especially in Mediterranean regions and on the northern fringes of Europe, while in eastern regions these events are even expected to increase (i.e. Germany until H1; Fig. 6). Different varieties provided insights into variations of risk exposure among those examined. A reduced frost events frequency is more evident for VE and

E varieties where the frost events frequency decreases at a higher rate with respect to ME and L varieties in western European regions. Similarly, Molitor et al. (2014) showed that frost events are expected to decrease for the early variety Muller Thurgau, as the earlier budbreak does not outweigh the seasonal temperature pattern.

By contrast, in Eastern Europe, frost events frequency is predicted to increase with respect to the baseline, especially for VE and E, while ME and L are less affected. These results therefore suggest the adoption of frost resistant and/or ME and L varieties, especially in those regions where frost events are predicted to increase. Indeed, although the climate conditions in some cooler areas are currently more favorable to VE and E varieties with a short growing season, the warmer conditions of future scenarios may lead to more suitable conditions for ME and L.

The impact of stressful temperatures during flowering is a key factor for final yield (Hale and Buttrose, 1974; Vasconcelos et al., 2009). Indeed, given that optimal temperatures for flowering range from 20 to 30 °C (Kozma, 2003; May, 2004), higher and lower temperatures during this stage impact negatively on flower formation, fruit-set, pollen germination and ultimately on grape production (Ewart and Kliwer, 1977). According to Ebadi et al. (1995), for example, a 30% decrease in flower size and pollen germination was found for Chardonnay and Shiraz with temperature drops before flowering.

In this study, the temperature around flowering date plays a key role in the FSI performances (Supplementary Material Fig. A.5, A.6, A.7 and A.8). Although the variability of FSI between countries is evident, very low differences have been found between variety and scenarios (Fig. 7). While the optimal FSI reported for southern regions (i.e. Italy) is related to the positive temperature conditions around flowering, the lower temperatures in northern areas (i.e. UK) show a negative effect on FSI performances. Moreover, flowering date estimations do not differ excessively between VE, E, ME and L varieties under future scenarios. The limited shift of the flowering stage between varieties led to complete the forcing requirement for flowering in a similar period. As mentioned before, this regulation process is due to the earlier budbreak in cooler time windows that slows the rate of forcing units accumulation for flowering (e.g. grapevine: Sadras and Moran, 2013; wheat: Sadras and Monzon, 2006).

Based on the results of this study, the effects of climate change and extreme events on early season phenology of grapevines are most evident on budbreak. Indeed, greater differences between VE, E, ME and L have been shown for frost events compared to FSI. More specifically, our results suggest that the effect of frost events at budbreak stage represents the most important factor for the selection of varieties.

4.5. Conclusions

This study highlighted the estimated dynamics of grapevine phenology (budbreak and flowering) in Europe at present and in the future considering the impact of mean climate change and the occurrence of extreme events at specific stages. Our results showed a general earlier occurrence of the phenology stages under future scenarios, which follows a latitudinal and longitudinal geographical gradient (e.g. over the H2 emission scenario budbreak occurs 28–31 days earlier in Germany and 7–11 days in Spain while flowering occurs 18–21 days earlier in France and 16–18 days in Italy). The interest in studying the impact of climate change on the phenology dynamics, as performed in this work, lies in understanding the frequency of the extreme events for four widespread varieties in Europe. In this context, the great impact of frost events at budbreak, more than suboptimal temperatures at flowering, resulted a key factor for the selection of grapevine varieties in Europe.

The phenological outcomes have been obtained taking into account the effect of temperature only and applied on the entire European domain. Accordingly, future researches should consider the effect of more weather variables (e.g. rainfall, daylength, etc.) excluding the marginal areas in which grapevine is not usually grown (e.g. unsuitable soil and climate). Future works can also take advantage of the combined impact assessment of climate change and extreme events, to be applied on grape biomass accumulation and quality process associated to different grapevine phenological cycles. An even more integrated assessment would likely be more informative about the overall effects derived from grapevine growing season shifts and on fruit/wine production in the future, ultimately allowing for greater understanding of appropriate adaptation strategies.

Chapter 5

General Discussion



Chapter 5 has been focused on the general discussions of the thesis

PhD candidate's contribution

Luisa Leolini wrote all the sections of the chapter.

5. General Discussion

5.1. UNIFI.GrapeML implementation

The UNIFI.GrapeML is a BioMA (<http://www.biomamodelling.org/>) extendible model library used for describing grapevine development and growth (Chapter 2). The most important features of BioMA biophysical models are the ease of implementation, maintenance and re-usability of both algorithms and modelling domain (Donatelli and Rizzoli, 2008). The fine-granularity of models implementation allows the discretization of the algorithms in single units, specific to isolate biophysical processes. In this context, the strength of this architecture is the introduction of alternative modelling approaches that extend the code of the original modelling solution (Donatelli et al., 2014). Indeed, the separation of data from algorithms, the reusability of I/O procedures and the fine granularity of the domain structure allow an easier implementation of alternative ways to the original modelling solutions and the hybridizing between model components (e.g., simulation of soil water and temperature; Donatelli et al., 2014). The structure of UNIFI.GrapeML, thus allows an easier discretization and implementation of the code compared to monolithic models (Donatelli et al., 2014; Donatelli and Rizzoli, 2008).

Based on these premises, the UNIFI.GrapeML has been presented in this thesis as a re-implementation of the original model of (Bindi et al., 1997a, 1997b) composed by a new structure of the model domain and new physiological modelling approaches for the single plant processes (Fig. 2.3 and 3.2).

For example, two alternative ways are adopted to describe the phenological development process. A chilling-forcing approach (CF model) was introduced without replacing the original model of Bindi et al. (1997a, 1997b) exclusively based on GDD accumulation. In this context, the model users can decide to activate CF or GDD phenological processes based on their needs. The use of a CF model, for example, may result more adequate for estimating grapevine phenology in a context of warmer climate. Under current climate conditions, indeed, CF and GDD models evidenced similar estimation accuracy and both models are considered to be appropriated to simulate phenological development. However, the impact of high temperature on dormancy release in the next future is expected to produce a delay in chilling units accumulation and a shortening forcing period playing a key role on budbreak estimation (Fila et al., 2014; García de Cortázar-Atauri et al., 2009a; Parker et al., 2011). In this case, GDD models do not account the chilling unit accumulation process and thus generally overestimate the budbreak date. According to Moriondo et al. (2015), some of the most famous grapevine simulation models are characterized by phenological development process based on thermal time accumulation that start from a fixed day of the year (Ben-Asher et al., 2006; Bindi et al., 1997a, 1997b; Cola

et al., 2014; García de Cortázar-Atauri et al., 2009a; Wermelinger and Baumgartner, 1991) without considering the dormancy period. However, the forthcoming effect of the mean climate change motivate the modelers to take into account the effect of higher temperature on both dormancy and post-dormancy period (Brisson et al., 2009; Godwin et al., 2002; Nendel and Kersebaum, 2004).

On these basis, despite the mean climate change is expected to produce detrimental effect on grapevine growth in future scenarios (i.e. advancement of phenological cycle), some authors evidenced as the combined effect of mean climate change and extreme events may lead to more negative impacts on grapevine yield and quality (White et al., 2006).

Accordingly, both the impact of mean climate change and the effect of extreme events should be considered in the crop simulation models for improving their estimation accuracy (Eitzinger et al., 2013; Moriondo et al., 2011b). However, the modelling of extreme events effect and their introduction in crop simulation models is currently limited (Barlow et al., 2015a; Eitzinger et al., 2013) and few examples of crop simulation models are able to reproduce the impact of extreme events (Palermi et al., 2015). Accordingly, the implementation in UNIFI.GrapeML of a strategy focused on the extreme events impact may play a key role for investigating the effect of these events on the final production. More specifically, the effect of suboptimal temperature conditions on flowering stage is considered for evaluating the reduction of fruit-set and final yield (Ewart and Kliewer, 1977; Haeseler and Fleming, 1967; Kliewer, 1977; Tukey, 1958). As mentioned before for phenology, an extreme events strategy is implemented in UNIFI.GrapeML as an alternative way of the existing model of (Bindi et al., 1997a, 1997b) and its activation is user-defined.

The introduction of the extreme temperature impact on flowering stage is useful for accounting the effect of high/low temperatures on final grapevine yield. However, despite the effect of extreme temperature, UNIFI.GrapeML considers the effect of water stress on above and below-ground biomass. As described in Chapter 2, the simulation of a soil water stress is allowed by the link between UNIFI.GrapeML (plant component) and UNIMI.SoilW (soil water balance; Donatelli et al., 2014). The UNIMI.SoilW is a soil water balance model able to investigate the dynamics of the water in the soil profile. Accordingly, UNIMI.SoilW provides to UNIFI.GrapeML the amount of water available for the plant (FTSW) useful for establishing the impact of water stress on leaf development and photosynthesis rate such as already shown in (Bindi et al., 2005, 1997a, 1997b). However, some studies evidenced that the effect of water stress influence not only aboveground biomass but also the root growth rate and consequently root elongation (Bota et al., 2004; Dry et al., 2000b). In general, crop models use a fixed root depth for their estimation even if very high differences in terms of root growth rate are shown, for instance, between young and old vines (Dry et al., 2000b; Nendel and Kersebaum, 2004). In UNIFI.GrapeML, the root growth rate

was based on two user-defined parameters for wet and dry conditions considering that the root growth rate in dry conditions is higher compared to wet conditions (Dry et al., 2000b).

Finally, a grape quality strategy for simulating sugar accumulation is implemented in UNIFI.GrapeML following the approach described by García de Cortázar-Atauri et al. (2009b). The introduction of a quality approach for investigating sugar contents during ripening period represents a new implementation method that was not accounted in the original solution of Bindi et al. (1997a, 1997b). Indeed, the importance to simulate grape sugar content results particularly evident in the high-quality wine-producing regions in which the increase of higher level of grape sugar content (and consequently alcohol level wine) and the decrease of total acidity are responsible of the production of unbalanced wines (Duchêne and Schneider, 2005; Jones et al., 2005; Jones and Davis, 2000). Accordingly, the UNIFI.GrapeML introduced a quality strategy focused on the estimation of berry sugar content concurrently to the berry water decrease. The main difference introduced in UNIFI.GrapeML compared to the approach of García de Cortázar-Atauri et al. (2009b) was related to the period of interest for sugar content accumulation (veraison-harvest vs flowering-harvest). In Chapter 3, indeed, the estimation of berry sugar content was performed from the beginning of ripening (veraison) to harvest date due to the strong relevance of sugar accumulation in this period (Coombe, 1992).

5.2. Sensitivity analysis, calibration and validation

The reliability of UNIFI.GrapeML to simulate grapevine growth, development, yield and quality was evaluated considering two cases of study in Spain and Italy (Chapter 2 and 3). In Chapter 2, the sensitivity analysis of UNIFI.GrapeML was performed using Latin Hypercube and Sobol methods on the environmental conditions of Penedès region (Spain) for assessing the most sensitive parameters that affect fruit biomass over the grapevine growing cycle. During sensitivity analysis, the model parameters varied around the default value with a narrow range of variation (Table 2.3) whose magnitude is expected to have a great impact on final output (Wang et al., 2013). For instance, our study reveals that using a specific range of variation the parameters related to leaf growth and crop partitioning processes strongly affect fruit dry biomass production. Indeed, being fruit biomass strictly dependent to light interception and biomass accumulation, parameters such as leaf area expansion or harvest index assume a high importance (Wang et al., 2013; Dzotsi et al., 2013). Moreover, our sensitivity results evidence the role of root length on fruit biomass supporting the study of Vanuytrecht et al. (2014) in which the EFAST sensitivity analysis method on AquaCrop model highlighted a significant impact of root parameters on maize yield. The response of sensitivity analysis was useful for evaluating the role of model parameters on fruit dry biomass before calibrating

phenology, soil water content and fruit biomass under the environmental conditions of Penedès region.

The calibration results evidenced satisfactory performance for the simulation of the main phenology phases (budbreak, flowering, veraison and maturity). In particular, the range of the statistical analysis (R and RMSE) reported for our results supports the studies proposed by Parker et al. (2011), Caffarra and Eccel (2010) and Fraga et al. (2015) for several varieties and different locations. In Penedès region, the limits of phenology estimation were particularly evident for budbreak and veraison while flowering and maturity showed higher performances (Chapter 2). These results are in agreement with the study of Chapter 3 with the exception of Maturity stage. Indeed, also at Susegana and Montalcino study areas higher performances of phenology simulation were found for flowering stage while lower results are showed for budbreak and veraison stages. Being phenological model driven by temperature conditions, no relationship can be found between maturity (physiological process) and harvest event (agro-management decision). Despite farmers usually harvest grapes at maturity stage, the phenological data of this phase are not always available and this information is replaced by harvest data (Barnuud et al., 2014).

After the setting of phenology, Chapter 2 presents the calibration of soil water content for evaluating the reliability of UNIFI.GrapeML and UNIMI.SoilW to simulate the soil water content dynamics of the observed data reported by Ramos and Martínez-Casasnovas (2014) for Chardonnay variety. As shown in Fig 2.6, the simulation of all four soil layers showed satisfactory performances during the period 2011-2012 in reproducing soil water dynamics with a lower accuracy for the first layer. Looking at the simulation, the slight overestimation of the first soil layer and its consequently lower accuracy should be traced back to its higher sensitivity to precipitation events (especially during spring and autumn seasons) that determine a sudden refill up to soil water content. However, the range of RRMSE value for all soil layers simulated was in agreement with the studies of Bregaglio et al., (2016), Constantin et al., (2015) and Markewitz et al. (2010). Moreover, the R and EF are consistent with the range of R proposed by Molina-Herrera et al. (2016) for soil water content at 10 cm and Toumi et al. (2016) who consider as soil water inputs both precipitation and irrigation provisions.

In Chapter 2, the calibration of fruit biomass of Chardonnay variety has been also shown. Although the LAI data were not available in the dataset, the range of LAI proposed by Pérez et al. (2013) and Chacón et al. (2009) for rainfed Spanish vines with similar bud ha^{-1} was adopted as reference value. On these basis, the satisfactory performance over the 15-years dataset evidenced a higher reliability to reproduce fruit dry biomass of the years with a relevant water deficit during the flowering-veraison period (Ramos and Martínez-Casasnovas, 2014) while lower performances are reported for the wet years (last years) in which a model overestimation was showed.

The use of a fixed coefficient for converting the observed fruit fresh biomass into fruit dry biomass allow to compare observed and simulated values. However, the alteration of wet and dry period with inter and intra-annual variability may lead to increase the variability of the berry water concentration. Future validation of fruit biomass simulation under different climate conditions could be useful for evaluating the reliability of the model to simulate fruit biomass.

Finally, the quality approach for estimating berries sugar concentration proposed by (García de Cortázar-Atauri et al., 2009b) was implemented in UNIFI.GrapeML (Chapter 3). As shown in this study and in Sadras et al. (2008), the increase of sugar content during the ripening period is related to a decrease of berry water content. Accordingly, the high performances of calibration and validation reported for the study area of Montalcino evidenced the reliability of this approach to simulate the sugar content accumulation process. In this context, some differences between simulated and observed results were found when the extreme years were showed. According to Duchêne and Schneider, (2005), Jones et al. (2005) and Jones and Davis (2000), the higher temperatures joint to lower precipitation influence grape quality reducing sugar concentration. Based on these premises, Petrie and Sadras (2008) highlighted that the advancement of maturity date caused by warmer temperature over the period 1993-2006 in Australia determined the increase of sugar concentration for Cabernet S. and Shiraz.

5.3. Application: the impact of mean climate change and extreme events at European scale

The impact of mean climate change on grapevine yield and quality has been already highlighted by several authors (Duchêne and Schneider, 2005; Jones et al., 2005; Santos et al., 2012, 2011). However, the current suitability of the most famous viticultural areas is threatened also by the effect of extreme events. Indeed, White et al. (2006) evidenced that the increase of frequency and magnitude of extreme events joint to the impact of mean climate change have a more detrimental effect on grapevine growth and quality. On these basis, several authors highlighted the fundamental role played by the effect of frost events at budbreak and high/low temperature at flowering on growth and yield (Hale and Buttrose, 1974; Molitor et al., 2014a; Mullins et al., 1992; Trought et al., 1999; Vasconcelos et al., 2009). In Chapter 4, the use of a chilling-forcing model (Chuine, 2000) was showed for assessing the impact of mean climate change on four different phenological cycles under present and future climate conditions. The variability of the phenological stages (e.g. shortening of the grapevine cycle) under different scenarios has been directly linked to the effect of the frost events at budbreak and the extreme temperatures at flowering. In particular, the equation for estimating extreme events effect around flowering was based on temperature factor of the photosynthesis scheme proposed after Farquhar

and Caemmerer (1982) and calibrated considering an extensive literature survey. This equation was also introduced in UNIFI.GrapeML for taking into account the effect of high/low temperature on fruit-set and final production.

Based on these premises, this study evidenced as the impact of mean climate change generates an advance of budbreak and flowering stages especially concentrated in central/eastern and less in southern European regions as also showed by Fraga et al. (2016). The higher advancement of budbreak in central/eastern regions compared to southern Europe was related to the delay of chilling accumulation evidenced in Mediterranean regions (Fig. 4.5). These results support the study of Gabaldòn-Leal et al., (2017) for olive tree in Andalusia (Spain) in which chilling accumulation is limited by high temperatures during winter. On the other hand, the less pronounced advancement of flowering compared to budbreak stage was correlated to the shift of budbreak stage into a relatively cooler climate window. This phenomenon determine a decrease of the forcing accumulation rate and, thus, a higher number of forcing units need to reach the final requirement (Sadras and Moran, 2013). In this context, the effect of mean climate change was also evident on the different phenological cycles. Indeed, late variety highlighted an earlier occurrence of budbreak compared to very-early and early in western European regions such as also shown by Webb et al. (2007) for Cabernet S. and Chardonnay in Australia.

The overall shift of budbreak and flowering stages is expected to expose grapevine to the effect of extreme events as shown for other crops (Barlow et al., 2015a; Chung et al., 2014; Gabaldòn-Leal et al., 2017). The impact of frost events, for example, is expected to decrease especially in western Europe while an increase of these events is showed in central/eastern Europe due to the advance of budbreak stage in these areas (Fig. 4.1 and 4.3). The decrease of frost events under future scenarios is more evident for very early and early varieties compared to middle-early and late varieties in westerns regions supporting the results of (Molitor et al., 2014a). Accordingly, the results of Chapter 4 suggest the use of frost resistant varieties for the next future especially for those regions in which frost events evidenced a possible increase. Indeed, the future warmer conditions may lead to a more suitable conditions for middle-early and late compared to very-early and early varieties currently more adapted to northern regions.

Finally, the impact of high/low temperature around flowering stage showed lower difference between varieties and scenarios compared to the results obtained for frost events (Fig.4.6 and 4.7). A more evident effect of Fruit-Set Index equation was showed comparing northern and southern European regions, showing as the northern areas appeared less suitable for fruit-set event. In general, the low variability highlighted by the application of Fruit-Set Index between varieties and scenarios was determined by the occurrence of flowering stage. Probably, the regulation process that determine the occurrence of budbreak in cooler time windows, especially for very-

early and early varieties, force a slow rate of forcing unit accumulation leading to similar flowering occurrence between varieties (Sadras and Moran, 2013). On these basis, a lower Fruit-Set Index, as found for the northern regions, is strongly correlated to the production of final yield (Hale and Buttrose, 1974; Vasconcelos et al., 2009). Indeed, the higher and lower temperatures conditions of flowering stage negatively influence the flower formation, fruit-set, pollen germination and thus on the grapevine production (Ewart and Kliewer, 1977; Kliewer, 1977). The results of the Chapter 4 suggest the need to test the equation of Fruit-Set Index in specific greenhouse experiments at different temperature regimes and on different varieties. Moreover, the combined effect of extreme events related to water stress conditions, different CO₂ concentrations, temperature regimes (high and low temperatures at different phenological stages), etc. should be furtherly investigated and proposed in crop simulation models as, for example, yield-reducing factors.

5.4. Future implementations

The main feature of the UNIFI.GrapeML in BioMA is the possibility to implement several alternative approaches compared to the original modelling solution. This aspect allows the extension of the component as new models on grapevine are developed.

Phenological development process, for example, may be integrated with new approaches to give the choice between alternative options. After the introduction of chilling-forcing and growing degree days models, existing sophisticated modelling approaches (Fishman et al., 1987a, 1987b) could be investigated through specific experiments and more dynamically implemented into crop simulation models.

Concerning the phenological stages, the introduction of the effects of extreme events as low temperatures around budbreak stage should be implemented. As evidenced in Chapter 4, the impact of frost events around budbreak was found to increase in some European regions playing a key role on grapevine growth and production. Accordingly, joint to the effect of high/low temperatures on flowering stage, the impact of frost events should also be added to UNIFI.GrapeML.

The atmospheric CO₂ increase is one of the main driver to be considered in climate change simulation studies. UNIFI.GrapeML presents models to simulate the effect of CO₂ concentration on radiation use efficiency and biomass accumulation process. However, some authors reported a similar effect of CO₂ on water use efficiency (Tubiello and Ewert, 2002). Accordingly, modelling the impact of CO₂ concentration on water use efficiency could allow the evaluation of the plant response in terms of biomass accumulation in a CO₂ enriched environment.

Moreover, despite the soil water dynamics play a fundamental role on the plant growth and production, also soil nutrients availability has a strong impact on

grapevine yield and quality. In future, the link between grape component and a soil nitrogen balance is strongly recommended. As showed by Nendel and Kersebaum (2004) and Wermelinger and Baumgartner (1991), the nitrogen content deficiency in the soil layers led to a reduced biomass accumulation with particular influences on shoot and leaf growth. However, several nitrogen models are mainly driven by abiotic variables (i.e. water, temperature, etc.; Soltani and Sinclair, 2012) without considering the impact of microorganisms on organic matter degradation (Brisson et al., 2009, 1998). Thus, a more integrate approach is need for introducing the micro-organisms dynamics on soil nitrogen degradation.

Finally, UNIFI.GrapeML presents the quality strategy for evaluating the sugar accumulation over the ripening period providing a useful tool for investigating the dynamics of grape quality under future scenarios. Despite the implementation of the sugar accumulation approach, quality strategy lacks an approach for assessing the titratable acidity. This aspect assumes a relevant importance especially under future climatic scenarios in which the warmer temperatures are expected to produce an increase of the berries sugar concentration and a decrease of the titratable acidity with the production of unbalanced wines.

Chapter 6

Conclusions



Chapter 6 shows the conclusions of the thesis

PhD candidate's contribution

Luisa Leolini wrote all the sections of the chapters

6. Conclusions

Over the last years, the grapevine simulations models have been recognized as promising tools for investigating vine behavior and production. Indeed, the role and importance of viticulture is largely spread around the world and, especially in the most famous wine-producing regions, the high-quality wine production plays a key role in local economy.

Building on these premises, this research reported the results of the implementation of a new software component (UNIFI.GrapeML) used for reproducing the main physiological processes of the grapevine. On these basis, for improving the extendibility and re-usability of the different parts and the easier implementation of the algorithms, the model was built in the BiOMA software environment in which the fine-granularity of the code represent the main prerogative of the biophysical models. Compared to the original model of Bindi et al. (1997a, 1997b), UNIFI.GrapeML showed new implementations, such as (i) the introduction of chilling-forcing approach for phenological development, (ii) the implementation of a fruit-set equation for estimating the extreme events around flowering, (iii) a root deepening approach for evaluating root growth according to water stress conditions of the soil and (iv) a quality method for sugar content estimation. These implementations were useful for improving the simulation accuracy such as shown in the field level application on phenology, soil water dynamics and fruit dry biomass. Indeed, the feasibility of the grape growth and development and quality process UNIFI.GrapeML was tested in Penedès region (Spain) and Montlacio (Italy) on two different varieties, Chardonnay and Sangiovese. In Penedès region, the results of sensitivity analysis evidenced a strong impact of leaf area and fruit partitioning parameters on the final fruit biomass. Moreover, the calibration of soil water content, phenology and yield showed satisfactory results. In Montalcino area, the quality approach based on the relationship between Brix degree accumulation and berry water content decrease was tested over the period 1998-2015. The results showed high performances during the calibration and validation procedures when simulated and observed sugar content data were compared.

Finally, in order to evaluate the impact of climate change and extreme events on grapevine development, the budbreak and flowering stages of some varieties with different phenological cycle length was analyzed at European scale under different climate scenarios. More specifically, the effect of the mean climate change was evaluated using a chilling-forcing model for accounting the endo-dormancy and eco-dormancy period. The impact of extremes was evaluated considering the minimum temperature at budbreak and the high and low temperature conditions at flowering stage. In this last case, the equation implemented in UNIFI.GrapeML for estimating Fruit-Set Index was applied in Europe for accounting the effect of extreme

temperature around flowering. The results showed an advance of both phases for all varieties evidencing a European latitudinal and longitudinal gradient as consequence of the mean climate change impact. Moreover, a strong decrease of frost events was highlighted especially in western Europe while a low sensitivity of Fruit-Set Index was showed between varieties and scenarios at flowering stage. The higher differences of Fruit-Set Index were showed comparing the Northern and Southern European regions.

Based on the previous results, the aim of this research has been reached through the presentation of the software library UNIFI.GrapeML, which models were calibrated and validated in different pedo-climatic conditions. Future steps and research should be focused on new functional implementations as well as on the applications of the model capabilities in different environments.

References

- Acutis, M., Confalonieri, R., 2006. Optimization algorithms for calibrating cropping systems simulation models. A case study with simplex-derived methods integrated in the WARM simulation environment. *Riv. Ital. di Agrometeorol.* 11, 26–34.
- Allison, L.E., 1965. Organic carbon. In: Black, C.A. (Ed.), *Methods of Soil Analysis. Part 2. Chemical and Microbiological Properties*. Am. Soc. Agron. Publ. 9, pp. 1367–1379.
- Allen, R.G., Pereira, L.S., Raes, D., Smith, M., Ab, W., 1998. *Crop evapotranspiration - Guidelines for computing crop water requirements*. Rome. doi:10.1016/j.eja.2010.12.001
- Amir, J., Sinclair, T.R., 1991. A model of water limitation on spring wheat growth and yield. *F. Crop. Res.* 28, 59–69.
- Asseng, S., Ewert, F., Rosenzweig, C., Jones, J.W., Hatfield, J.L., Ruane, A.C., Brisson, N., 2013. Uncertainty in simulating wheat yields under climate change. *Nat. Clim. Chang.* 3, 827–832. doi:10.1038/nclimate1916.
- Bannayan, M., Crout, N., 1999. A stochastic modelling approach for real-time forecasting of winter wheat yield. *F. Crop. Res.* 62, 85–95. doi:10.1016/S0378-4290(99)00008-8.
- Barlow, K.M., Christy, B.P., O’Leary, G.J., Riffkin, P.A., Nuttall, J.G., 2015. Simulating the impact of extreme heat and frost events on wheat crop production: A review. *F. Crop. Res.* 171, 109–119. doi:10.1016/j.fcr.2014.11.010.
- Barnuud, N.N., Zerihun, A., Gibberd, M., Bates, B., 2014. Berry composition and climate: Responses and empirical models. *Int. J. Biometeorol.* 58, 1207–1223. doi:10.1007/s00484-013-0715-2.
- Bassu, S., Brisson, N., Durand, J.L., Boote, K., Lizaso, J., Jones, J.W., Rosenzweig, C., Ruane, A.C., Adam, M., Baron, C., Basso, B., Biernath, C., Boogaard, H., Conijn, S., Corbeels, M., Deryng, D., De Sanctis, G., Gayler, S., Grassini, P., Hatfield, J., Hoek, S., Izaurrealde, C., Jongschaap, R., Kemanian, A.R., Kersebaum, K.C., Kim, S.H., Kumar, N.S., Makowski, D., Müller, C., Nendel, C., Priesack, E., Pravia, M.V., Sau, F., Shcherbak, I., Tao, F., Teixeira, E., Timlin, D., Waha, K., 2014. How do various maize crop models vary in their responses to climate change factors? *Glob. Chang. Biol.* 20, 2301–2320. doi:10.1111/gcb.12520.
- Becker N., Zimmermann H. 1984. Influence de divers apports d’eau sur les vignes en pots, sur la maturité des sarments, le développement des baies et la qualité du vin. *Bulletin de l’OIV*, 573–583.

- Bellocchi, G., Rivington, M., Donatelli, M., Matthews, K., 2010. Validation of biophysical models: Issues and methodologies. *Agron. Sustain. Dev.* 30, 109–130.
- Ben-Asher, J., van Dam, J., Feddes, R.A., Jhorar, R.K., 2006. Irrigation of grapevines with saline water. II. Mathematical simulation of vine growth and yield. *Agric. Water Manag.* 83, 22–29. doi:10.1016/j.agwat.2005.11.006
- Bettini, O., 2015. Eu-27. Wine Annual Report and Statistics 2015.
- Bindi, M., Bellesi, S., Orlandini, S., Fibbi, L., Moriondo, M., Sinclair, T., 2005. Influence of Water Deficit Stress on Leaf Area Development and Transpiration of Sangiovese Grapevines Grown in Pots 3, 68–72.
- Bindi, M., Fibbi, L., Lanini, M., Miglietta, F., 2001a. Free Air CO₂ Enrichment (FACE) of grapevine (*Vitis vinifera* L.): I. Development and testing of the system for CO₂ Enrichment. *Eur. J. Agron.* 14, 135–143. doi:10.1016/S1161-0301(00)00092-7.
- Bindi, M., Fibbi, L., Miglietta, F., 2001b. Free Air CO₂ Enrichment (FACE) of grapevine (*Vitis vinifera* L.): II. Growth and quality of grape and wine in response to elevated CO₂ concentrations. *Eur. J. Agron.* 14, 145–155. doi:10.1016/S1161-0301(00)00093-9.
- Bindi, M., Miglietta, F., Gozzini, B., Orlandini, S., Seghi, L., 1997a. A simple model for simulation of growth and development in grapevine (*Vitis vinifera* L.). II. Model validation. *Vitis* 36, 73–76.
- Bindi, M., Miglietta, F., Gozzini, B., Orlandini, S., Seghi, L., 1997b. A simple model for simulation of growth and development in grapevine (*Vitis vinifera* L.). I. Model Description. *Vitis* 36, 67–71.
- BioMA. <http://www.biomamodelling.org/>. (accessed 21 October 2017).
- Bock, A., Sparks, T.H., Estrella, N., Menzel, A., 2013. Climate-Induced Changes in Grapevine Yield and Must Sugar Content in Franconia (Germany) between 1805 and 2010. *PLoS One* 8, e69015. doi:10.1371/journal.pone.0069015.
- Bota, J., Stasyk, O., Flexas, J., Medrano, H., 2004. Effect of water stress on partitioning of 14 C-labelled photosynthates in *Vitis vinifera*. *Funct. Plant Biol.* 31, 697–708. doi:10.1071/FP03262.
- Botelho, R.V., Pavanello, A.P., José, E., Pires, P., Terra, M.M., Marques, M., Müller, L., 2007. Effects of Chilling and Garlic Extract on Bud Dormancy Release in Cabernet Sauvignon Grapevine Cuttings. *Am. J. Enol. Vitic.* 58, 402–404.
- Boulton, R.B., Singleton, V.L., Bisson, L.F., Kunkee, R.E., 1996. Nitrogen metabolism during fermentation. *Princ. Pract. Winemak.* 153–167.
- Bregaglio, S., Donatelli, M., 2015. A set of software components for the simulation of plant airborne diseases. *Environ. Model. Softw.* 72, 426–444. doi:10.1016/j.envsoft.2015.05.011.

- Bregaglio, S., Orlando, F., Forni, E., Gregorio, T. De, Falzoi, S., Boni, C., Pisetta, M., Confalonieri, R., 2016. Development and evaluation of new modelling solutions to simulate hazelnut (*Corylus avellana* L.) growth and development. *Ecol. Modell.* 329, 86–99. doi:10.1016/j.ecolmodel.2016.03.006.
- Brilli, L., Buscioni, G., Moriondo, M., Bindi, M., Vincenzini, M., 2014. Influence of Interannual Meteorological Variability on Yeast Content and Composition in Sangiovese Grapes. *Am. J. Enol. Vitic.* 65, 375–380. doi:10.5344/ajev.2014.13116.
- Brisson, N., Launay, M., Mary, B., Beaudoin, N., 2009. Conceptual basis, formalisations and parameterization of the STICS crop model, QUAE. ed. Versailles.
- Brisson, N., Mary, B., Ripoche, D., Jeuffroy, M.H., Ruget, F., Nicoullaud, B., Gate, P., Devienne-Barret, F., Antonioletti, R., Durr, C., Richard, G., Beaudoin, N., Recous, S., Tayot, X., Plenet, D., Cellier, P., Machet, J.-M., Meynard, J.M., Delécolle, R., 1998. STICS: a generic model for the simulation of crops and their water and nitrogen balances. I. Theory and parameterization applied to wheat and corn. *Agronomie* 18, 311–346. doi:10.1051/agro:19980501.
- Brun and Cellier. 1992. Les gelées de printemps dans les vignobles septentrionaux. *Progrès Agricole et Viticole*.
- Bucelli, P., Costantini, E.A.C., Storchi, P., 2010. It is possible to predict sangiovese wine quality through a limited number of variables measured on the vines. *J. Int. des Sci. la Vigne du Vin* 44, 207–218. doi:10.20870/oenone.2010.44.4.1473.
- Bucur, G.M., Babes, A.C., 2015. Research on Trends in Extreme Weather Conditions and their Effects on Grapevine in Romanian Viticulture, *Bulletin UASVM Horticulture*. doi:10.15835/buasvmcn-hort.
- Caffarra, A., Eccel, E., 2010. Increasing the robustness of phenological models for *Vitis vinifera* cv. Chardonnay. *Int. J. Biometeorol.* 54, 255–267. doi:10.1007/s00484-009-0277-5.
- Campbell, G.S., 1985. *Soil physics with BASIC: transport models for soil-plant systems*. Elsevier.
- Cappelli, G., Bregaglio, S., Romani, M., Feccia, S., Confalonieri, R., 2014. A software component implementing a library of models for the simulation of pre-harvest rice grain quality. *Comput. Electron. Agric.* 104, 18–24. doi:10.1016/j.compag.2014.03.002
- Celette, F., Ripoche, A., Gary, C., 2010. WaLIS-A simple model to simulate water partitioning in a crop association: The example of an intercropped vineyard. *Agric. Water Manag.* 97, 1749–1759. doi:10.1016/j.agwat.2010.06.008
- Chacón, J.L., García, E., Martínez, J., Romero, R., Gómez, S., 2009. Impact of the vine water status on the berry and seed phenolic composition of “Merlot” (*Vitis vinifera* L.) cultivated in a warm climate: Consequence for the style of wine. *Vitis - J. Grapevine Res.* 48, 7–9.

- Challinor, A.J., Watson, J., Lobell, D.B., Howden, S.M., Smith, D.R., Chhetri, N., 2014. A meta-analysis of crop yield under climate change and adaptation. *Nat. Clim. Chang.* 4, 287–291. doi:10.1038/nclimate2153.
- Chaves, M.M., Santos, T.P., Souza, C.R., Ortuño, M.F., Rodrigues, M.L., Lopes, C.M., Maroco, J.P., Pereira, J.S., 2007. Deficit irrigation in grapevine improves water-use efficiency while controlling vigour and production quality. *Ann. Appl. Biol.* 150, 237–252. doi:10.1111/j.1744-7348.2006.00123.x
- Chaves, M.M., Zarrouk, O., Francisco, R., Costa, J.M., Santos, T., Regalado, A.P., Rodrigues, M.L., Lopes, C.M., 2010. Grapevine under deficit irrigation: hints from physiological and molecular data. *Ann. Bot.* 105, 661–676. doi:10.1093/aob/mcq030
- Chuine, I., 2000. A Unified Model for Budburst of Trees. *J. Theor. Biol.* 207, 337–347. doi:10.1006/jtbi.2000.2178
- Chuine, I., Cour, P., Rousseau, D.D., 1999. Selecting models to predict the timing of flowering of temperate trees : implications for tree phenology modelling. *Plant, Cell Environ.* 22, 1–13.
- Chung, U., Gbegbelegbe, S., Shiferaw, B., Robertson, R., Yun, J.I., Tesfaye, K., Hoogenboom, G., Sonder, K., 2014. Modeling the effect of a heat wave on maize production in the USA and its implications on food security in the developing world. *Weather Clim. Extrem.* 5, 67–77. doi:10.1016/j.wace.2014.07.002.
- Clayden, J., 2014. General-Purpose optimisation with the Self-Organising Migrating Algorithm.
- Cola, G., Mariani, L., Salinari, F., Civardi, S., Bernizzoni, F., Gatti, M., Poni, S., 2014. Description and testing of a weather-based model for predicting phenology, canopy development and source-sink balance in *Vitis vinifera* L. cv. Barbera. *Agric. For. Meteorol.* 184, 117–136. doi:10.1016/j.agrformet.2013.09.008.
- Confalonieri, R., Bellocchi, G., Bregaglio, S., Donatelli, M., Acutis, M., 2010. Comparison of sensitivity analysis techniques : A case study with the rice model WARM. *Ecol. Modell.* 221, 1897–1906. doi:10.1016/j.ecolmodel.2010.04.021.
- Constantin, J., Willaume, M., Murgue, C., Lacroix, B., Therond, O., 2015. The soil-crop models STICS and AqYield predict yield and soil water content for irrigated crops equally well with limited data. *Agric. For. Meteorol.* 206, 55–68. doi:10.1016/j.agrformet.2015.02.011.
- Costantini, E.A.C. and Bucelli, P. 2014. Soil and Terroir, in: Soil security for ecosystem management. Springer International Publishing, pp. 97-113. doi:10.1007/978-3-319-00699-4_6.
- Coombe, B.G., 1992. Research on Development and Ripening of the Grape Berry. *Am. J. Enol. Vitic.* 43, 101–110. doi:10.1111/j.1755-0238.2000.tb00171.x

- Corduas, M., Cinquanta, L., Ievoli, C., 2013. The importance of wine attributes for purchase decisions: A study of Italian consumers' perception. *Food Qual. Prefer.* 28, 407–418. doi:10.1016/j.foodqual.2012.11.007
- Costantini, E.A.C., Bucelli, P., 2014. Soil and terroir, in: *Soil Security for Ecosystem Management*. Springer, pp. 97–133.
- Dai, Z.W., Vivin, P., Robert, T., Milin, S., Li, S.H., Genard, M., 2009. Model-based analysis of sugar accumulation in response to sourcesink ratio and water supply in grape (*Vitis vinifera*) berries. *Funct. Plant Biol.* 36, 527–540. doi:10.1071/FP08284.
- DAR, 2008. Mapa de Sòls (1:25.000) de l'àmbitgeogràfic de la Denominació d'Origen Penedès. Vilafranca del Penedès-Lleida. Departament d'Agricultura, Alimentació i Acció Rural, Generalitat de Catalunya.
- De la Hera-Orts, M., Martínez-Cutillas, A., López-Roca, J.M., Gómez-Plaza, E., 2005. Effect of moderate irrigation on grape composition during ripening. *Spanish J. Agric. Res.* 3, 352–361.
- Del Furia, L., Rizzoli, A., Arditi, R., 1995. Lakemaker: A general object-oriented software tool for modelling the eutrophication process in lakes. *Environ. Softw.* 10, 43–64. doi:10.1016/0266-9838(94)00016-Z
- Delgado, R., Martín, P., DelÁlamo, M., González, M.-R., 2004. Changes in the phenolic composition of grape berries during ripening in relation to vineyard nitrogen and potassium fertilisation rates. *J. Sci. Food Agric.* 84, 623–630. doi:10.1002/jsfa.1685
- Des Gachons, C.P., Van Leeuwen, C., Tominaga, T., Soyer, J.P., Gaudillère, J.P., Dubourdieu, D., 2005. Influence of water and nitrogen deficit on fruit ripening and aroma potential of *Vitis vinifera* L cv Sauvignon blanc in field conditions. *J. Sci. Food Agric.* 85, 73–85. doi:10.1002/jsfa.1919
- Dokoozlian, N.K., 1999. Chilling temperature and duration interact on the budbreak of “Perlette” grapevine cuttings. *HortScience* 34, 1054–1056.
- Donatelli, M., Bregaglio, S., Confalonieri, R., De Mascellis, R., Acutis, M., 2014. A generic framework for evaluating hybrid models by reuse and composition - A case study on soil temperature simulation. *Environ. Model. Softw.* 62, 478–486. doi:10.1016/j.envsoft.2014.04.011
- Donatelli, M., Confalonieri, R., Cerrani, I., Fanchini, D., Acutis, M., Tarantola, S., Baruth, B., 2009. LUISA (Library User Interface for Sensitivity Analysis): a generic software component for sensitivity analysis of bio-physical models, in: 18th World IMACS Congress and MODSIM09 International Congress on Modelling and Simulation. Modelling and Simulation Society of Australia and New Zealand and International Association for Mathematics and Computers in Simulation. pp. 2377–2383.

- Donatelli, M., Rizzoli, A.E., 2008. A design for framework-independent model components of biophysical systems, in: 4th Biennial Meeting of International Congress on Environmental Modelling and Software: Integrating Sciences and Information Technology for Environmental Assessment and Decision Making, iEMSs 2008. pp. 727–734.
- Donatelli, M., Van Evert, F.K., Di Guardo, A., Adam, M., Kansou, K., 2006. A component to simulate agricultural management. In: Voinov, A., Jakeman, A.J., Rizzoli, A.E. (Eds.), iEMSs Third Biannual Meeting: “Summit on Environmental Modelling and Software”. International Environmental Modelling and Software Society, Burlington, Vermont.
- Dos Santos, T.P., Lopes, C.M., Rodrigues, M.L., De Souza, C.R., Maroco, J.P., Pereira, J.S., Silva, J.R., Chaves, M.M., 2003. Partial rootzone drying: Effects on growth and fruit quality of field-grown grapevines (*Vitis vinifera*). *Funct. Plant Biol.* 30, 663–671. doi:10.1071/FP02180.
- Dry, P.R. 1988. Climate change and the Australian grape and wine industry. *The Australian Grapegrower and Winemaker* 300, 14–15.
- Dry, P.R., Loveys, B.R., Düring, H., 2000a. Partial drying of the rootzone of grape. I. Transient changes in shoot growth and gas exchange. *Vitis* 39, 3–7.
- Dry, P.R., Loveys, B.R., Düring, H., 2000b. Partial drying of the rootzone of grape. II. Changes in the pattern of root development. *Vitis* 39, 9–12.
- Duchêne, E., Schneider, C., 2005. Grapevine and climatic changes: a glance at the situation in Alsace. *Agron. Sustain. Dev.* 24, 93–99. doi:10.1051/agro:2004057
- Dzotsi, K.A., Basso, B., Jones, J.W., 2013. Development, uncertainty and sensitivity analysis of the simple SALUS crop model in DSSAT. *Ecol. Modell.* 260, 62–76. doi:10.1016/j.ecolmodel.2013.03.017
- Ebadi, A., May, P., Sedgley, M., Coombe, B.G., 1995. Effect of low temperature near flowering time on ovule development and pollen tube growth in the grapevine (*Vitis vinifera* L.), cvs Chardonnay and Shiraz. *Aust. J. Grape Wine Res.* 1, 11–18.
- Edwards, E.J., Unwin, D.J., Sommer, K.J., Downey, M.O., Mollah, M., 2016. The response of commercially managed, field grown, grapevines (*Vitis vinifera* L.) to a simulated future climate consisting of elevated CO₂ in combination with elevated air temperature, in: *Acta Horticulturae*. pp. 103–109. doi:10.17660/ActaHortic.2016.1115.16
- Eitzinger, J., Thaler, S., Schmid, E., Strauss, F., Ferrise, R., Moriondo, M., Bindi, M., Palosuo, T., Rotter, R., Kersebaum, K.C., Olesen, J.E., Patil, R.H., Saylan, L., Caldag, B., Caylak, O., 2013. Sensitivities of crop models to extreme weather conditions during flowering period demonstrated for maize and winter wheat in Austria. *J. Agric. Sci.* 151, 813–835. doi:10.1017/S0021859612000779.

- Erez, A., Couvillon, G.A., 1987. Characterization of the influence of moderate temperatures on rest completion in peach. *J. Am. Soc. Hortic. Sci.* 112, 677-680.
- Ewart, A., Kliewer, W.M., 1977. Effects of controlled day and night temperatures and nitrogen on fruit-set, ovule fertility, and fruit composition of several wine grape cultivars. *Am. J. Enol. Vitic.* 28, 88-95.
- FAO, 2017. <http://www.fao.org> (accessed 08 December 2017).
- FAOSTAT, 2016. <http://www.fao.org/faostat/en/> (accessed 13 October 2017).
- Farquhar, Caemmerer, 1982. Modelling of photosynthetic response to environmental conditions, in: *Physiological Plant Ecology II*. Springer, pp. 549-587.
- Ferrise, R., Trombi, G., Moriondo, M., Bindi, M., 2016. Climate Change and Grapevines: A Simulation Study for the Mediterranean Basin. *J. Wine Econ.* 11, 88-104. doi:10.1017/jwe.2014.30
- Fila, G., 2012. Modelli matematici per l'analisi della variabilità spatio-temporale della fenologia della vite. University of Padova.
- Fila, G., Di Lena, B., Gardiman, M., Storchi, P., Tomasi, D., Silvestroni, O., Pitacco, A., 2012. Calibration and validation of grapevine budburst models using growth-room experiments as data source. *Agric. For. Meteorol.* 160, 69-79. doi:10.1016/j.agrformet.2012.03.003
- Fila, G., Gardiman, M., Belvini, P., Meggio, F., Pitacco, A., 2014. A comparison of different modelling solutions for studying grapevine phenology under present and future climate scenarios. *Agric. For. Meteorol.* 195-196, 192-205. doi:10.1016/j.agrformet.2014.05.011.
- Fishman, S., Erez, A., Couvillon, G.A., 1987a. The temperature dependence of dormancy breaking in Plants: computer simulation of processes studied under controlled temperatures. *J. Theor. Biol.* 126, 309-321.
- Fishman, S., Erez, A., Couvillon, G.A., 1987b. The temperature dependence of dormancy breaking in Plants: mathematical analysis of a two-step model involving a cooperative transition. *J. Theor. Biol.* 124, 473-483.
- Flexas, J., Niinemets, Ü., Gallé, A., Barbour, M.M., Centritto, M., Diaz-Espejo, A., Douthe, C., Galmés, J., Ribas-Carbo, M., Rodriguez, P.L., Rosselló, F., Soolanayakanahally, R., Tomas, M., Wright, I.J., Farquhar, G.D., Medrano, H., 2013. Diffusional conductances to CO₂ as a target for increasing photosynthesis and photosynthetic water-use efficiency. *Photosynth. Res.* 117, 45-59. doi:10.1007/s11120-013-9844-z.
- Forrester, J.W. 1961. *Industrial Dynamics*, MIT Press, Cambridge, MA.
- Fraga, H., Costa, R., Moutinho-pereira, J., Correia, C.M., 2015. Modeling Phenology, Water Status, and Yield Components of Three Portuguese Grapevines Using the STICS Crop Model. *Am. J. Enol. Vitic.* doi:10.5344/ajev.2015.15031.

- Fraga, H., García De Cortazar-Atauri, I., Malheiro, A.C., Santos, J.A., 2016. Modelling climate change impacts on viticultural yield, phenology and stress conditions in Europe. *Glob. Chang. Biol.* 22, 3774–3788. doi:10.1111/gcb.13382.
- Gabaldón-Leal, C., Ruiz-Ramos, M., de la Rosa, R., Leòn, L., Belaj, A., Rodríguez, A., Santos, C., Lorite, I.J., 2017. Impact of changes in mean and extreme temperatures caused by climate change on olive flowering in southern Spain. *Int. J. Climatol.* doi:10.1002/joc.5048
- Gao, X., Giorgi, F., 2008. Increased aridity in the Mediterranean region under greenhouse gas forcing estimated from high resolution simulations with a regional climate model. *Glob. Planet. Change* 62, 195–209. doi:10.1016/j.gloplacha.2008.02.002
- Gao, X., Pal, J.S., Giorgi, F., 2006. Projected changes in mean and extreme precipitation over the Mediterranean region from a high resolution double nested RCM simulation. *Geophys. Res. Lett.* 33, 2–5. doi:10.1029/2005GL024954
- García de Cortázar-Atauri, I., Brisson, N., Gaudillere, J.P., 2009a. Performance of several models for predicting budburst date of grapevine (*Vitis vinifera* L.). *Int. J. Biometeorol.* 53, 317–326. doi:10.1007/s00484-009-0217-4
- García de Cortázar-Atauri, I., Brisson, N., Ollat, N., Jacquet, O., Payan, J.C., 2009b. Asynchronous Dynamics of Grapevine (*Vitis Vinifera*) Maturation: Experimental Study for a Modelling Approach. *J. Int. des Sci. la Vigne du Vin* 43, 83–97.
- Gee, G.W., Bauder, J.W., 1986. Particle-size analysis, *Methods of soil analysis: Part 1—Physical and mineralogical methods*. Soil Science Society of America, American Society of Agronomy.
- Génard, M., Lescouret, F., Gomez, L., Habib, R. 2003. Changes in fruit sugar concentrations in response to assimilate supply, metabolism and dilution: a modeling approach applied to peach fruit (*Prunus persica*). *Tree Physiology*, 23(6), 373–385. doi:10.1093/treephys/23.6.373
- Giannakopoulos, C., Sager, P., Le, Bindi, M., Moriondo, M., Kostopoulou, E., Goodess, C.M., 2009. Climatic changes and associated impacts in the Mediterranean resulting from a 2 ° C global warming. *Glob. Planet. Change* 68, 209–224. doi:10.1016/j.gloplacha.2009.06.001
- Girona, J., Marsal, J., Mata, M., Campo, J.D.E.L., Basile, B., 2009. Phenological sensitivity of berry growth and composition of Tempranillo grapevines (*Vitis vinifera* L.) to water stress. *Aust. J. Grape Wine Res.* 15, 268–277. doi:10.1111/j.1755-0238.2009.00059.x
- Godwin, D.C., White, R.J.G., Sommer, K.J., Walker, R.R., Goodwin, I., Clingeffer, P.R., 2002. VineLOGIC—a model of grapevine growth, development and water use, Eds C Dund. ed, *Managing Water*'.

- Grechi, I., Vivin, P., Hilbert, G., Milin, S., Robert, T., Gaudillère, J.-P., 2007. Effect of light and nitrogen supply on internal C:N balance and control of root-to-shoot biomass allocation in grapevine. *Environ. Exp. Bot.* 59, 139–149. doi:10.1016/j.envexpbot.2005.11.002
- Green, I.R.A., Stephenson, D., 1986. Criteria for comparison of single event models. *Hydrol. Sci. J.* 31, 395–411. doi:10.1080/02626668609491056.
- Greer, D.H., Weston, C., 2010. Heat stress affects flowering, berry growth, sugar accumulation and photosynthesis of *Vitis vinifera* cv. Semillon grapevines grown in a controlled environment. *Funct. Plant Biol.* 37, 206–214. doi:10.1071/FP09209
- Haeseler, C.W., Fleming, H.K., 1967. Response of Concord grapevines to various controlled day-temperatures. *Pennsylvania State Univ. Bull.* 739, 16.
- Hale, C.R., Buttrose, M.S., 1974. Effect of temperature on ontogeny of berries of *Vitis vinifera* L. cv. Cabernet Sauvignon. *J. Am. Soc. Hortic. Sci.* 99, 390–394.
- Hannah, L., Roehrdanz, P.R., Ikegami, M., Shepard, A. V, Shaw, M.R., Tabor, G., Zhi, L., Marquet, P.A., Hijmans, R.J., 2013. Climate change, wine, and conservation. *Proc. Natl. Acad. Sci.* 110, 6907–6912. doi:10.1073/pnas.1210127110
- Hargreaves, G.H., Samani, Z.A., 1982. Estimating potential evapotranspiration. *J. Irrig. Drain. Div.* 108, 225–230.
- Hilbert, G., Soyer, J.P., Molot, C., Giraudon, J., Milin, S., Gaudillere, J.P., 2003. Effects of nitrogen supply on must quality and anthocyanin accumulation in berries of cv. Merlot. *Vitis* 42, 69–76.
- Hlaszny, E., Hajdu, E., Bisztray, G.Y., Ladanyi, M., 2011. Comparison Of Budburst Models Predictions For kekfrankos. *Appl. Ecol. Environ. Res.* 10, 75–86.
- Huglin, P., 1978. Nouveau mode d'évaluation des possibilités héliothermiques d'un milieu viticole, in: *Proceedings of the Symposium International Sur L'écologie de La Vigne*. Ministère de l'Agriculture et de l'Industrie Alimentaire, Contança, pp. 88–98.
- Huglin, P., Schneider, C., 1998. *Biologie et écologie de la vigne*, Lavoisier. ed. Tec & Doc Lavoisier, Paris.
- Hunter, A. H., Lechowicz, M. J. 1992. Predicting the timing of budburst in temperate trees, *J. Appl. Ecol.*, 29, 597–604.
- IDESCAT, 2013. <https://www.idescat.cat/?lang=es>. (accessed 13 October 2017).
- IPCC, 2014. *Fifth Assessment Report of the Intergovernmental Panel on Climate Change*.
- IUSS Working Group, F., 2014. *World reference base for soil resources 2014 international soil classification system for naming soils and creating legends for soil maps*, FAO. Rome.

- James, L.D., Burges, S.J., 1982. Selection, calibration, and testing of hydrologic models, in: Haan, C., Johnson, H., Brakensiek, D. (Eds.), *Hydrologic Modeling of Small Watersheds*. American Society of Agricultural Engineers, St. Joseph, Mich. USA, pp. 437–472.
- Jamieson, P.D., Semenov, M.A., Brooking, I.R., Francis, G.S., 1998. Sirius: a mechanistic model of wheat response to environmental variation. *Eur. J. Agron.* 8, 161–179.
- Jones, G. V., Davis, R.E., 2000. Climate influences on grapevine phenology, grape composition, and wine production and quality for Bordeaux, France. *Am. J. Enol. Vitic.* 51, 249–261.
- Jones, G. V., White, M.A., Cooper, O.R., Storchmann, K., 2005. Climate Change and Global Wine Quality. *Clim. Change* 73, 319–343. doi:10.1007/s10584-005-4704-2
- Jones, G. V., Duff, A.A., Hall, A., Myers, J.W., 2010. Spatial Analysis of Climate in Winegrape Growing Regions in the Western United States. *Am. J. Enol. Vitic.*, 3, 313–326.
- Kliewer, W.M., 1977. Effect of High Temperatures during the Bloom-Set Period on Fruit-Set, Ovule Fertility, and Berry Growth of Several Grape Cultivars. *Am. J. Enol. Vitic.* 28, 215–222.
- Köppen, W., 1936. *Das geographische System der Klimate (Handbuch der Klimatologie, Bd. 1, Teil C)*, Apud. Beck, C.
- Kozma, P., 2003. Exploration of flower types in grapes, Floral Biology, Pollination and Fertilisation in Temperate Zone Fruit Species and Grape. *Akadémiai Kiadó, Budapest*.
- Lakso, A. N., & Johnson, R. S. (1989, September). A simplified dry matter production model for apple using automatic programming simulation software. In: II International Symposium on Computer Modelling in Fruit Research and Orchard Management, 276, pp. 141-148.
- Lavee, S., May, P., 1997. Dormancy of grapevine buds - facts and speculation. *Aust. J. Grape Wine Res.* 3, 31–46. doi:10.1111/j.1755-0238.1997.tb00114.x.
- Lawless, C., Semenov, M.A., Jamieson, P.D., 2005. A wheat canopy model linking leaf area and phenology. *Eur. J. Agron.* 22, 19–32. doi:10.1016/j.eja.2003.11.004.
- Lebon, E., Dumas, V., Pieri, P., Schultz, H.R., 2003. Modelling the seasonal dynamics of the soil water balance of vineyards. *Funct. Plant Biol.* 30, 699. doi:10.1071/FP02222.
- Lebon, E., Pellegrino, A., Louarn, G., Lecoœur, J., 2006. Branch development controls leaf area dynamics in grapevine (*Vitis vinifera*) growing in drying soil. *Ann. Bot.* 98, 175–185. doi:10.1093/aob/mcl085.

- Li, T., Hasegawa, T., Yin, X., Zhu, Y., Boote, K., Adam, M., Bregaglio, S., Buis, S., Confalonieri, R., Fumoto, T., Gaydon, D., Marcaida, M., Nakagawa, H., Oriol, P., Ruane, A.C., Ruget, F., Singh, B., Singh, U., Tang, L., Tao, F., Wilkens, P., Yoshida, H., Zhang, Z., Bouman, B., 2015. Uncertainties in predicting rice yield by current crop models under a wide range of climatic conditions. *Glob. Chang. Biol.* 21, 1328–1341. doi:10.1111/gcb.12758
- Liu, H.F., Wu, B.H., Fan, P.G., Xu, H.Y., Li, S.H., 2007. Inheritance of sugars and acids in berries of grape (*Vitis vinifera* L.). *Euphytica* 153, 99–107. doi:10.1007/s10681-006-9246-9.
- Loague, K., Green, R.E., 1991. Statistical and graphical methods for evaluating solute transport models: Overview and application. *J. Contam. Hydrol.* 7, 51–73. doi:10.1016/0169-7722(91)90038-3.
- Markewitz, D., Devine, S., Davidson, E.A., Brando, P., Nepstad, D.C., 2010. Soil moisture depletion under simulated drought in the Amazon: impacts on deep root uptake. *New Phytol.* 187, 592–607. doi:10.1111/j.1469-8137.2010.03391.x.
- Martre, P., Wallach, D., Asseng, S., Ewert, F., Jones, J.W., Rötter, R.P., Boote, K.J., Ruane, A.C., Thorburn, P.J., Cammarano, D., Hatfield, J.L., Rosenzweig, C., Aggarwal, P.K., Angulo, C., Basso, B., Bertuzzi, P., Biernath, C., Brisson, N., Challinor, A.J., Doltra, J., Gayler, S., Goldberg, R., Grant, R.F., Heng, L., Hooker, J., Hunt, L.A., Ingwersen, J., Izaurralde, R.C., Kersebaum, K.C., Müller, C., Kumar, S.N., Nendel, C., O’leary, G., Olesen, J.E., Osborne, T.M., Palosuo, T., Priesack, E., Ripoche, D., Semenov, M.A., Shcherbak, I., Steduto, P., Stöckle, C.O., Stratonovitch, P., Streck, T., Supit, I., Tao, F., Travasso, M., Waha, K., White, J.W., Wolf, J., 2015. Multimodel ensembles of wheat growth: Many models are better than one. *Glob. Chang. Biol.* 21, 911–925. doi:10.1111/gcb.12768
- Matthews, M. A., & Anderson, M. M. (1988). Fruit ripening in *Vitis vinifera* L.: responses to seasonal water deficits. *American Journal of Enology and viticulture*, 39(4), 313-320.
- May, P., 2004. Flowering and fruitset in grapevines. Lythrum Press, Adelaide, Australia.
- McGovern, P.E., Michel, R.H., 1995. The analytical and archaeological challenge of detecting ancient wine: two case studies from the ancient Near East. *Orig. Anc. Hist. wine* 57–67.
- McKay, M.D., Beckman, R.J., Conover, W.J., 1979. Comparison of three methods for selecting values of input variables in the analysis of output from a computer code. *Technometrics* 21, 239–245.
- Medrano, H., Escalona, J.M., Cifre, J., Bota, J., Flexas, J., 2003. A ten-year study on the physiology of two Spanish grapevine cultivars under field conditions: Effects of water availability from leaf photosynthesis to grape yield and quality. *Funct. Plant Biol.* 30, 607–619. doi:10.1071/FP02110.

- Miglietta, F., Gozzini, B., Orlandini, S., 1992. Simulation of leaf appearance in grapevine. *Vitic. Enol. Sci.* 47, 41–45.
- Moberg, A., Jones, P.D., 2005. Trends in indices for extremes in daily temperature and precipitation in central and western Europe, 1901 – 99. *Int. J. Climatol.* 25, 1149–1171. doi:10.1002/joc.1163.
- Molina-Herrera, S., Haas, E., Klatt, S., Kraus, D., Augustin, J., Magliulo, V., Tallec, T., Ceschia, E., Ammann, C., Loubet, B., Skiba, U., Jones, S., Brümmer, C., Butterbach-Bahl, K., Kiese, R., 2016. A modeling study on mitigation of N₂O emissions and NO₃ leaching at different agricultural sites across Europe using LandscapeDNDC. *Sci. Total Environ.* 553, 128–140. doi:10.1016/j.scitotenv.2015.12.099.
- Molitor, D., Caffarra, A., Sinigoj, P., Pertot, I., Hoffmann, L., Junk, J., 2014. Late frost damage risk for viticulture under future climate conditions: a case study for the Luxembourgish winegrowing region. *Aust. J. Grape Wine Res.* 20, 160–168. doi:10.1111/ajgw.12059.
- Moriondo, M., Bindi, M., 2006. Comparison of temperatures simulated by GCMs, RCMs and statistical downscaling: potential application in studies of future crop development. *Clim. Res.* 30, 149–160.
- Moriondo, M., Bindi, M., 2007. Impact of climate change on the phenology of typical Mediterranean crops. *Ital. J. Agrometeorol.* 5–12. doi:10.1007/s00425-010-1258-y.
- Moriondo, M., Bindi, M., Kundzewicz, Z.W., Szwed, M., 2010. Impact and adaptation opportunities for European agriculture in response to climatic change and variability. *Mitig. Adapt. Strateg. Glob. Chang.* 15, 657–679. doi:10.1007/s11027-010-9219-0.
- Moriondo, M., Bindi, M., Fagarazzi, C., Ferrise, R., Trombi, G., 2011a. Framework for high-resolution climate change impact assessment on grapevines at a regional scale. *Reg. Environ. Chang.* 11, 553–567. doi:10.1007/s10113-010-0171-z.
- Moriondo, M., Giannakopoulos, C., Bindi, M., 2011b. Climate change impact assessment: The role of climate extremes in crop yield simulation. *Clim. Change* 104, 679–701. doi:10.1007/s10584-010-9871-0.
- Moriondo, M., Ferrise, R., Trombi, G., Brilli, L., Dibari, C., Bindi, M., 2015. Modelling olive trees and grapevines in a changing climate. *Environ. Model. Softw.* 72, 387–401. doi:10.1016/j.envsoft.2014.12.016.
- Moriondo, M., Jones, G. V., Bois, B., Dibari, C., Ferrise, R., Trombi, G., Bindi, M., 2013. Projected shifts of wine regions in response to climate change. *Clim. Change* 119, 825–839.
- Moutinho-Pereira, J.M., Correia, C., Falco, V., 2006. Effects of elevated CO₂ on grapevines grown under Mediterranean field conditions – impact on grape and wine composition, in: *Proceedings XXXth OIV World Congress, Budapest*. pp. 2–12.

- Mullins, M.G., Bouquet, A., Williams, L.E., 1992. *Biology of the grapevine*. Cambridge University Press, Great Britain.
- Murthy, V.R.K., 2004. Crop Growth Modeling and Its Applications in Agricultural Meteorology. *Satell. Remote Sens. GIS Appl. Agric. Meteorol.* 235–261.
- Narciso, G., Ragni, P., Venturi, A., 1992. Agrometeorological aspects of crops in Italy, Spain and Greece: a summary review for common and durum wheat, barley, maize, rice, sugar beet, sunflower, soya bean, rape, potato, tobacco, cotton, olive and grape crops. Commission of the European Communities.
- Nelder, J.A., Mead, R., 1965. A simplex method for function minimization. *Comput. J.* 7, 308–313.
- Nendel, C., Kersebaum, K.C., 2004. A simple model approach to simulate nitrogen dynamics in vineyard soils. *Ecol. Modell.* 177, 1–15. doi:10.1016/j.ecolmodel.2004.01.014.
- Nendel, C., 2010. Grapevine bud break prediction for cool winter climates. *Int. J. Biometeorol.* 54, 231–241. doi:10.1007/s00484-009-0274-8.
- Oberholster, A., Botes, M.P., Lambrechts, M., 2010. Phenolic composition of Cabernet Sauvignon (*Vitis vinifera*) grapes during ripening in four South African winegrowing regions. *J. Int. Sci. Vigne Vin, Spec. issue Macrowine* 33–40.
- OIV, 2015. Global state of conditions report: developments and trends.
- OIV, 2016. State of the Vitiviniculture World Market, International Organization of Vine and Wine.
- OIV, 2017. State of the Vitiviniculture World Market, 38th OIV World Congress of vine and wine.
- Ojeda, H., Andary, C., Kraeva, E., Carbonneau, A., Deloire, A., 2002. Influence of pre- and postveraison water deficit on synthesis and concentration of skin phenolic compounds during berry growth of *Vitis vinifera* cv. Shiraz. *Am. J. Enol. Vitic.* 53, 261–267.
- Olesen, J.E., Bindi, M., 2002. Consequences of climate change for European agricultural productivity, land use and policy. *Eur. J. Agron.* 16, 239–262.
- Oliveira, M., 1998. Calculation of Budbreak and Flowering Base Temperatures for *Vitis vinifera* cv. Touriga Francesa in the Douro Region of Portugal. *Am. J. Enol. Vitic.* 49, 74–78.
- Oyarzun, R.A., Stockle, C.O., Whiting, M.D., 2007. A simple approach to modeling radiation interception by fruit-tree orchards. *Agric. For. Meteorol.* 142, 12–24. doi:10.1016/j.agrformet.2006.10.004.
- Paleari, L., Movedi, E., Pagani, V., Bregaglio, S., Confalonieri, R., 2015. A software component for simulation of the impacts of weather extremes on agricultural production.

- Pallas, B., Loi, C., Christophe, A., Cournede, P.H., Lecoeur, J., 2011. Comparison of three approaches to model grapevine organogenesis in conditions of fluctuating temperature, solar radiation and soil water content. *Ann. Bot.* 107, 729–745. doi:10.1093/aob/mcq173.
- Parker, A.K., De Cortázar-Atauri, I.G., Van Leeuwen, C., Chuine, I., 2011. General phenological model to characterise the timing of flowering and veraison of *Vitis vinifera* L. *Aust. J. Grape Wine Res.* 17, 206–216. doi:10.1111/j.1755-0238.2011.00140.x.
- Parker, A., de Cortázar-Atauri, I.G., Chuine, I., Barbeau, G., Bois, B., Boursiquot, J.M., Cahurel, J.Y., Claverie, M., Dufourcq, T., Gény, L., Guimberteau, G., Hofmann, R.W., Jacquet, O., Lacombe, T., Monamy, C., Ojeda, H., Panigai, L., Payan, J.C., Lovelle, B.R., Rouchaud, E., Schneider, C., Spring, J.L., Storchi, P., Tomasi, D., Trambouze, W., Trought, M., van Leeuwen, C., 2013. Classification of varieties for their timing of flowering and veraison using a modelling approach: A case study for the grapevine species *Vitis vinifera* L. *Agric. For. Meteorol.* 180, 249–264. doi:10.1016/j.agrformet.2013.06.005.
- Pellegrino, A., Gozé, E., Lebon, E., Wery, J., 2006. A model-based diagnosis tool to evaluate the water stress experienced by grapevine in field sites. *Eur. J. Agron.* 25, 49–59. doi:10.1016/j.eja.2006.03.003.
- Pérez, D., Castel, J., Intrigliolo, D.S., Castel, J.R., 2013. Response of “Muscat of Alexandria” wine grapes to irrigation in eastern Spain, in: IX International Symposium on Grapevine Physiology and Biotechnology. pp. 343–350. doi:10.17660/ActaHortic.2017.1157.48.
- Petrie, P.R., Trought, M.C.T., Howell, G.S., 2000. Fruit composition and ripening of Pinot Noir (*Vitis vinifera* L.) in relation to leaf area. *Aust. J. Grape Wine Res.* 6, 46–51.
- Petrie, P.R., Sadras, V.O., 2008. Advancement of grapevine maturity in Australia between 1993 and 2006: Putative causes, magnitude of trends and viticultural consequences. *Aust. J. Grape Wine Res.* 14, 33–45. doi:10.1111/j.1755-0238.2008.00005.x.
- Poni, S., Palliotti, A., Bernizzoni, F., 2006. Calibration and Evaluation of a STELLA Software- based Daily CO₂ Balance Model in *Vitis vinifera* L. *J. Am. Soc. Hortic. Sci.* 131, 273–283.
- Pouget, R., 1963. Recherches physiologiques sur le repos végétatif de la vigne (*Vitis vinifera* L.): la dormance des bourgeons et le mécanisme de sa disparition. *Ann. Amélior. Plant.* 13(1):1-247.
- Pouget, R., 1968. Nouvelle conception du seuil de croissance chez la vigne. *Vitis* 7, 201–205.
- Quamme, H.A., Cannon, A.J., Neilsen, D., Caprio, J.M., Taylor, W.G., 2010. The potential impact of climate change on the occurrence of winter freeze events in six fruit crops grown in the Okanagan Valley. *Can. J. Plant Sci.* 90 (1), 85–93.

- R Core Team, 2015. R: A language and environment for statistical computing.
- Ramos, M.C., Jones, G. V., Martínez-Casasnovas, J.A., 2008. Structure and trends in climate parameters affecting winegrape production in northeast Spain. *Clim. Res.* 38, 1–15. doi:10.3354/crPAGE00759
- Ramos, M.C., Martínez-Casasnovas, J.A., 2014. Soil water variability and its influence on transpirable soil water fraction with two grape varieties under different rainfall regimes. *Agric. Ecosyst. Environ.* 185, 253–262. doi:10.1016/j.agee.2013.12.025
- Reynolds, A.G., Lowrey, W.D., Tomek, L., Hakimi, J., de Savigny, C., 2007. Influence of irrigation on vine performance, fruit composition, and wine quality of Chardonnay in a cool, humid climate. *Am. J. Enol. Vitic.* 58, 217–228.
- Richards, L.A., 1931. Capillary conduction of liquids through porous mediums. *Physics (College. Park. Md).* 1, 318–333.
- Ritchie, J.T., 1972. Model for predicting evaporation from a row crop with incomplete cover. *Water Resour. Res.* 8, 1204–1213.
- Ritchie, J.T., 1974. Atmospheric and soil water influences on the plant water balance. *Agric. Meteorol.* 14, 183–198. doi:10.1016/0002-1571(74)90018-1
- Ritchie, J.T., Otter, S., 1984. CERES-Wheat: A user oriented wheat yield model. Preliminary documentation. United States Department of Agriculture. *Agric. Res. Serv. ARS* 38, 159–175.
- Ritchie, J.T., 1998. Soil water balance and plant water stress, in: *Understanding Options for Agricultural Production*. Springer Netherlands, pp. 41–54.
- Rötter, R.P., Carter, T.R., Olesen, J.E., Porter, J.R., 2011. Crop–climate models need an overhaul. *Nat. Clim. Chang.* 1, 175–177. doi:10.1038/nclimate1152
- Ruget, F., Brisson, N., Delecolle, R., Faivre, R., 2002. Sensitivity analysis of a crop simulation model, STICS, in order to choose the main parameters to be estimated. *Agronomie* 22, 133–158. doi:10.1051/agro
- Ruti, P.M., Somot, S., Giorgi, F., Dubois, C., Flaounas, E., Obermann, A., Dell’Aquila, A., Pisacane, G., Harzallah, A., Lombardi, E., 2016. MED-CORDEX initiative for Mediterranean climate studies. *Bull. Am. Meteorol. Soc.* 97, 1187–1208.
- Sadras, V.O., Mccarthy, M.G., 2007. Quantifying the dynamics of sugar concentration in berries of *Vitis vinifera* cv. Shiraz: A novel approach based on allometric analysis. *Aust. J. Grape Wine Res.* 13, 66–71. doi:10.1111/j.1755-0238.2007.tb00236.x.
- Sadras, V.O., Collins, M., Soar, C.J., 2008. Modelling variety-dependent dynamics of soluble solids and water in berries of *Vitis vinifera*. *Aust. J. Grape Wine Res.* 14, 250–259. doi:10.1111/j.1755-0238.2008.00025.x.

- Sadras, V.O., Moran, M.A., 2013. Nonlinear effects of elevated temperature on grapevine phenology. *Agric. For. Meteorol.* 173, 107–115. doi:10.1016/j.agrformet.2012.10.003.
- Sáenz-Navajas, M. P., Campo, E., Sutan, A., Ballester, J., Valentin, D. 2013. Perception of wine quality according to extrinsic cues: The case of Burgundy wine consumers. *Food Quality and Preference*, 27(1), 44-53.
- Sáenz-Navajas, M. P., Ballester, J., Peyron, D., Valentin, D. 2014. Extrinsic attributes responsible for red wine quality perception: A cross-cultural study between France and Spain. *Food Quality and Preference*, 35, 70-85.
- Salazar-Parra, C., Aguirreolea, J., Sánchez-Díaz, M., Irigoyen, J.J., Morales, F., 2012a. Photosynthetic response of Tempranillo grapevine to climate change scenarios. *Ann. Appl. Biol.* 161, 277–292. doi:10.1111/j.1744-7348.2012.00572.x.
- Salazar-Parra, C., Aguirreolea, J., Sánchez-Díaz, M., Irigoyen, J.J., Morales, F., 2012b. Climate change (elevated CO₂, elevated temperature and moderate drought) triggers the antioxidant enzymes' response of grapevine cv. Tempranillo, avoiding oxidative damage. *Physiol. Plant.* 144, 99–110. doi:10.1111/j.1399-3054.2011.01524.x.
- Saltelli, A., Andres, T.H., Homma, T., 1995. Sensitivity analysis of model output. Performance of the iterated fractional factorial design method. *Comput. Stat. Data Anal.* 20, 387–407. doi:10.1016/0167-9473(95)92843-M.
- Saltelli, A., Tarantola, S., Chan, K.P.-S., 1999. A Quantitative Model-Independent Method for Global Sensitivity Analysis of Model Output. *Technometrics* 41, 39–56. doi:10.1080/00401706.1999.10485594.
- Santos, T.P., Lopes, C.M., Rodrigues, M.L., Souza, C.R. DE, Ricardo da Silva, J.M., Maroco, J.P., Pereira, J.S., Chaves, M.M., 2005. Effects of partial root-zone drying irrigation on cluster microclimate and fruit composition of field-grown Castelão grapevines. *Vitis - J. Grapevine Res.* 44, 117–125. doi:10.1016/j.scienta.2007.01.006.
- Santos, J.A., Malheiro, A.C., Karremann, M.K., Pinto, J.G., 2011. Statistical modelling of grapevine yield in the Port Wine region under present and future climate conditions. *Int. J. Biometeorol.* 55, 119–131. doi:10.1007/s00484-010-0318-0.
- Santos, J.A., Malheiro, A.C., Pinto, J.G., Jones, G. V., 2012. Macroclimate and viticultural zoning in Europe: Observed trends and atmospheric forcing. *Clim. Res.* 51, 89–103. doi:10.3354/cr01056.
- Schultz, H.R., 2000. Climate change and viticulture: A European perspective on climatology, carbon dioxide and UV-B effects. *Aust. J. Agric. Res.* 1, 2–12.
- Seguin, G., 1986. “Terroirs” and pedology of wine growing. *Experientia* 42, 861–873.

- Seguin, G., 1988. Ecosystems of the great red wines produced in the maritime climate of Bordeaux, in: Fuller-Perrine (Ed.), Proceedings of the Symposium on Maritime Climate Winegrowing. Department of Horticultural Sciences, Cornell University, Geneva, NY, pp. 36–53.
- Semenov, M.A., Barrow, E.M., 1997. Use of a stochastic weather generator in the development of climate change scenarios. *Clim. Change* 35, 397–414. doi:10.1023/A:1005342632279.
- Smart, R.E., 1985. Principles of Grapevine Canopy Microclimate Manipulation with Implications for Yield and Quality. A Review. *Am. J. Enol. Vitic.* 3, 230–239.
- Smart, R.E., Dick, J.K., Gravett, I.M., Fisher, B.M., 1990. Canopy management to improve grape yield and wine quality principles and practices. *South African J. Enol. Vitic.* 11, 3–17.
- Soltani, A., Sinclair, T., 2012. Modeling physiology of crop development, growth and yield. CABI.
- Somers, T.C., Verette, E., 1988. Phenolic composition of natural wine types. *Wine Anal.* 6, 219–257.
- Stella, T., Frasso, N., Negrini, G., Bregaglio, S., Cappelli, G., Acutis, M., Confalonieri, R., 2014. Model simplification and development via reuse, sensitivity analysis and composition: A case study in crop modelling. *Environ. Model. Softw.* 59, 44–58. doi:10.1016/j.envsoft.2014.05.007.
- Stöckle, C.O., Donatelli, M., Nelson, R., 2003. CropSyst, a cropping systems simulation model. *Eur. J. Agron.* 18, 289–307.
- Swanson, C.A., El-Shishiny, E.D.H., 1958. Translocation of sugars in the concord grape. *Plant Physiol.* 33, 33.
- Tang, Y., Reed, P., Van Werkhoven, K., Wagener, T., 2007. Advancing the identification and evaluation of distributed rainfall-runoff models using global sensitivity analysis. *Water Resour. Res.* 43, 1–14. doi:10.1029/2006WR005813.
- Tanner, C.B., Sinclair, T.R., 1983. Efficient water use in crop production: research or re-research? Limitations to Effic. water use *Crop Prod.* 1–27.
- Tate, A.B., 2001. Global warming's impact on wine. *J. Wine Res.* 12, 95–109.
- Terral, J.-F., Tabard, E., Bouby, L., Ivorra, S., Pastor, T., Figueiral, I., Picq, S., Chevance, J.-B., Jung, C., Fabre, L., Tardy, C., Compan, M., Bacilieri, R., Lacombe, T., This, P., 2010. Evolution and history of grapevine (*Vitis vinifera*) under domestication: new morphometric perspectives to understand seed domestication syndrome and reveal origins of ancient European cultivars. *Ann. Bot.* 105, 443–455. doi:10.1093/aob/mcp298.
- Teslic, N., Zinzani, G., Parpinello, G.P., Versari, A., 2016. Climate change trends, grape production, and potential alcohol concentration in wine from the “Romagna Sangiovese” appellation area (Italy). *Theor. Appl. Climatol.* 1–11. doi:10.1007/s00704-016-2005-5.

- Therond, O., Hengsdijk, H., Casellas, E., Wallach, D., Adam, M., Belhouchette, H., Oomend, R., Russellf, G., Ewert, F., Bergez, J.E., Janssend, S., Wery, J., Van Ittersumd, M.K., 2011. Using a cropping system model at regional scale: Low-data approaches for crop management information and model calibration. *Agric. Ecosyst. Environ.* 142, 85–94.
- Thorntwaite, C.W., 1948. An Approach toward a Rational Classification of Climate 38, 55–94.
- Tomasi, D., Jones, G. V., Giust, M., Lovat, L., Gaiotti, F., 2011. Grapevine Phenology and Climate Change: Relationships and Trends in the Veneto Region of Italy for 1964-2009. *Am. J. Enol. Vitic.* 62, 329–339. doi:10.5344/ajev.2011.10108.
- Tonietto, J., Carbonneau, A., 2004. A multicriteria climatic classification system for grape-growing regions worldwide. *Agric. For. Meteorol.* 124, 81–97. doi:10.1016/j.agrformet.2003.06.001.
- Toumi, J., Er-Raki, S., Ezzahar, J., Khabba, S., Jarlan, L., Chehbouni, A., 2016. Performance assessment of AquaCrop model for estimating evapotranspiration, soil water content and grain yield of winter wheat in Tensift Al Haouz (Morocco): Application to irrigation management. *Agric. Water Manag.* 163, 219–235. doi:10.1016/j.agwat.2015.09.007.
- Trought, M.C., Howell, G.S., Cherry, N.J., 1999. Practical considerations for reducing frost damage in vineyards. Lincoln University Report to New Zealand Winegrowers.
- Tubiello, F.N., Ewert, F., 2002. Simulating the effects of elevated CO₂ on crops: Approaches and applications for climate change. *Eur. J. Agron.* 18, 57–74. doi:10.1016/S1161-0301(02)00097-7.
- Tukey, L.D., 1958. Effects of Controlled Temperatures Following Bloom on Berry Development of the Concord Grape (*Vitis labrusca*). *Proc. Am. Soc. Hortic. Sci* 71, 157–166.
- Van Keulen, H., Seligman, N.G., 1987. Simulation of water use, nitrogen nutrition and growth of a spring wheat crop. *Simulation Monograph*, Wageningen.
- Van Leeuwen, C., Seguin, G., 1994. Incidences de l'alimentation en eau de la vigne, appréciée par l'état hydrique du feuillage, sur le développement de l'appareil végétatif et la maturation du raisin (*Vitis vinifera* variété Cabernet franc, Saint-Emilion, 1990). *J. Int. Sci. Vigne Vin* 28, 81–110.
- Van Leeuwen, C., Friant, P., Choné, X., Tregoat, O., Koundouras, S., Dubourdieu, D., 2004. Influence of Climate, Soil, and Cultivar on Terroir.pdf. *Am. J. Enol. Vitic.* 3, 207–217.
- Van Leeuwen, C., Tregoat, O., Chone, X., Gaudillère, J.P., Pernet, D., Leeuwen, C. Van, Trégoat, O., Choné, X., Gaudillère, J.P., Pernet, D., 2008. Different environmental conditions, different results: the role of controlled environmental stress on grape quality potential and the way to monitor it., in: 13th Australian Wine Industry Technical Conference, p. 8.

- Van Leeuwen, C., Tregoat, O., Choné, X., Bois, B., Pernet, D., Gaudillère, J.P., 2009. Vine water status is a key factor in grape ripening and vintage quality for red bordeaux wine. How can it be assessed for vineyard management purposes? *J. Int. des Sci. la Vigne du Vin* 43, 121–134. doi:10.20870/oenone.2009.43.3.798.
- Vanuytrecht, E., Raes, D., Willems, P., 2014. Global sensitivity analysis of yield output from the water productivity model. *Environ. Model. Softw.* 51, 323–332. doi:10.1016/j.envsoft.2013.10.017.
- Varella, H., Guérf, M., Buis, S., 2010. Global sensitivity analysis measures the quality of parameter estimation: The case of soil parameters and a crop model. *Environ. Model. Softw.* 25, 310–319. doi:10.1016/j.envsoft.2009.09.012.
- Vasconcelos, M.C., Greven, M., Winefield, C.S., Trought, M.C.T., Raw, V., 2009. The flowering process of *vitis vinifera*: A review. *Am. J. Enol. Vitic.* 60, 411–434.
- Von Hoyningen-Huene, J. 1981. Die Interzeption des Niederschlags in landwirtschaftlichen Pflanzenbeständen. Arbeitsbericht Deutscher Verband für Wasserwirtschaft und Kulturbau, DVWK.
- Vose, J.M., Sullivan, N.H., Clinton, B.D., Bolstad, P.V., 1995. Vertical leaf area distribution, light transmittance, and application of the Beer–Lambert law in four mature hardwood stands in the southern Appalachians. *Can. J. For. Res.* 25, 1036–1043.
- Wang, J., Li, X., Lu, L., Fang, F., 2013. Parameter sensitivity analysis of crop growth models based on the extended Fourier Amplitude Sensitivity Test method. *Environ. Model. Softw.* 48, 171–182. doi:10.1016/j.envsoft.2013.06.007
- Wang, X., He, X., Williams, J.R., Izaurrealde, R.C., Atwood, J.D., 2005. Sensitivity and uncertainty analyses of crop yields and soil organic carbon simulated with EPIC. *Am. Soc. Agric. Eng.* 48, 1041–1054.
- Webb, L., Whetton, P., Barlow, E.W.R., 2007. Modelled impact of future climate change on phenology of wine grapes in Australia. *Aust. J. Grape Wine Res.* 13, 165–175.
- Webb, L., Whetton, P., Barlow, E., 2008. Modelling the relationship between climate, winegrape price and winegrape quality in Australia. *Clim. Res.* 36, 89–98. doi:10.3354/cr00739
- Webb, L.B., Whetton, P.H., Barlow, E.W.R., 2011. Observed trends in winegrape maturity in Australia. *Glob. Chang. Biol.* 17, 2707–2719. doi:10.1111/j.1365-2486.2011.02434.x.
- Wermelinger, B., Baumgartner, J., 1991. A demographic model of assimilation and allocation of carbon and nitrogen in grapevines. *Ecol. Modell.* 53, 1–26. doi:10.1016/0304-3800(91)90138-Q.

- White, M.A., Diffenbaugh, N.S., Jones, G. V, Pal, J.S., Giorgi, F., 2006. Extreme heat reduces and shifts United States premium wine production in the 21st century. *Proc. Natl. Acad. Sci. U. S. A.* 103, 11217–22. doi:10.1073/pnas.0603230103.
- Williams, J.R., Jones, C.A., Kiniry, J.R., Spanel, D.A., 1989. The EPIC Crop Growth Model. *Trans. Am. Soc. Agric. Eng.* 32, 497–511. doi:10.13031/2013.31032
- Williams, L.E., Ayars, J.E., 2005. Grapevine water use and the crop coefficient are linear functions of the shaded area measured beneath the canopy. *Agric. For. Meteorol.* 132, 201–211. doi:10.1016/j.agrformet.2005.07.010.
- Winkler, A.J., Cook, J.A., Kliever, W.M., Lider, L.A., 1974. *General Viticulture*, 2nd ed. University of California Press, Berkeley.
- Yang, X., Tian, Z., Sun, L., Chen, B., Tubiello, F.N., Xu, Y., 2017. The impacts of increased heat stress events on wheat yield under climate change in China. *Clim. Change* 140, 605–620. doi:10.1007/s10584-016-1866-z.
- Yuyuen, P., Boonkerd, N., Wanapu, C., 2015. Effect of grape berry quality on wine quality 22, 349–356.
- Zapata, D., Salazar, M., Chaves, B., Keller, M., Hoogenboom, G., 2015. Estimation of the base temperature and growth phase duration in terms of thermal time for four grapevine cultivars. *Int. J. Biometeorol.* 59, 1771–1781. doi:10.1007/s00484-015-0985-y.
- Zapata, D., Salazar-Gutierrez, M., Chaves, B., Keller, M., Hoogenboom, G., 2017. Predicting key phenological stages for 17 grapevine cultivars (*Vitis vinifera* L.). *Am. J. Enol. Vitic.* 68, 60–72. doi:10.5344/ajev.2016.15077.
- Zhai, P., Zhang, X., Wan, H., Pan, X., 2005. Trends in Total Precipitation and Frequency of Daily Precipitation Extremes over China. *J. Clim.* 18, 1096–1108.
- Zohary, D., 1996. The mode of domestication of the founder crops of Southwest Asian agriculture. *Orig. spread Agric. Pastor. Eurasia* 142–158.

Supplementary Material

Supplementary Material contains all the annexes of the thesis separated in Chapters. The Supplementary Material includes also the List of Tables and Figures, the Curriculum Vitae and the List of Publications.

Supplementary Material I

2. A model library to simulate grapevine growth and development: software implementation, sensitivity analysis and field level application

Model documentation

BioMA component name

UNIFI.GrapeML

Developers

Luisa Leolini, Fabrizio Ginaldi, Simone Bregaglio

Availability and Online Documentation

UNIFI.GrapeML is available as Software Development Kit (SDK) upon request from the Corresponding Author (provided at Supplementary Material for the Reviewers. Please note that the .rar folder must be unlocked before unzipping). The SDK contains a help file with the documentation of algorithms and models, and two sample applications showing how to use UNIFI.GrapeML component as single software unit and in a modelling solution. UNIFI.GrapeML is released as C# libraries compiled for the NET 4.5 platform.

Tables**Table S.2.1.** Average maximum and minimum air temperatures, cumulated precipitation and evapotranspiration, over the grape growing seasons (1998-2012) in the study area.

Year	Budbreak-Flowering				Flowering-Veraison				Veraison-Maturity			
	T _x	T _n	P	ET ₀	T _x	T _n	P	ET ₀	T _x	T _n	P	ET ₀
1998	19.9	8.3	26.6	383.6	28.6	16.3	104.8	428.4	33.2	19.6	48.6	317.2
1999	21.5	9.3	75.8	366.8	28.5	15.8	45.2	466.3	31.1	19.5	25.8	258.9
2000	18.9	9.0	79.8	310.1	26.1	15.8	89.9	425.2	28.3	18.1	33.9	198.1
2001	20.6	8.8	37.6	325.6	29.3	16.0	44	593.0	32.6	19.5	35.4	157.4
2002	18.6	9.6	178.6	327.9	26.6	16.0	28.6	364.5	27.7	17.9	69.4	357.3
2003	20.2	8.9	81.2	324.2	29.8	16.7	12.2	375.7	32.1	20.4	1.4	342.8
2004	16.5	7.1	205.0	287.0	25.2	13.5	57.6	447.8	28.5	16.3	49.4	192.8
2005	20.1	9.4	54.0	329.7	28.4	17.1	18.2	447.9	29.4	18.6	39	175.4
2006	21.5	10.4	15.2	229.3	29.0	16.9	11	495.6	32.1	19.9	44.2	236.8
2007	21.0	10.0	234.4	264.8	28.2	15.2	12.4	453.3	29.3	17.7	68.8	215.5
2008	19.2	8.1	167.9	314.5	25.4	14.7	159	350.6	29.9	18.5	19.9	264.3
2009	18.9	8.3	158.8	231.6	27.5	16.1	92.3	378.4	31.1	18.7	33.9	207.1
2010	17.7	7.8	163.6	241.9	26.9	15.3	73.8	346.9	29.3	18.2	63.2	236.6
2011	20.3	9.4	86.3	235.9	25.9	14.9	184.6	381.4	28.8	17.7	35.1	246.8
2012	20.2	9.3	217.8	274.2	28.4	16.6	52.8	249.5	31.4	19.3	31	221.8

Table S.2.2. Acronyms, description, default value and unit of the model parameters calibrated. CU =Chilling Units, FU=Forcing Units.

Parameters	Description	Calibrated value	Default value	Measured value	Units
Phenological development					
aParam	Curve shape parameter	0.006	0.005		unitless
cParam	Optimal chilling temperature	1.79	2.8		°C
ChillingReq	Chilling requirement	59.28	78.692		CU
db	Slope of forcing unit eq. (budbreak)	-0.23	-0.26		unitless
df	Slope of forcing unit eq. (flowering)	-0.13	-0.26		unitless
dv	Slope of forcing unit eq. (veraison)	-0.40	-0.26		unitless
dm	Slope of forcing unit eq. (maturity)	-0.40	-0.26		unitless
eb	Base forcing temperature (budbreak)	15.15	16.06		°C
ef	Base forcing temperature (flowering)	9.43	16.06		°C
ev	Base forcing temperature (veraison)	10.93	16.06		°C
em	Base forcing temperature (maturity)	17.24	16.06		°C
Col	Curve shape parameter	108.36	176.26		unitless
co2	Curve shape parameter	-0.014	-0.015		unitless
LimitForcingReq	Last day of CU effect on forcing req.	200	234		day
FloweringReq	Forcing requirement for flowering	38.81	24.7		FU
VeraisonReq	Forcing requirement for veraison	57.31	51.14		FU
MaturityReq	Forcing requirement for maturity	30.73	-		FU
Leaf growth					
ShootNumber	Number of shoots per plant	16		16	Number
ShootLeafNumberIntercept	Curve shape param. of SLN eq.	-0.22	-0.28		unitless
LeafAppearanceRate1	Curve shape param. of SLN eq.	0.06	0.04		unitless
LeafAppearanceRate2	Curve shape param. of SLN eq.	-0.015	-0.015		unitless
ShootLeafAreaSlope	Curve shape param. of SLA eq.	5.39	5.39		unitless
ShootLeafAreaExp	Curve shape param. of SLA eq.	1.48	2.13		unitless

Table S.2.3. Acronyms, description, default value and unit of the model parameters calibrated. CU =Chilling Units, FU=Forcing Units (continue).

Parameters	Description	Calibrated value	Default value	Measured value	Units
ProportionShadedArea	Proportion of the area shaded by plant	0.75	0.75		unitless
PlantArea	Squared meters of soil per plant	4		4	m ² plant ⁻¹
SLN1	Coeff. of WS eq. on leaf develop.	39.92	25.9		unitless
SLN2	Coeff. of WS eq. on leaf develop.	39.16	17.3		unitless
Light interception					
CropCoeff	Extinction coefficient for RadIntercept	0.6	0.6		Unitless
InitialRUE	Initial RUE at 350 ppm of CO ₂	1.001	1.001		g MJ ⁻¹
qRUE550	Intercept of the CO ₂ 550 ppm eq.	0.633	0.633		g MJ ⁻¹
mRUE550	Coeff. of the CO ₂ 550 ppm eq.	0.00105	0.00105		g MJ ⁻¹ ppm ⁻¹
PHO1	Coeff. for WS effect on photosyn.	6.01	12.9		unitless
PHO2	Coeff. for WS effect on photosyn.	8.59	14.1		unitless
qRUE700	Intercept of the CO ₂ 700 ppm eq.	0.954	0.95		g MJ ⁻¹
mRUE700	Coeff. of the CO ₂ 700 ppm eq.	0.000468	0.00047		g MJ ⁻¹ ppm ⁻¹
FTSWLimitRoot	FTSW Limit for Root Growth	0.5	0.5		unitless
DayForStress	N° Days for water stress on root	2	2		day
Biomass partitioning					
HarvestIndex	Slope of Fruit Biomass Index eq.	0.0035	0.00443		d ⁻¹
HarvestIndexCutOff	Harvest Index cut off	0.5	0.5		d ⁻¹
InitialRootLength	Initial value of root depth	100		100	cm
RootGrowthBasic	Root growth rate for not limiting water	0.001	0.001		cm day ⁻¹
RootGrowthStress	Root growth rate for limiting water	0.05	0.05		cm day ⁻¹
Evapotranspiration					
WUE	Water use efficiency	3.86	6.1		Pa
Extreme event impact					
Tmax	Max temp. for fruit-set at flowering	40	41		°C
Tmin	Min temp. for fruit-set at flowering	1	1		°C
Topt	Optimum temp. for fruit-set at flowering	25	25		°C
q	Curve shape param.	1.9	1.9		unitless

Figures

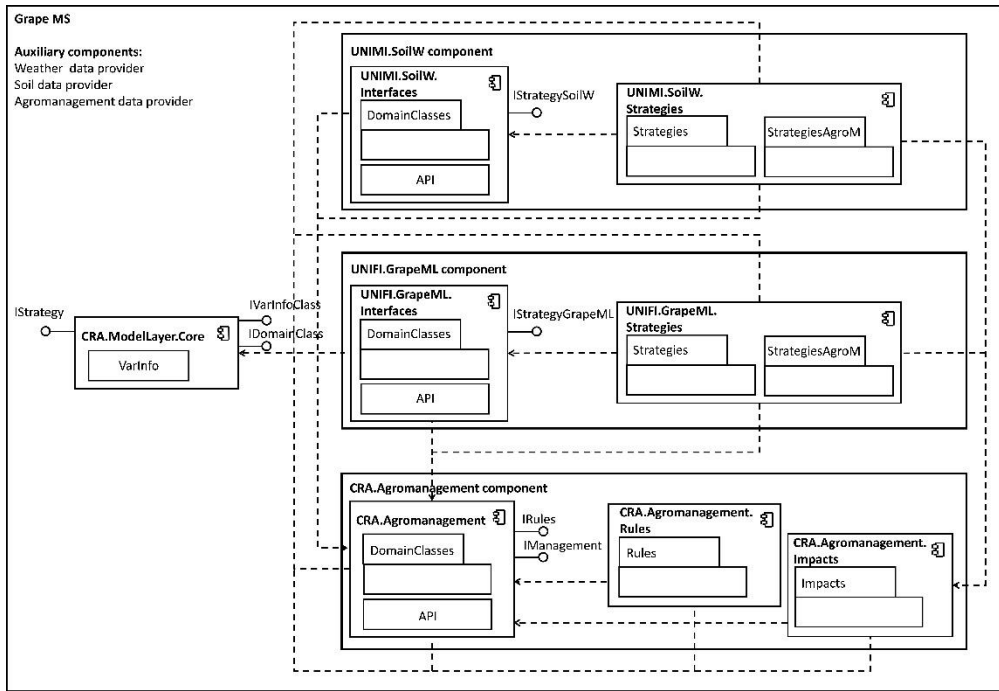


Figure S.2.1. Unified Modelling Language (UML) of the UNIFI.GrapeRunner modelling solution. The graph shows the dependencies (arrow dotted line) between software components.

Supplementary Material II

3. UNIFI.GrapeML implementation for estimating sugar content of Sangiovese grape variety

Figures

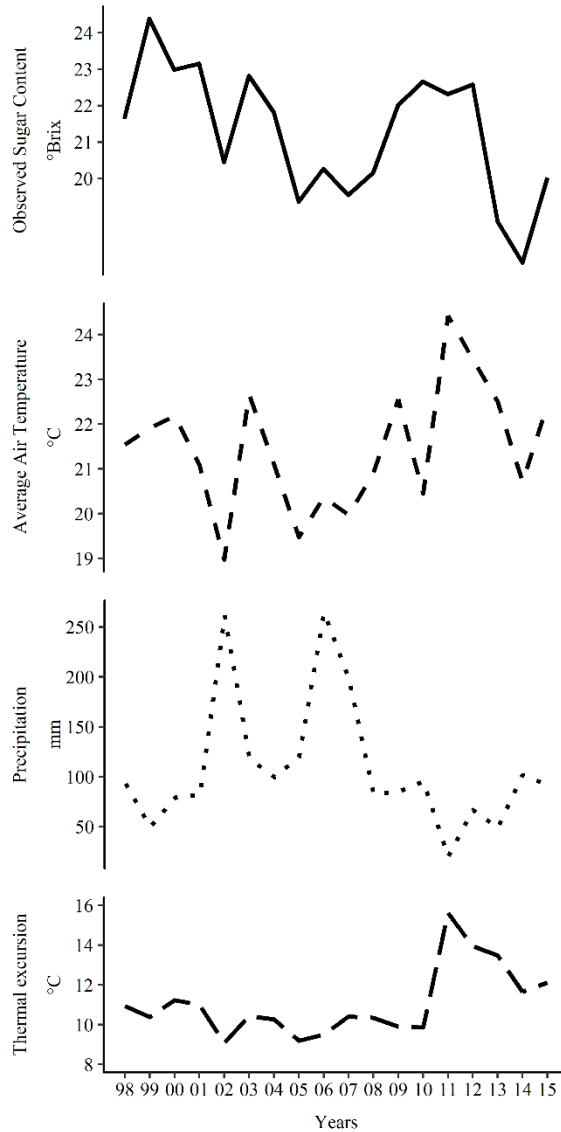


Figure S.3.1. Dynamics of observed Brix data compared to the main weather variables over the period 1998-2015. The observed Brix data are represented as the annual average of the measurements recorded during the year.

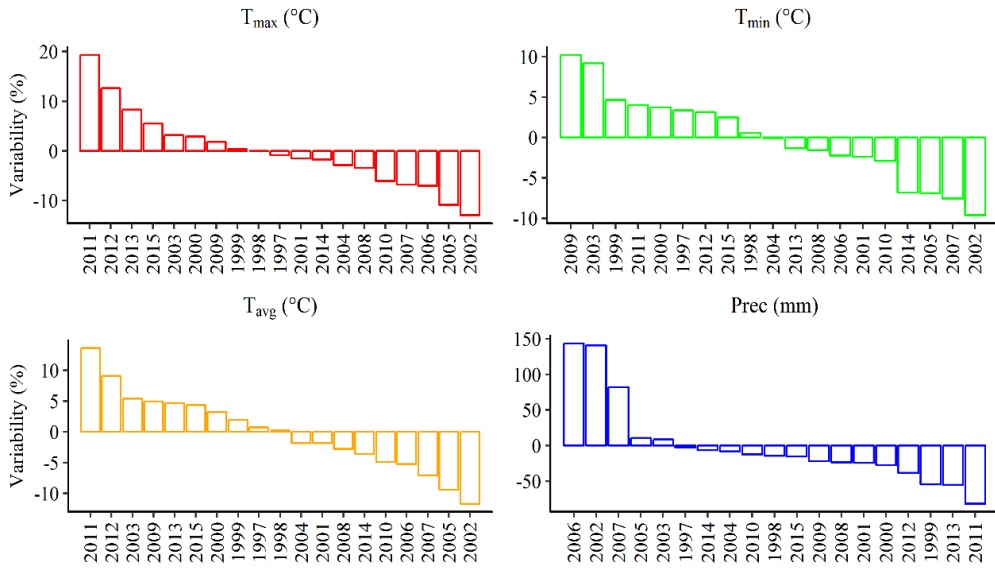


Figure S.3.2. Long-Term Average (LTA) over the period 1998-2015. The four graphs represent the percentage variability of each weather variable average during the ripening period (from August to September). T_{max} = maximum air temperature (°C), T_{min} = minimum air temperature (°C), T_{avg} = average air temperature (°C), $Prec$ = precipitation (mm).

Supplementary Material III

4. Frost impacts on grapevine distribution in Europe

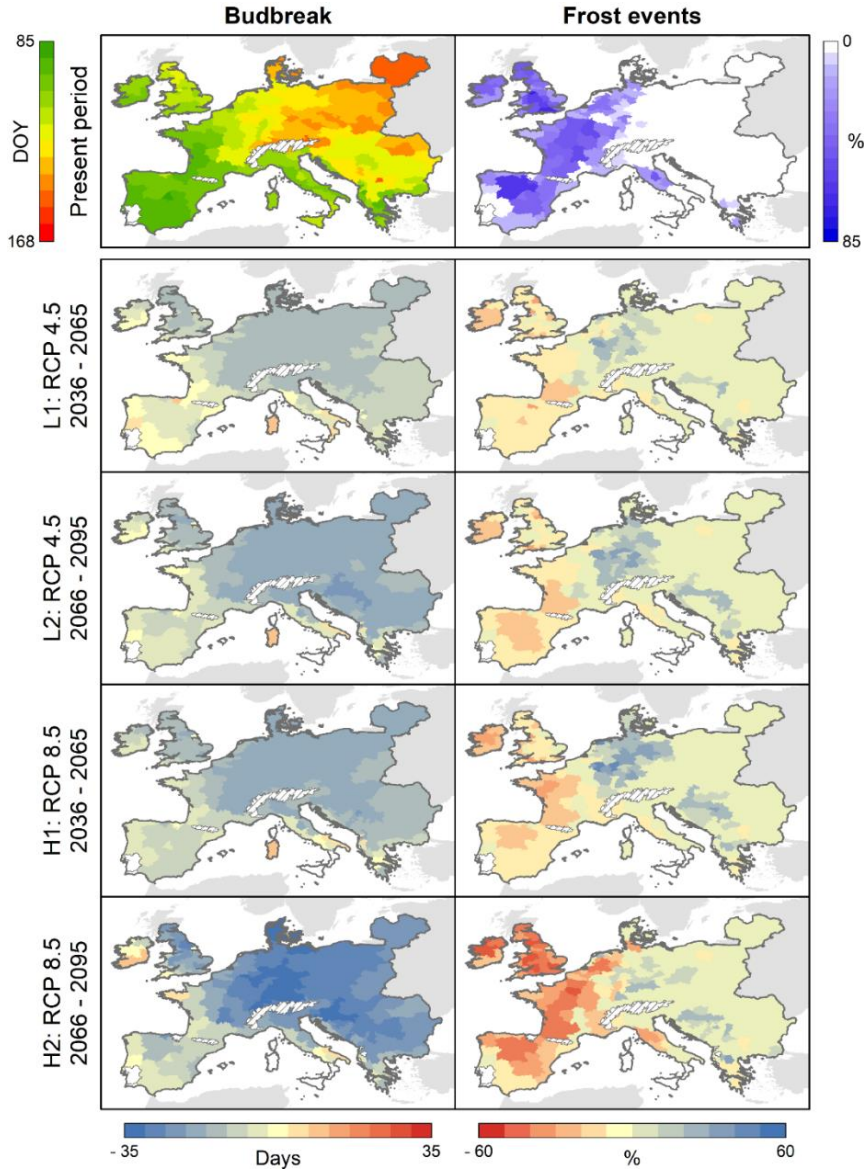


Figure S.4.1. Budbreak stage and frost events for Chardonnay variety at European NUTS2 regional scale. The maps of future emission scenarios (L1, L2, H1, H2) are obtained comparing present with future data (Days = number of days in advance or delay compared to the present period). The white areas on the map correspond to the NUTS2 zones in which budbreak is not reached while the stippled areas refer to the grid points excluded by the simulation.

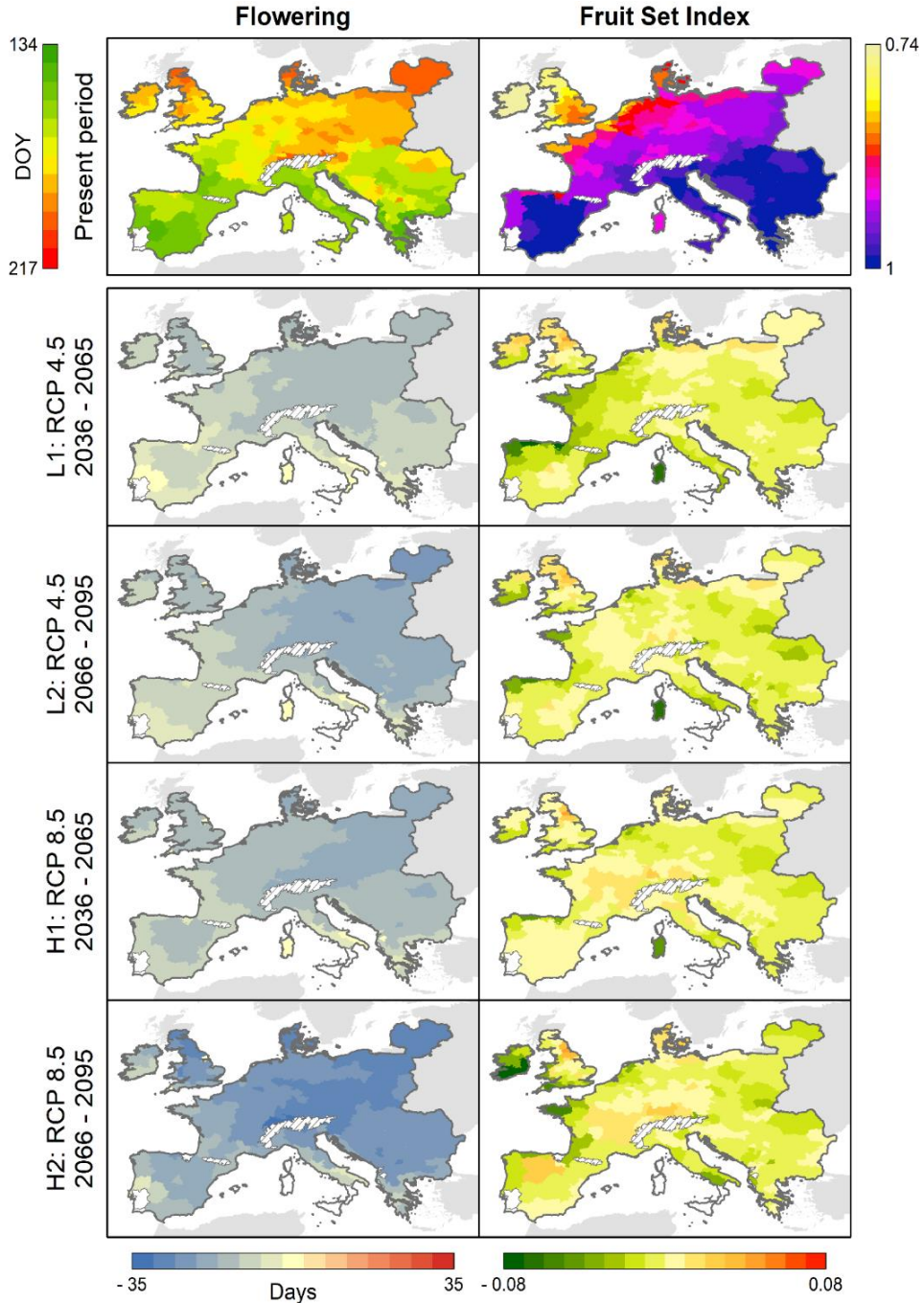


Figure S.4.2. Flowering stage and fruit-set index for Chardonnay variety at European NUTS2 regional scale. The maps of future emission scenarios (L1, L2, H1, H2) are obtained comparing present with future data (Days = number of days in advance or delay compared to the present period). The white areas on the map correspond to the NUTS2 zones in which budbreak is not reached while the stippled areas refer to the grid points excluded by the simulation.

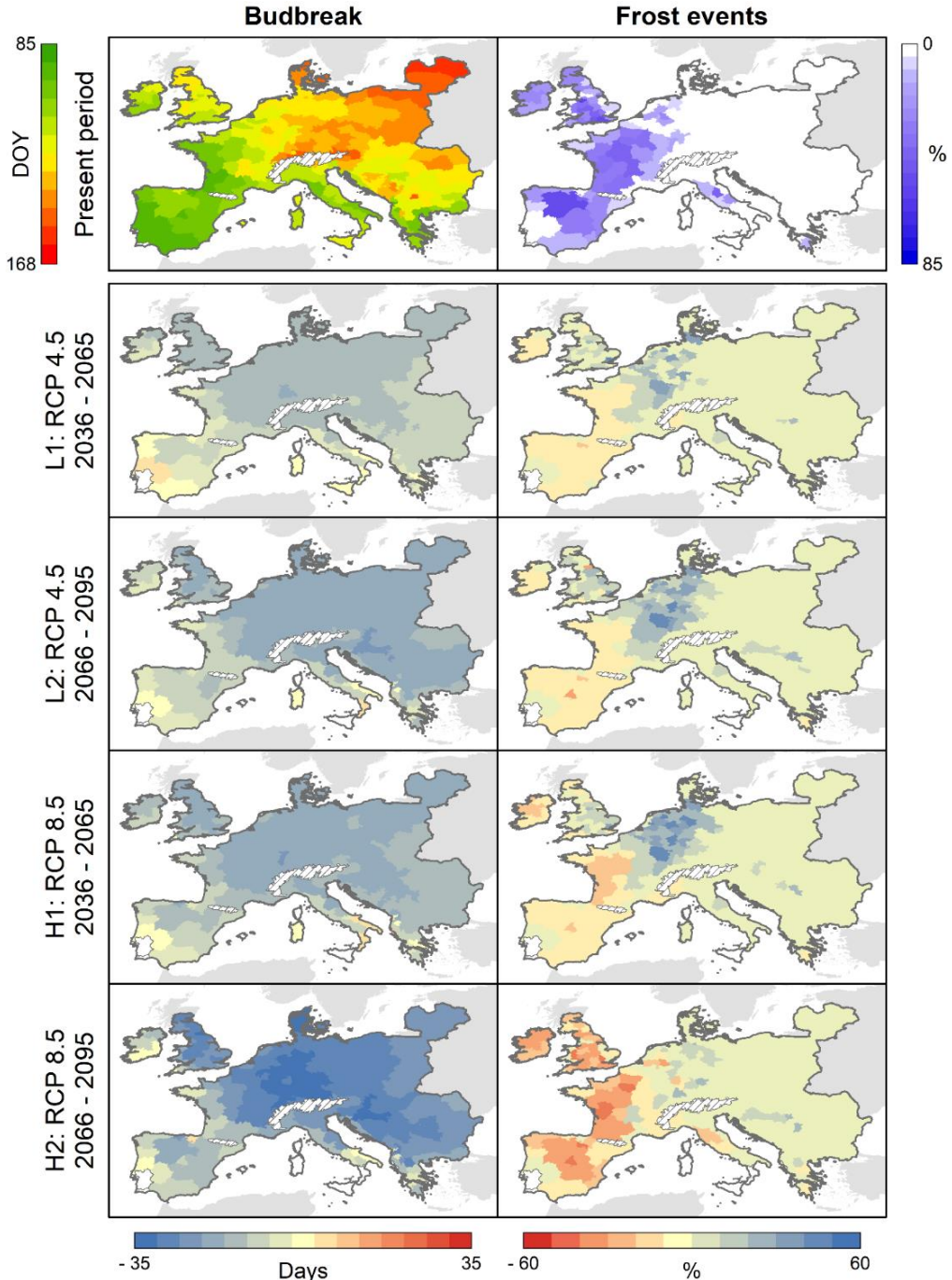


Figure S.4.3. Budbreak stage and frost events for Merlot variety at European NUTS2 regional scale. The maps of future emission scenarios (L1, L2, H1, H2) are obtained comparing present with future data (Days = number of days in advance or delay compared to the present period). The white areas on the map correspond to the NUTS2 zones in which budbreak is not reached while the stippled areas refer to the grid points excluded by the simulation.

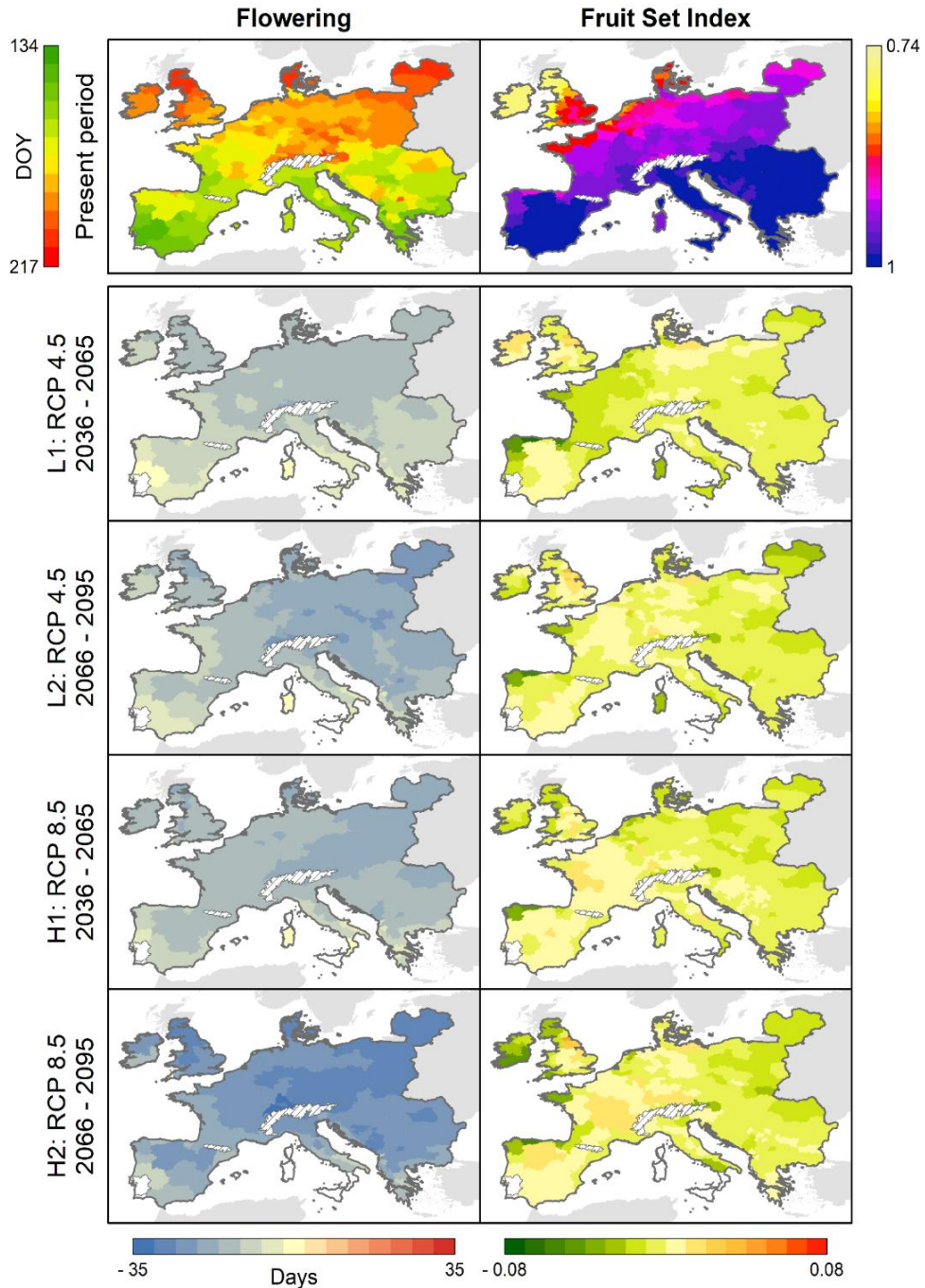


Figure S.4.4. Flowering stage and fruit-set index for Merlot variety at European NUTS2 regional scale. The maps of future emission scenarios (L1, L2, H1, H2) are obtained comparing present with future data (Days = number of days in advance or delay compared to the present period). The white areas on the map correspond to the NUTS2 zones in which budbreak is not reached while the stippled areas refer to the grid points excluded by the simulation.

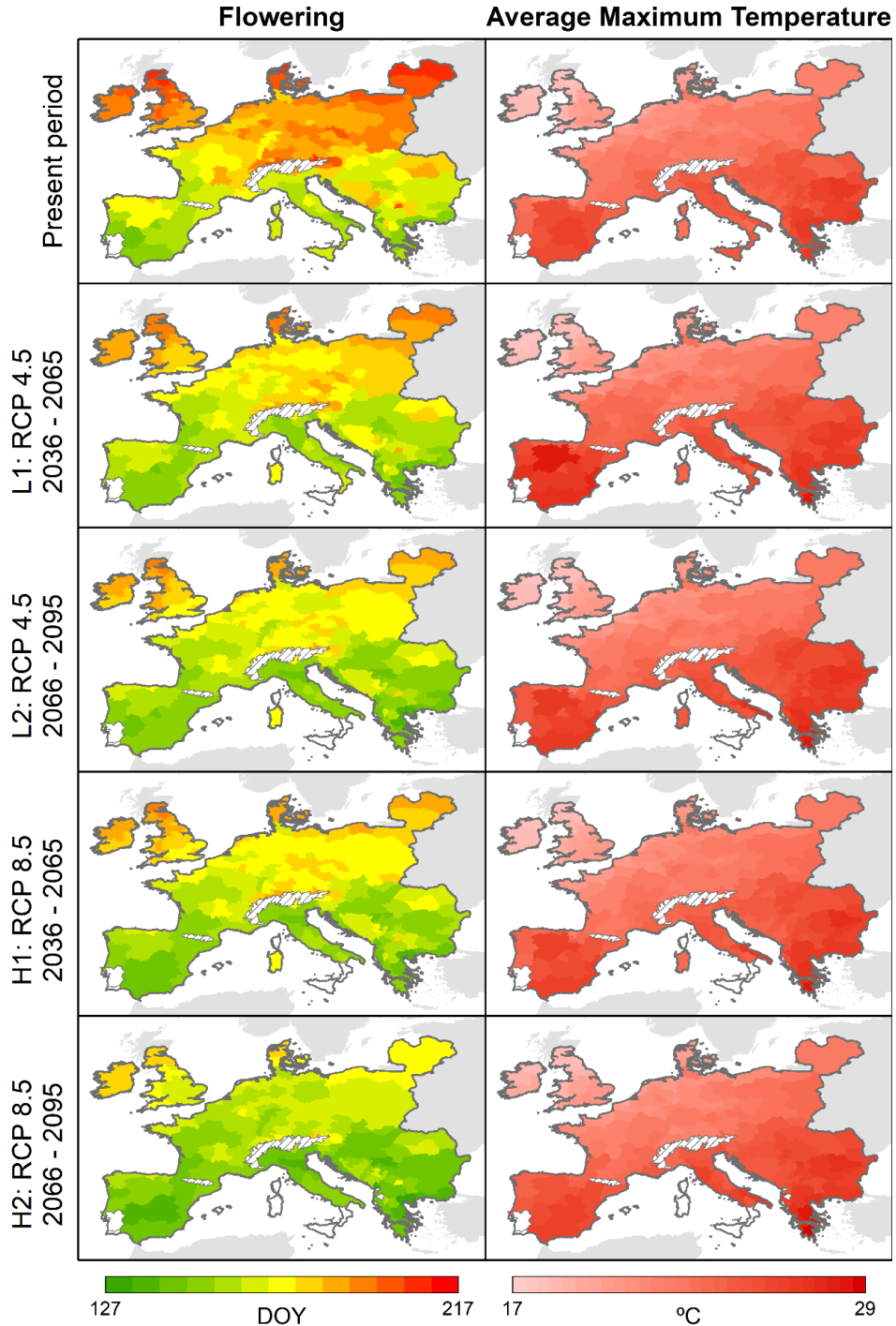


Figure S.4.5. Flowering stage and Average Maximum Temperature estimated in seven days around flowering for *Glera* variety at European NUTS2 regional scale. The white areas on the map correspond to the NUTS2 zones in which flowering is not reached while the stippled areas correspond to the grid points excluded by the simulation.

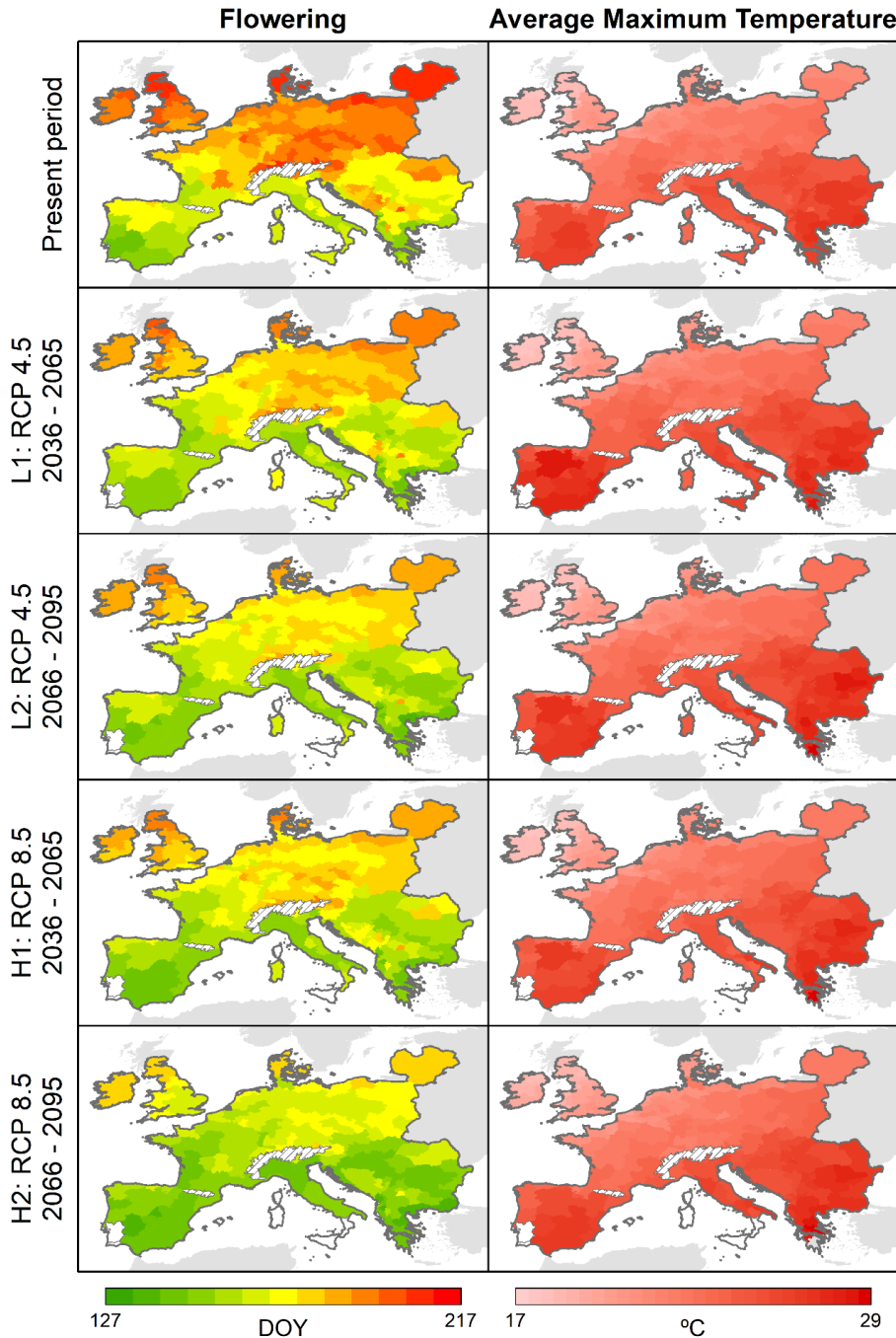


Figure S.4.6. Flowering stage and Average Maximum Temperature estimated in seven days around flowering for Cabernet Sauvignon variety at European NUTS2 regional scale. The white areas on the map correspond to the NUTS2 zones in which flowering is not reached while the stippled areas correspond to the grid points excluded by the simulation.

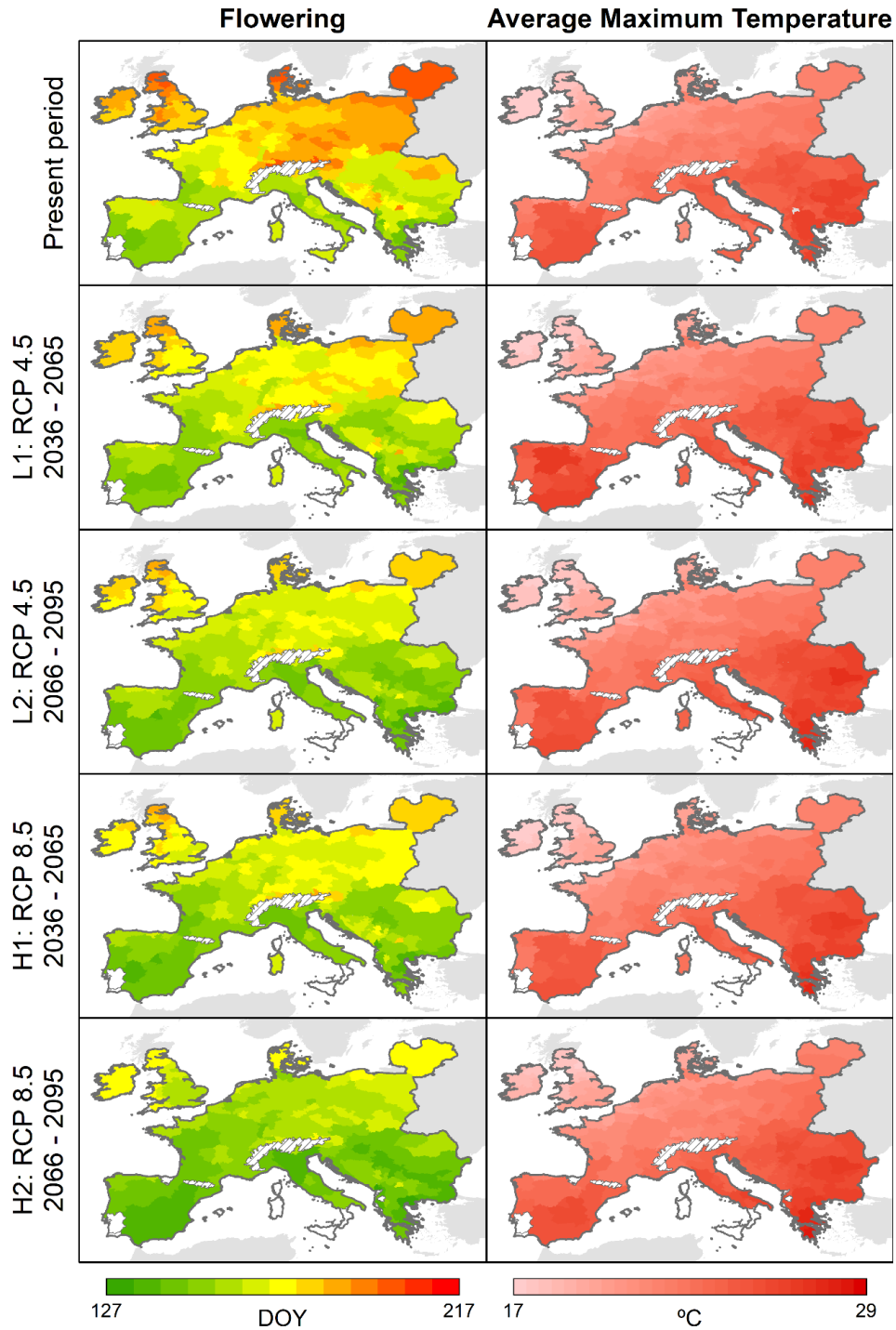


Figure S.4.7. Flowering stage and Average Maximum Temperature estimated in seven days around flowering for Chardonnay variety at European NUTS2 regional scale. The white areas on the map correspond to the NUTS2 zones in which flowering is not reached while the stippled areas correspond to the grid points excluded by the simulation.

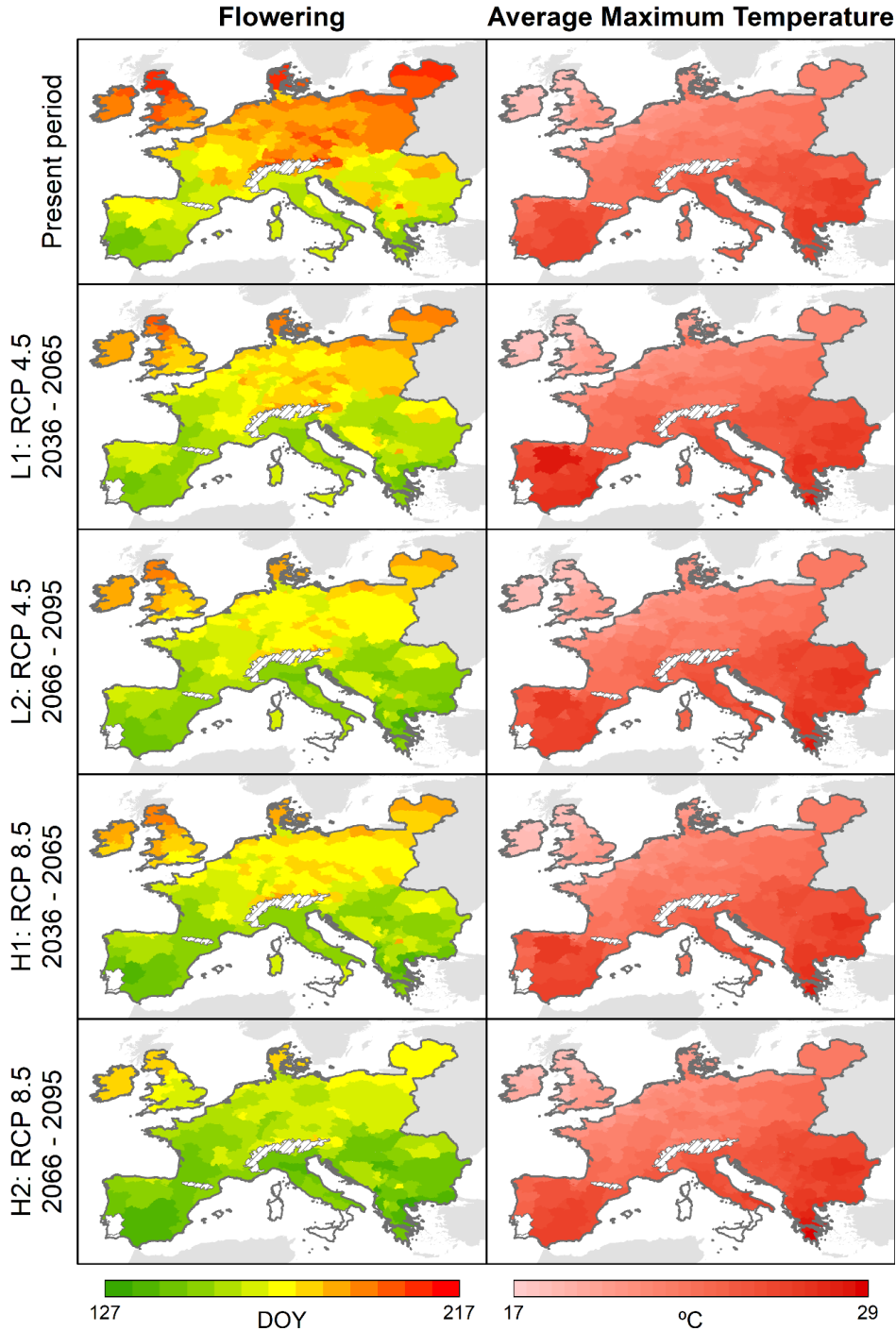


Figure S.4.8. Flowering stage and Average Maximum Temperature estimated in seven days around flowering for Merlot variety at European NUTS2 regional scale. The white areas on the map correspond to the NUTS2 zones in which flowering is not reached while the stippled areas correspond to the grid points excluded by the simulation.

List of Tables and Figures

Tables

Chapter 2

Table 2.1. Equations of the CF method to simulate phenological development in the four main phenological stages of grapevine (Caffarra and Eccel, 2010).

Table 2.2. Average and standard deviations of maximum (T_x) and minimum (T_n) air temperatures, cumulated precipitation (Prec) and evapotranspiration (ET0) in the grape growing seasons (1998-2012) in the study area.

Table 2.3. Acronyms, description, default value and unit of the model parameters evaluated via sensitivity analysis, with relevant source of information. CU =Chilling Units, FU=Forcing Units.

Chapter 3

Table 3.1. Calibration of the UNIFI.GrapeML parameters for assessing grape phenology and sugar content in cv. Sangiovese.

Chapter 4

Table 4.1. Equations of UniChill model for chilling and forcing accumulation.

Table 4.2. UniChill model calibration for different grape varieties. Source: Fila (2012).

Table 4.3. Control temperature experiments used for describing the fruit-set index curve.

Supplementary Material I

Table S.2.1. Average maximum and minimum air temperatures, cumulated precipitation and evapotranspiration, over the grape growing seasons (1998-2012) in the study area.

Table S.2.2. Acronyms, description, default value and unit of the model parameters calibrated. CU =Chilling Units, FU=Forcing Units.

Figures

Chapter 1

Figure 1.1. Distribution of the current suitable wine regions around the world.

Figure 1.2. Estimation of Budbreak (Day Of Year; DOY) of four different grape varieties under two different climatic scenarios and two time slice in Spain (L1: RCP 4.5 2036-2065; L2: RCP 4.5 2066-2095; H1: RCP 8.5 2036-2065; H2: RCP 8.5 2066-2095).

Figure 1.3. Grape phenology development.

Figure 1.4. Biomass partitioning among single plant organs.

Chapter 2

Figure 2.1. Workflow of the activities presented in this study, with relevant objectives and BioMA tools, downloadable at www.biomamodelling.org.

Figure 2.2. Unified Modelling Language (UML) component diagram of the UNIFI.GrapeML component. Software units (UNIFI.GrapeML.Interfaces and UNIFI.GrapeML.Strategies) have a dependency (arrow dotted line) to CRA.Core.ModelLayer and CRA.AgroManagement component, belonging to the core of the BioMA framework.

Figure 2.3. Workflow of the strategies currently implemented in UNIFI.GrapeML. The scheme presents the logical order in which models are called during a daily time step. T_x = daily maximum air temperature ($^{\circ}\text{C}$), T_n = daily minimum air temperature ($^{\circ}\text{C}$), P = precipitation (mm), GSR = global solar radiation (MJ m^{-2}), CF = Chilling-Forcing, GDD = Growing Degree Days.

Figure 2.4. Sensitivity Analysis (SA) using LHS and Sobol' methods. The Spearman's correlation coefficient (Fig. 2.4a) and Sobol' Total Order (Fig. 2.4b) were used as metrics to determine which parameters of the modelling solution is more sensitive.

Figure 2.5. Scatterplots presenting the comparison of simulated (X-axis) and observed (Y-axis) day of the year (DOY) referred to the main phenological phases of the Chardonnay grape variety (budbreak, flowering, veraison and maturity). Within each plot, the values of root mean square error (RMSE), Pearson's coefficient (r), the modelling efficiency (EF), and the coefficient of residual mass (CRM) are reported.

Figure 2.6. Simulated (continuous lines) and observed (empty points) soil water content at different depths in two cropping seasons (2010-2012) in the experimental vineyard. Precipitation is reported on the secondary y-axis as grey line. The table at the top right of the figure resumes the performances of the modelling solution in the different layers, considering the relative root mean square error (RRMSE), the coefficient of residual mass (CRM), the modelling efficiency (EF), and the Pearson's coefficient (r).

Figure 2.7. Comparison of simulated (lines) and measured (histogram) fruit dry biomass (kg ha^{-1}) over the period 1998-2012. In the top right of the figure, the values of Pearson's coefficient (r), relative root mean square error (RRMSE), the modelling efficiency (EF) and the coefficient of residual mass (CRM) are reported.

Chapter 3

Figure 3.1. Study Area: (A) Susegana (Treviso, $45^{\circ}51'00''\text{N}$, $12^{\circ}15'31''\text{E}$) and (B) Montalcino (Siena, $43^{\circ}03'33''\text{N}$; $11^{\circ}29'26''\text{E}$).

Figure 3.2. UNIFI.GrapeML workflow modified with the implementation of grape quality strategy.

Figure 3.3. Model calibration of the four phenology phases (i.e. budbreak, flowering, veraison and maturity) at Susegana (TV) and Montalcino (SI).

Figure 3.4. Correlations between observed and simulated Brix data in Montalcino area: model calibration and validation.

Chapter 4

Figure 4.1. Budbreak stage and frost events for Glera variety at European NUTS2 regional scale. The maps of future emission scenarios (L1, L2, H1, H2) are obtained comparing present with future data (Days = number of days in advance or delay compared to the present period). The white areas on the map correspond to the NUTS2 zones in which budbreak is not reached while the stippled areas refer to the grid points excluded by the simulation.

Figure 4.2. Flowering stage and fruit-set index for Glera variety at European NUTS2 regional scale. The maps of future emission scenarios (L1, L2, H1, H2) are obtained comparing present with future data (Days = number of days in advance or delay compared to the present period). The white areas on the map correspond to the NUTS2 zones in which budbreak is not reached while the stippled areas refer to the grid points excluded by the simulation.

Figure 4.3. Budbreak stage and frost events for Cabernet Sauvignon variety at European NUTS2 regional scale. The maps of future emission scenarios (L1, L2, H1, H2) are obtained comparing present with future data (Days = number of days in advance or delay compared to the present period). The white areas on the map correspond to the NUTS2 zones in which budbreak is not reached while the stippled areas refer to the grid points excluded by the simulation.

Figure 4.4. Flowering stage and fruit-set index for Cabernet Sauvignon variety at European NUTS2 regional scale. The maps of future emission scenarios (L1, L2, H1, H2) are obtained comparing present with future data (Days = number of days in advance or delay compared to the present period). The white areas on the map correspond to the NUTS2 zones in which budbreak is not reached while the stippled areas refer to the grid points excluded by the simulation.

Figure 4.5. Trend of endo-dormancy and eco-dormancy period under different climatic scenarios considering an average year calculated using the mean of each day of 300 years of simulation on two representative grid points of Spain and Germany (Pr=Present; L1=Low emission Scenario RCP 4.5 2036-2065; L2=Low emission Scenario RCP 4.5 2066-2095; H1=High emission Scenario RCP 8.5 2036-2065; H2=High emission Scenario RCP 8.5 2066-2095; CU =Chilling Units; FU = Forcing Units).

Figure 4.6. Distribution of frost events for present and future scenarios for each variety and country (Pr=Present; L1=Low emission Scenario RCP 4.5 2036-2065; L2=Low emission Scenario RCP 4.5 2066-2095; H1=High emission Scenario RCP 8.5 2036-2065; H2=High emission Scenario RCP 8.5 2066-2095).

Figure 4.7. Distribution of the fruit-set index for present and future scenarios for each variety and country (Pr=Present; L1=Low emission Scenario RCP 4.5 2036-2065; L2=Low emission Scenario RCP 4.5 2066-2095; H1=High emission Scenario RCP 8.5 2036-2065; H2=High emission Scenario RCP 8.5 2066-2095).

Supplementary Material I

Figure S.2.1. Unified Modelling Language (UML) of the UNIFI.GrapeRunner modelling solution. The graph shows the dependencies (arrow dotted line) between software components.

Supplementary Material II

Figure S.3.1. Dynamics of observed Brix data compared to the main weather variables over the period 1998-2015. The observed Brix data are represented as the annual average of the measurements recorded during the year.

Figure S.3.2. Long-Term Average (LTA) over the period 1998-2015. The four graphs represent the percentage variability of each weather variable average during the ripening period (from August to September). T_{max} = maximum air temperature ($^{\circ}\text{C}$), T_{min} = minimum air temperature ($^{\circ}\text{C}$), T_{avg} = average air temperature ($^{\circ}\text{C}$), Prec = precipitation (mm).

Supplementary Material III

Figure S.4.1. Budbreak stage and frost events for Chardonnay variety at European NUTS2 regional scale. The maps of future emission scenarios (L1, L2, H1, H2) are obtained comparing present with future data (Days = number of days in advance or delay compared to the present period). The white areas on the map correspond to the NUTS2 zones in which budbreak is not reached while the stippled areas refer to the grid points excluded by the simulation.

- Figure S.4.2.** Flowering stage and fruit-set index for Chardonnay variety at European NUTS2 regional scale. The maps of future emission scenarios (L1, L2, H1, H2) are obtained comparing present with future data (Days = number of days in advance or delay compared to the present period). The white areas on the map correspond to the NUTS2 zones in which budbreak is not reached while the stippled areas refer to the grid points excluded by the simulation.
- Figure S.4.3.** Budbreak stage and frost events for Merlot variety at European NUTS2 regional scale. The maps of future emission scenarios (L1, L2, H1, H2) are obtained comparing present with future data (Days = number of days in advance or delay compared to the present period). The white areas on the map correspond to the NUTS2 zones in which budbreak is not reached while the stippled areas refer to the grid points excluded by the simulation.
- Figure S.4.4.** Flowering stage and fruit-set index for Merlot variety at European NUTS2 regional scale. The maps of future emission scenarios (L1, L2, H1, H2) are obtained comparing present with future data (Days = number of days in advance or delay compared to the present period). The white areas on the map correspond to the NUTS2 zones in which budbreak is not reached while the stippled areas refer to the grid points excluded by the simulation.
- Figure S.4.5.** Flowering stage and Average Maximum Temperature estimated in seven days around flowering for Glera variety at European NUTS2 regional scale. The white areas on the map correspond to the NUTS2 zones in which flowering is not reached while the stippled areas correspond to the grid points excluded by the simulation.
- Figure S.4.6.** Flowering stage and Average Maximum Temperature estimated in seven days around flowering for Cabernet Sauvignon variety at European NUTS2 regional scale. The white areas on the map correspond to the NUTS2 zones in which flowering is not reached while the stippled areas correspond to the grid points excluded by the simulation.
- Figure S.4.7.** Flowering stage and Average Maximum Temperature estimated in seven days around flowering for Chardonnay variety at European NUTS2 regional scale. The white areas on the map correspond to the NUTS2 zones in which flowering is not reached while the stippled areas correspond to the grid points excluded by the simulation.
- Figure S.4.8.** Flowering stage and Average Maximum Temperature estimated in seven days around flowering for Merlot variety at European NUTS2 regional scale. The white areas on the map correspond to the NUTS2 zones in which flowering is not reached while the stippled areas correspond to the grid points excluded by the simulation.

Curriculum Vitae

Luisa Leolini was born on 12th January, 1989 in Florence (Italy). In 2008, she started the University course of Agriculture and Forestry Sciences (Bachelor degree-3 years) at the University of Florence. She concluded the course in 2012 with 110/110 cum laude and she started the University course in Agriculture and Technologies Sciences (Master degree- 2 years) at the same University. From February 2013 to June 2013, she participated at the Erasmus Placement program and she moved at the department of horticulture, fruit growing botany and gardening University of Lleida (Spain) in the research group of Prof. Maria Teresa Sebastià. At that time, she started her Master's thesis titled "Climatic and biodiversity effects on litter decomposition in semi-natural grassland". In July 2014, and from January 2014 to March 2014, she obtained two scholarships from the University of Lleida. She completed the Master course in 2014 with 110/110 cum laude. From September to November 2014, she worked at the University of Florence collaborating with the research group of Prof. Marco Bindi. In November 2014, she started her PhD working on the thesis "A model library for estimating grapevine development and growth under different pedo-climatic conditions". During her PhD, she participated to workshops (second science workshop of MODEXTREME project at FAO-Rome), international conference (ClimWine in Bordeaux, France) and international award (Premio Soldera 2015 and 2016, Rome, Italy). In 2016, she gained a scholarship from the Embassy of France in Italy and she spent 3 months (May-July 2016) at the INRA of Bordeaux (France) under the supervision of Dr. Zhanwu Dai for improving her knowledges in grape simulation models.



Publications

M. Moriondo, **L. Leolini**, N. Staglianò, G. Argenti, G. Trombi, L. Brilli, C. Dibari, C. Leolini, M. Bindi. 2016. Use of digital images to disclose canopy architecture in olive tree. *Sci. Hortic.* 209, 1–13.

***L. Leolini**, M. Moriondo, G. Fila, S. Costafreda-Aumedes, R. Ferrise, M. Bindi. (in press). Late spring frost impacts on grapevine distribution in Europe. *Field Crops Res.* <https://doi.org/10.1016/j.fcr.2017.11.018>

M. Moriondo, **L. Leolini**, L. Brilli, C. Dibari, R. Tognetti, A. Giovannelli, B. Rapi, P. Battista, G. Caruso, R. Gucci, G. Argenti, A. Raschi, M. Centritto, M. Bindi. (*submitted*). A simple model simulating development and growth of an olive grove. *Agric. For. Meteorol.*

***L. Leolini**, S. Bregaglio, M. Moriondo, M.C. Ramos, M. Bindi, F. Ginaldi. (*submitted*). A model library to simulate grapevine growth and development: software implementation, sensitivity analysis and field level application. *Eur. J. Agron.*

*Publications included in the thesis